ASC

ASTRO
SCIENCES
CENTER

N 70 37046
CR112773

Report No. M-21

SOLAR ELECTRIC PROPULSION - A SURVEY
TECHNOLOGY STATUS AND MISSION APPLICATIONS

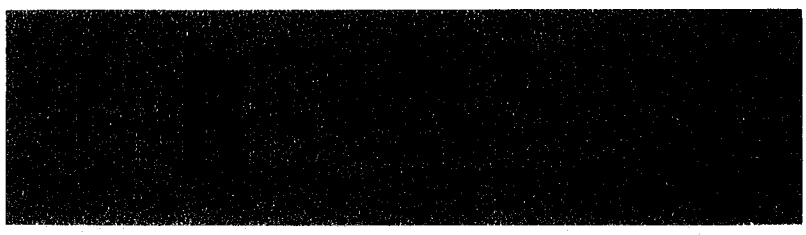

Report No. M-21

SOLAR ELECTRIC PROPULSION - A SURVEY TECHNOLOGY STATUS AND MISSION APPLICATIONS

by

A. L. Friedlander
Project Leader
Astro Sciences

IIT Research Institute
Chicago, Illinois 60616

This work was performed
for the Jet Propulsion Laboratory,
California Institute of Technology,
as sponsored by the National Aeronautics
and Space Administration under
Contract NAS7-100, Task Order No. RD-26

Contract No. 952701

APPROVED:

D. L. Roberts, Manager
Astro Sciences

March 1970

IIT RESEARCH INSTITUTE

FOREWORD

This Technical Report is the final documentation on all data and information required by Task 1: Surveys of Solar-Electric Studies, and Task 2: Scaling Law Development and Validity. The work reported herein represents the first phase of the study, Support Analysis for Solar-Electric Propulsion Data Summary and Mission Applications, conducted by IIT Research Institute for the Jet Propulsion Laboratory, California Institute of Technology, under JPL Contract No. 952701. Phase 1 study objectives are to perform a literature review of previous investigations of solar-electric propulsion applications and to provide an up-to-date data compilation and interpretive summary thereof. The second phase of this study concerns a mission analysis of Jupiter and Saturn orbiters which employ the solar-electric propulsion flight mode. Phase 2 study results will be documented in a separate final report at the end of the contract period in July 1970.

SUMMARY AND CONCLUSIONS

This report reviews solar electric propulsion (SEP) flight systems and their application to planetary and other missions throughout the solar system. The current status of SEP technology is described in terms of the hardware parameters which impact on mission analysis and spacecraft design; e.g., propulsion system specific mass, efficiency and power rating. Primary emphasis is placed upon the characteristics and performance capabilities of the SEP flight mode and comparisons with the contemporary ballistic flight mode. This survey report is thus directed at the mission planning task wherein SEP and ballistic spacecraft may be viewed as tradeoff alternatives for accomplishing space exploration goals.

Summary Table 1 presents the SEP system parameters which are representative of 1970 technology. Rollout solar arrays having a specific mass of 15 kg/kw are assumed. Thrust subsystem specific mass is conservatively estimated to be 12 kg/kw; this includes power conditioning, thrusters and feed system, thruster array gimbal-translation mechanisms, and component redundancy. A 20 percent contingency factor is assigned to the power subsystem to account for possible solar cell damage due to radiation and micrometeoroid impacts, array performance uncertainty, and spacecraft subsystem auxiliary power requirements. This brings the total propulsion system specific mass to 30 kg/kw. Propulsion system efficiency at specific impulse values of 3000, 4000 and 5000 sec is, respectively, 62 percent, 68 percent and 71 percent. This assumes the 30 cm mercury electron bombardment thruster operating in the power range 2-3 kw and a power conditioning efficiency

of 91 percent. Current tankage design for mercury propellant gives a dry weight, including pressurization and expulsion systems, of about 3 percent of the propellant loading.

Performance estimates of SEP missions depend upon the above system input parameters and, hence, should be adjusted from time to time as technology changes. To meet this requirement in a relatively simple manner, a set of performance scaling relationships has been developed. This scaling method circumvents the need for expensive trajectory reoptimization. In addition to the propulsion system parameters, scaling applies to changes in launch vehicle selection, planet orbit size, and chemical retro system specific impulse and inert fraction. It is shown that performance results obtained by scaling generally agree to within a few percent of optimized results.

Summary Table 2 compares SEP and ballistic performance for such mission classes as planet flyby and orbiter, asteroid belt fly-through, asteroid and comet rendezvous, and out-of-ecliptic and solar probes. The performance measure here is the flight time required by SEP and ballistic spacecraft to deliver the same net spacecraft mass to the target. Net mass includes the science payload, structure and other engineering support subsystems. It does not include the solar array or thruster subsystem in the SEP case, or the terminal retro system, if needed, in either case. One basis for comparison is the same launch vehicle assumption for both ballistic and SEP flight modes. The currently planned Burner II (2300) is used as the ballistic upper stage example. In some cases a smaller launch vehicle is also shown for the SEP application, e.g., the Titan IIIC. Summary Table 3 lists the propulsion power, specific impulse and hyperbolic velocity at launch for each of the example SEP missions. In most cases these are optimum parameter values.

Highly energetic missions which are uniquely suited to SEP spacecraft are Mercury orbiter, comet rendezvous, large out-of-the-ecliptic excursions, and close solar probes. Performance advantages over ballistic spacecraft include significantly shorter flight times, high power availability at the target and, in some cases, a smaller launch vehicle. These missions can all be accomplished with the programmed Titan class vehicles; either the Titan IIIC or Titan IIIX(1205)/Centaur. The ballistic Mercury orbiter is completely infeasible even with the Saturn V/Centaur, and some comet rendezvous missions would require the (1207) version of the Titan IIIX. Other missions which show significant flight time reductions using SEP spacecraft are flybys and orbiters of all the outer planets but particularly flybys of Uranus and Neptune and orbiters of Saturn and Uranus. The Neptune orbiter mission, even with SEP, requires a flight time greater than 13 years. There does not appear to be any significant SEP advantage for orbiters of Venus and Mars except, perhaps, for high data-rate mapping missions requiring close circular orbits, very large orbiting payloads, and high power availability. If this were the case, the Titan IIIX(1205)/Centaur/SEP could be employed to deliver a net mass of 2000 kg or more with power capability of at least 10 kw. For asteroid rendezvous missions, the ballistic flight mode may be adequate if a net spacecraft mass of 420 kg or less were acceptable. The advantage of SEP for this mission would depend upon the need to deliver a larger payload than the maximum ballistic capability of the Titan IIIX(1205)/Centaur/BII.

It should be noted that the above comparisons are based on a circular, coplanar model of planet motion, and a launch window of zero length. When a real planet ephemeris and finite-length launch window (15-30 days) are used, the comparative advantage of SEP spacecraft over ballistic spacecraft becomes significantly greater.

The optimum power rating depends on the mission, flight time and launch vehicle. This power falls within the range 10-25 kw for the Titan IIIC and 25-55 kw for the Titan IIIX(1205)/ Centaur. It is shown in the report that off-optimum power operation, even down to 50 percent of optimum power, incurs only a modest payload penalty. The importance of this result is that a smaller solar array design allows a simpler SEP spacecraft configuration and lower cost (solar array cost is about 1/2 million dollars per killowatt). Another important result of the off-optimum power characteristic is that it becomes reasonable to consider a fixed SEP powerplant and spacecraft for multimission application. For example, a 10-15 kw SEP powerplant with thruster operation at about 3500 sec specific impulse could be launched by the Titan IIIC and perform many of the missions listed in Summary Table 2 with a net spacecraft mass of about 400 kg. Outer planet orbiters would likely require a common powerplant of 15-25 kw and the Titan IIIX(1205)/ Centaur launch vehicle.

There has been an understandable reluctance among space program planners to accept the new technology of solar electric propulsion. Many missions of interest, particularly the high priority missions, can be flown with existing or soon to be available chemical launch vehicles and ballistic spacecraft. It has not been possible to justify the SEP concept for most single mission applications. In the first instance, the single mission SEP cost would be about 10-15 percent higher than the ballistic mission. Secondly, the excess payload capability of SEP has not been readily appreciated in that the science payload matched to the ballistic capability is often said to be sufficient for the mission objectives. This may or may not be so but the question cannot be argued here.

It would seem that the acceptance and incorporation of SEP into flight programs depends first, on the demonstration of realistic hardware and reliable spacecraft operation, and,

second, on showing the cost effectiveness of a given SEP design for multimission use. The technology demonstration has been essentially accomplished as of 1970 with the SERT II flight test, continuing laboratory development and test programs, and recently completed spacecraft design studies. Multimission cost advantages would result from the savings in existing launch vehicle cost and development of future high energy chemical upper stages and retro systems. However, SEP cost effectiveness can be established best if there exists a long range space exploration program encompassing many missions to which this propulsion concept could be applied.

Summary Table 1

SOLAR ELECTRIC PROPULSION PARAMETER VALUES*

1970 TECHNOLOGY STATUS

1.	Power subsystem specific mass, α_w (rollout solar array)	15 kg/kw
2.	Thrust subsystem specific mass, α_{ts} (includes power conditioner, thruster array, thrust vector control and redundancy)	12 kg/kw
3.	Effective propulsion system specific mass, α_{ps} (20 percent contingency factor on α_w for solar cell degradation, losses and auxiliary power requirement)	30 kg/kw
4.	Propulsion system efficiency, η (4000 sec)	68%
	Thruster efficiency at I_{sp} = 4000 sec	75%
	Power conditioning efficiency	91%
5.	Propellant tankage factor, k_p (percent of propellant mass)	3%

*2-3 kw thruster modules
10-15 kw system power rating

Summary Table 2

COMPARISON OF SOLAR ELECTRIC PROPULSION AND BALLISTIC FLIGHT MODES FOR PLANETARY MISSIONS

1. OUTER PLANET FLYBY (Net Spacecraft Mass = 450 kg)

	Jupiter	Saturn	Uranus	Neptune
Titan IIIC/SEP	565 days	1300	2100	3100
Titan IIIX(1205)/Centaur/SEP	360 days	750	1625	2700
Titan IIIX(1205)/Centaur/BII	425 days	925	2500	5000

2. OUTER PLANET ORBITER (Net Spacecraft Mass = 750 kg)
   2 x 38 planet radii

	Jupiter	Saturn	Uranus	Neptune
Titan IIIX(1205)/Centaur/SEP	630 days	1450	3570	5000 (560 kg)
Titan IIIX(1205)/Centaur/BII	780 days	2000 (600 kg)	5000 (430 kg)	5000 (190 kg)

3. INNER PLANET ORBITER (Net Spacecraft Mass = 1400 kg)
   2 x 38 planet radii

	Mercury	Venus	Mars
Titan IIIC/SEP	550 days (1000 kg)	135	285
Titan IIIC/BII	--	112	250

4. ASTEROID BELT FLY-THROUGH (Net Spacecraft Mass = 400 kg)
   3.5 a.u. aphelion

Atlas/Centaur/SEP	750 days to 3.5 a.u. (1075 days in belt)
Atlas/Centaur/BII	615 days to 3.5 a.u. (908 days in belt)

Summary Table 2 (Cont'd)

5. ASTEROID (CERES) RENDEZVOUS (Net Spacecraft Mass = 450 kg)
2.77 a.u. circular orbit

Titan IIIC/SEP	560 days
Titan IIIX(1205)/Centaur/SEP	475 days
Titan IIIX(1205)/Centaur/BII	500 days (425 kg)

6. COMET RENDEZVOUS (Net Spacecraft Mass ≈ 450 kg)

	Encke/80	D'Arrest/82	Kopff/83
Titan IIIC/SEP	900 days	700	700
Titan IIIX(1205)/Centaur/SEP*	900 days	700	700
Titan IIIX(1205)/Centaur		1700(BII)	1360
Titan IIIX(1207)/Centaur	1200 days		

7. OUT-OF-ECLIPTIC, 45° (Net Spacecraft Mass ≥ 300 kg)

Titan IIIC/SEP	500 days (300 kg)
Titan IIIX(1205)/Centaur/SEP	600 days (1180 kg)
Titan IIIX(1205)/Centaur/BII with Jupiter swingby	1400 days (1180 kg)

8. SOLAR PROBE, 0.1 a.u. (Net Spacecraft Mass ≥ 300 kg)

Titan IIIC/SEP	400 days (315 kg)
Titan IIIX(1205)/Centaur/SEP	400 days (800 kg)
Titan IIIX(1205)/Centaur/BII with Jupiter swingby	970 days (800 kg)

*Off-optimum power design, $P_o \approx 15$ kw.

Summary Table 3

SOLAR ELECTRIC PROPULSION SYSTEM POWER,
SPECIFIC IMPULSE AND HYPERBOLIC LAUNCH VELOCITY
FOR PLANETARY MISSIONS

Mission	Launch Vehicle	P_o(kw)	I_{sp}(sec)	V_{hL} (km/sec)	Trajectory Mode*
Jupiter Flyby	Titan IIIX(1205)/Centaur	19	2400	9.1	D
Saturn Flyby	"	25	2500	8.2	D
Uranus Flyby	"	25	2500	8.1	D
Neptune Flyby	"	26	2500	8.0	D
Jupiter Orbiter	Titan IIIX(1205)/Centaur	27	2700	5.9	D
Saturn Orbiter	"	34	2800	5.6	D
Uranus Orbiter	"	47	4000	2.0	I
Neptune Orbiter	"	47	4000	2.2	I
Mercury Orbiter	Titan IIIC	23	6000	0	I
Venus Orbiter	"	2	2900	2.3	D
Mars Orbiter	"	6	3100	1.9	D
Asteroid Belt	Atlas/Centaur	7.8	3500	3.5	D
Asteroid Rendezvous	Titan IIIC	21	2400	2.4	D
Comet Rendezvous	Titan IIIC	20	3500	3.0	D
Out-of-Ecliptic, 45°	Titan IIIC	Data Not Available			D
Solar Probe, 0.1 a.u.	Titan IIIX(1205)/Centaur	22	4100	7.6	I

*D - Direct trajectory
I - Indirect trajectory (transfer angle greater than 360°)

TABLE OF CONTENTS

TABLE OF CONTENTS (Cont'd)

LIST OF ILLUSTRATIONS

LIST OF ILLUSTRATIONS (Cont'd)

LIST OF ILLUSTRATIONS (Cont'd)

LIST OF ILLUSTRATIONS (Cont'd)

LIST OF TABLES

LIST OF TABLES (Cont'd)

Report No. M-21

SOLAR ELECTRIC PROPULSION - A SURVEY TECHNOLOGY STATUS AND MISSION APPLICATIONS

1. INTRODUCTION

During the past several years, considerable attention has been directed at the role of solar powered electric spacecraft in planetary exploration. The electric propulsion concept had been under intensive study since 1958 and was viewed, in some quarters, as offering the potential for significant improvement in mission capability and performance as compared to ballistic flight systems. Electric thruster technology, particularly the mercury electron bombardment engine, was undergoing a successful development and test program. However, early expectations of developing a nuclear reactor power source were being diminished by the technological difficulties experienced. In 1964 the alternative prospect of developing a high power but light-weight array of photovoltaic cells was first suggested as being feasible. Since that time NASA programs, both in-house and contractual, have been aimed at demonstrating the feasibility of this propulsion concept along several lines of attack: (1) hardware development and test of thruster systems and large solar arrays, (2) computer programs for trajectory and payload optimization, (3) mission application studies, and (4) spacecraft design at the pre-Phase A level for selected missions. A representative sample of the work accomplished to date is shown by the accompanying list of references.

Solar electric propulsion (SEP) studies have been performed by many different organizations often acting independently of one another. While this approach has been of definite

advantage during the early growth period, it has also led in some instances to widely varying results which causes some confusion for mission planning purposes. This statement refers particularly to mission application studies. The reason for this variability lies in the different ground rules and assumptions regarding technology status (propulsion and power system parameters), launch vehicles, thrust vector constraints, performance optimality conditions, and payload definition. It would appear that an up-to-date compilation and interpretive summary of this previous work would serve a useful purpose. This is the objective of the present report.

The intent of this survey report is to communicate a clear understanding of SEP characteristics and capability for performing automated missions throughout the solar system. The SEP flight mode is primarily a method of transport; to deliver a given science payload and its support subsystems to a specified target in order to carry out the mission objectives. As such the SEP mode may be viewed as a tradeoff option as against the contemporary ballistic mode of transport via chemical propulsion. Vital questions of concern to mission planning are:

(1) How do SEP and ballistic flight modes compare with regard to such performance parameters as flight time, launch vehicle requirement and payload for various missions?

(2) Which missions are uniquely suited to SEP performance capability and operation features such as power availability and path flexibility?

(3) Would the development of a basic SEP stage for multimission use extend the range of existing launch vehicles through the Titan class and be a cost-effective approach for a total exploration program?

An attempt is made to provide answers to these questions through the literature review[1-35] and summary presented herein. Although the report is directed primarily at the mission planning task, those working in the area of SEP mission analysis may find useful information on the application and validity of mass scaling relationships (Appendix A), and new results on comet rendezvous trajectories.

The report is organized as follows: Section 2 presents a brief discussion of the basic characteristics of the SEP flight mode; Section 3 defines the terminology of parameters relevant to mission analysis and summarizes the mathematical interrelationship between trajectory, vehicle and propulsion parameters; Section 4 describes the current status of SEP hardware technology in terms of system parameter values as specific mass and propulsion efficiency, and reviews conceptual SEP spacecraft design studies; Section 5 presents the performance data on SEP mission applications, compares results of different studies through the use of scaling laws, and compares SEP and ballistic performance for various mission classes. The Summary section included in the report is essentially a distillation of Section 5. Appendix A discusses the motivation for developing performance scaling laws and the assumptions invoked, presents the scaling formulas derived, and gives numerical data on scaling accuracy. One page abstracts of the survey articles and reports are presented in Appendix B.

2. BASIC CHARACTERISTICS OF THE SEP FLIGHT MODE

The electrically propelled spacecraft derives its potential performance advantage from the efficient use of propellant mass. Ion thrusters characteristically operate at low thrust levels and high specific impulse (2000-8000 sec) -- an order of magnitude greater than high thrust chemical propulsion systems. Because of the low thrust acceleration (under 10^{-4} g's), the propulsion system must operate over a large fraction of the total flight time. The required mission velocity increment is acquired at a gradual rate as a consequence of the low acceleration. Characteristics of continuous low-thrust trajectories differ appreciably from those of the familiar ballistic trajectories. Inherent properties of flight path flexibility and control of terminal velocity can be important advantages for interplanetary missions.

The SEP spacecraft may be considered as an upper stage of a high-thrust chemical launch vehicle. It must be boosted, at least, to Earth orbital energy before thruster startup. Two flight modes for Earth escape have been investigated. The first assumes thruster startup in a circular orbit with a subsequent slow orbit-raising spiral about the Earth until escape conditions are attained. At a typical acceleration of 2×10^{-5} g's several hundred days are required for Earth escape. Because of this flight time penalty, the spiral escape mode is generally not desirable except, perhaps, for certain long duration missions requiring very large payloads. The second escape mode assumes a high-thrust launch and injection to some hyperbolic excess velocity; this is the usual mode employed in SEP mission analysis. Thruster startup occurs several days after launch at a distance somewhere near the Earth's sphere of influence. The injected mass capability of the launch vehicle decreases with the magnitude of the hyperbolic excess velocity. However, the SEP propellant requirement also decreases with higher initial velocity. Obviously these two opposite effects offer

the opportunity for optimizing the launch velocity. This is a positive but complicating factor in SEP mission analysis. In effect, the interplanetary trajectory requirements cannot be separated from the launch vehicle performance as in ballistic mission analysis. An optimum trajectory and SEP stage is defined herein as that which delivers the maximum net spacecraft mass to the target for a given launch vehicle and flight time. Net mass includes the science payload and engineering support subsystems but not the solar arrays or thrust subsystem.

Since the SEP spacecraft derives its thruster power from solar radiation the variation of solar flux density with distance from the Sun has a strong influence on the optimum trajectory. For outbound missions the available solar power decreases approximately as $R^{-1.7}$. This characteristic is obtained rather than the inverse-square variation of solar radiation because of improved solar cell efficiency with lower temperatures. The power output at Mars radius is about 50 percent of that at 1 a.u. while at Jupiter it falls off to 6 percent. On inbound missions the power output is limited to a factor of about 1.2-1.3 times the power at 1 a.u. due to restrictions on solar cell operating temperatures. In theory the power can be maintained at this constant level within the region 0.15-0.7 a.u. by tilting the solar array away from the Sun-spacecraft line (a more practical lower limit would be 0.3 a.u.). This would be an important design consideration for solar probe missions and Mercury orbiter missions.

The influence of the solar power characteristic on the heliocentric trajectory can best be illustrated by two mission examples. Figure 2-1 shows two different SEP trajectories to Jupiter's orbital radius each having a flight time of 1000 days.[24] The "direct" trajectory is characterized by a steadily increasing radial distance and a transfer angle of less than one revolution. The "indirect" trajectory makes more than one revolution about the Sun first going out to about

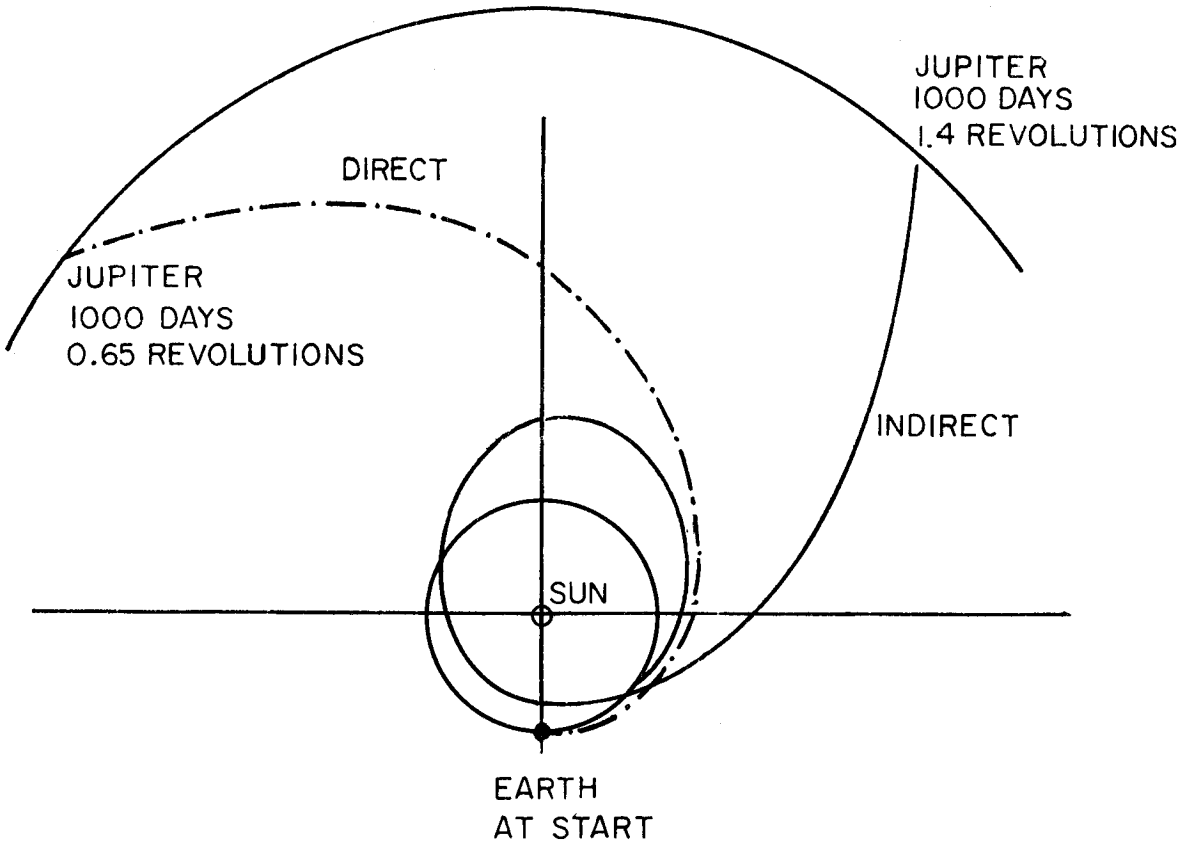

FIGURE 2-1. 1000-DAY SOLAR ELECTRIC PROPULSION MISSIONS TO JUPITER.

1.5 a.u. and then inward to about 0.8 a.u. before heading out to Jupiter's radius. This type of trajectory usually optimizes at a hyperbolic excess velocity of 0-2 km/sec whereas the direct trajectory has an optimum velocity in the range 3-7 km/sec. For the same flight time, indirect trajectories have larger propellant requirements, longer propulsion times, and arrive at the target planet with higher approach velocities. In the example shown both trajectories deliver about the same net spacecraft mass to Jupiter. However, at shorter flight times the direct trajectory will deliver more payload, the reverse being true at longer flight times. Indirect trajectories have significantly better performance for missions beyond Saturn. This looping type trajectory derives its performance advantage by remaining closer to the Sun for a longer time, thus making more efficient use of the solar power system.

Optimum SEP trajectories of the indirect type which make several loops about the Sun have also been identified. Figure 2-2 illustrates a 2-1/2 revolution trajectory for a 400 day solar probe mission.[3] The flight path spirals in toward the Sun with gradually decreasing orbit size. Three coast periods around the perihelion are found to be optimum.

Trajectory calculations for performance purposes are usually made without consideration of the actual thrust subsystem to be employed. One of the trajectory design outputs is the power profile given either as a function of distance or time along the trajectory. The thrust subsystem must then be designed to closely match the optimum power profile since the required thrust level varies directly with the power variation. Figure 2-3 illustrates the SEP propulsion system concept in block diagram form.[16] The power conditioning system must be designed to provide the proper load in the face of the constantly varying power and voltage outputs of the solar array. This could be accomplished by continuously varying the propellant mass flow rate to a single thruster. However, the throttling

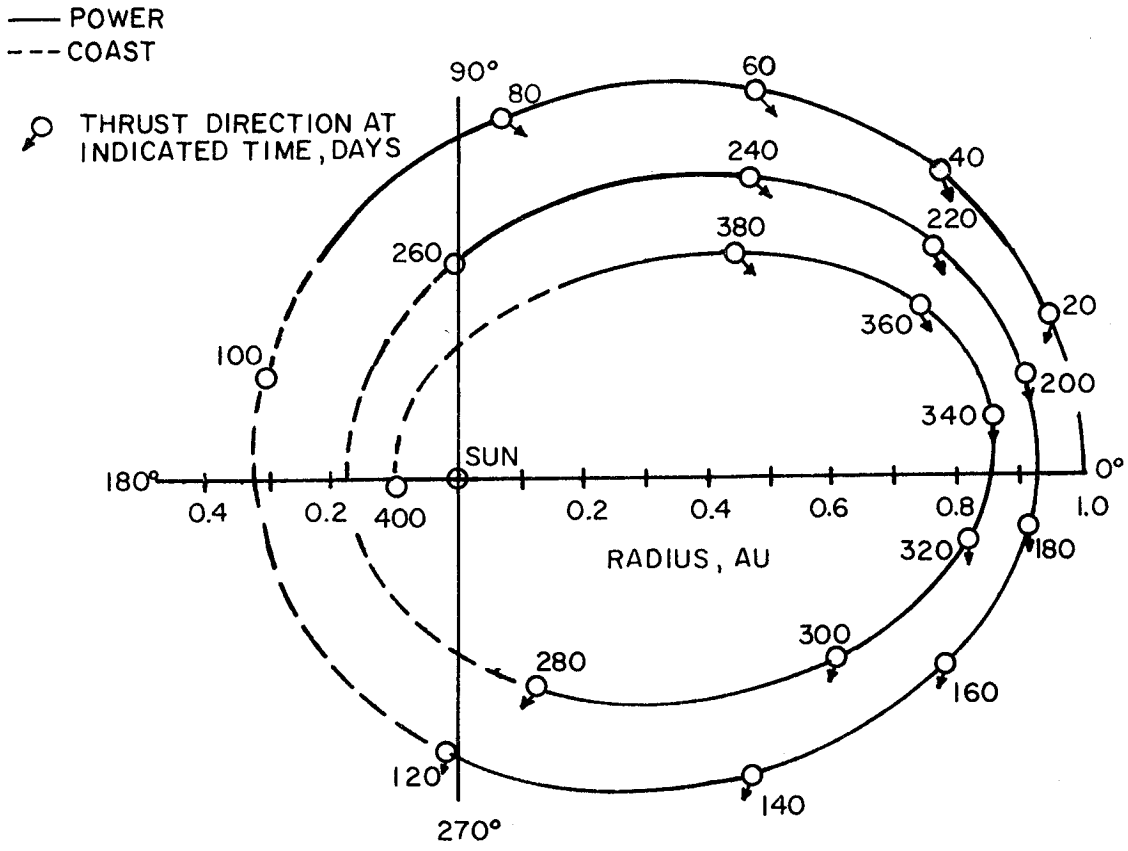

FIGURE 2-2. 400-DAY SOLAR ELECTRIC MISSION TO 0.1 AU.

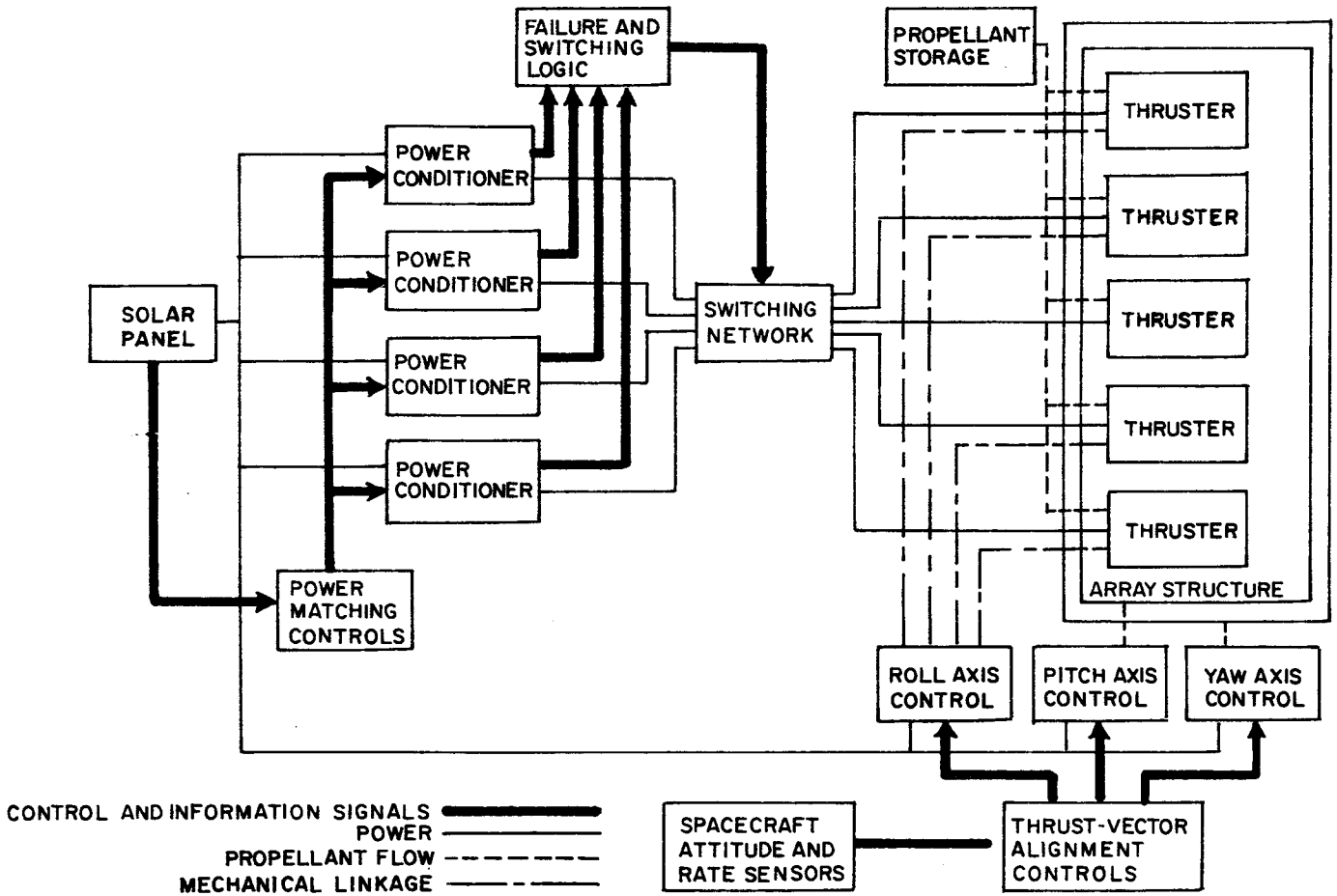

FIGURE 2-3. SOLAR-POWERED ELECTRIC-PROPULSION SYSTEM CONCEPT

ratio of any one thruster (operating at constant specific impulse) is limited by efficiency losses and instability problems to a ratio of about 2:1. The practical design solution is to use multiple thrusters and power conditioners; i.e., a modular design approach. Depending upon the number of modules, individual units would be switched off at appropriate times in the mission as the power available decreases. For inbound missions the modules would be switched on as power increases. The propellant flow rate would still be varied between switching times in order to match the power profile. As indicated in the diagram thrust vector control is necessary to account for shifts in the center of thrust with respect to the spacecraft center of mass.

A number of spacecraft configurations have evolved from different mission application studies. Figure 2-4 illustrates one such configuration for a Jupiter flyby mission.[12] The most striking feature is the large size of the spacecraft due to the solar array area requirement. The relatively small central bus consists of the power conditioning units, thruster array, antenna, science platform and experiments, and support subsystems. A more detailed description of the Jupiter mission will be given in Section 4 of this report.

1. LOW GAIN ANTENNA BOOM WITH COLD GAS JETS MOUNTED.
2. 5 THRUSTER ARRAY 4 OPERATING, 1 STANDBY.
3. 1 DEGREE OF FREEDOM 22.5 db HI-GAIN ANTENNA.
4. POWER CONDITIONING UNITS (4).
5. MAST CONNECTING SOLAR PANEL YOKES - BUS ROTATES ON THIS MAST.
6. 1472 FT^2 SOLAR ARRAY 9.5 W/FT^2 – AT 1 AU
   20.7 W/LB AT 1 AU 11.1 KW TO THE THRUSTERS.

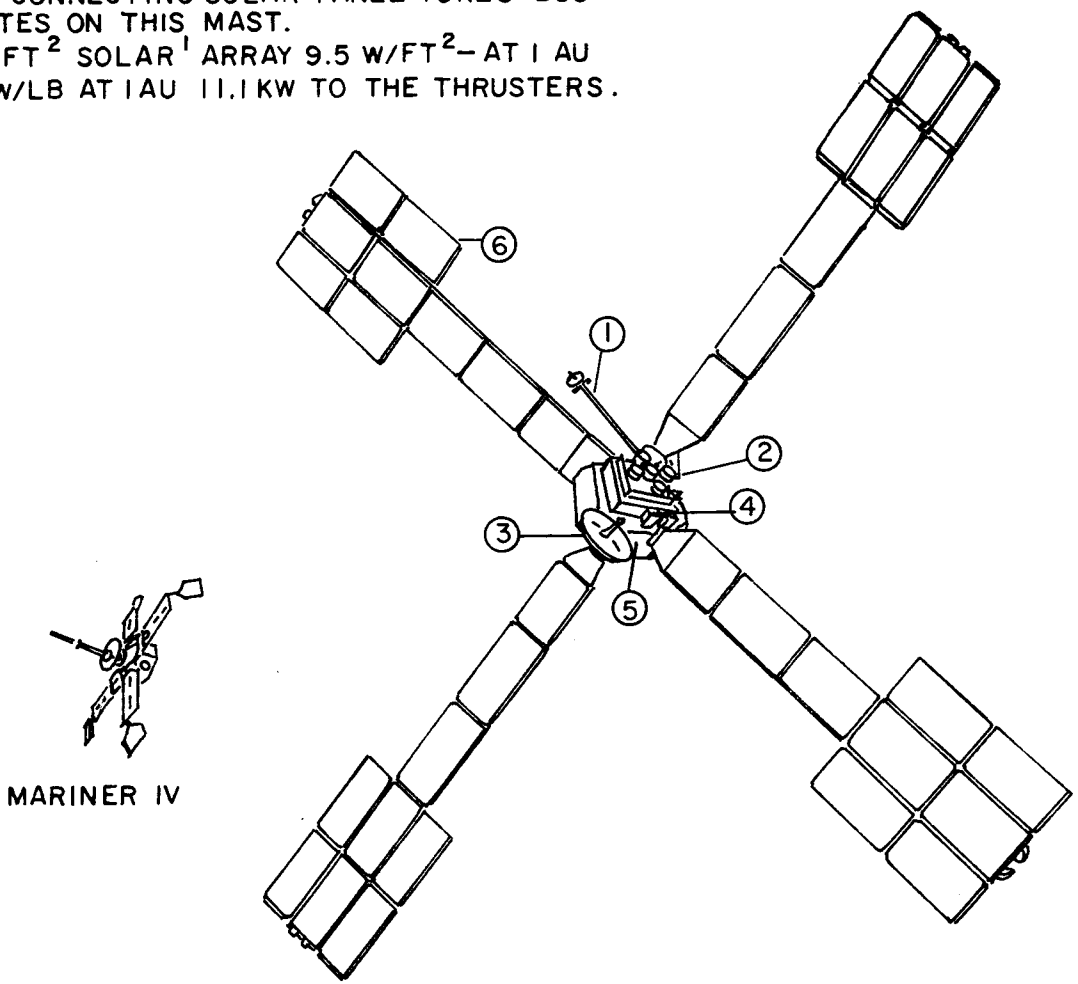

MARINER IV

FIGURE 2-4. JUPITER SOLAR ELECTRIC SPACECRAFT. (JPL DESIGN CONCEPT)

3. MISSION ANALYSIS PARAMETERS

The purpose of this section is to summarize the mathematical relationships which are relevant to mission analysis of solar-electric propulsion. These relationships describe the interdependence of trajectory, vehicle and propulsion system parameters. Standardized terminology recently compiled by a NASA analysis task group is employed.[31] Table 3-1 lists the mission analysis parameters which are discussed in the following paragraphs.

3.1 Spacecraft Mass Allocation

Spacecraft mass at the initiation of low-thrust propulsion is equivalent to that injected by the launch vehicle after discarding the inert mass of the last stage including the shroud and adapter. The injected mass is a function of the launch vehicle selection and the launch characteristic velocity (or hyperbolic excess velocity). Initial spacecraft mass m_o is defined as consisting of the sum of the following masses: low-thrust propulsion system m_{ps}, low-thrust propellant m_p, propellant tankage and plumbing m_t, structure m_s, chemical retro system (if applicable) m_r, and net spacecraft m_n.

$$m_o = m_{ps} + m_p + m_t + m_s + m_r + m_n \ , \ kg \qquad (3.1)$$

The overall propulsion system is made up of the power subsystem m_w and the thrust subsystem m_{ts},

$$m_{ps} = m_w + m_{ts} \qquad (3.2)$$

where m_w consists of the solar cell array and integrating structure, and m_{ts} includes the power conditioning, electric thrusters, thruster array gimbaling, translation actuators, and the integrating structure of the thrust subsystem.

Table 3-1

SUMMARY OF MISSION ANALYSIS PARAMETERS

A. INPUT PARAMETERS	COMMENTS
1) Flight time, t_f	Mission tradeoff
2) Launch vehicle performance, $m_o(V_{hL})$	Mission tradeoff
3) Solar power curve, G(R)	Design dependent
4) Propulsion system efficiency, $\eta(I_{sp})$	Technology dependent
5) Propulsion system specific mass, α_{ps}	Technology dependent
6) Propellant tankage factor, k_p	Technology dependent
7) Spacecraft structure factor, k_o	Design dependent
8) Planet orbit size, r_p and r_a	Mission tradeoff
9) Retro system specific impulse, I_{sc}	Design dependent
10) Retro system inert factor, k_r	Mission tradeoff
11) Retro system jettisoned, yes or no	Mission tradeoff
B. OPTIMIZATION PARAMETERS	
1) Launch date, t_L	Generally free
2) Initial power, P_o	May be constrained
3) Specific impulse, I_{sp}	May be constrained
4) Launch hyperbolic velocity, V_{hL}	Generally free
5) Arrival hyperbolic velocity, V_{hp}	Generally free
6) Thrust vector program, $\hat{\underline{\lambda}}(t)$	May be constrained
7) Propulsion and coast periods, $\sigma(t)$	May be constrained
C. PERFORMANCE PARAMETERS	
1) Net spacecraft mass, m_n	Usually maximized
2) Science payload, m_{sci}	Depends on mission objectives and subsystem requirements
3) Power availability at target, $P_o\ G(R_f)$	Mission dependent, mass tradeoff

Tankage mass is assumed to be proportional to the propellant loading

$$m_t = k_p m_p \tag{3.3}$$

The structural mass is often taken as being proportional to the initial mass,

$$m_s = k_o m_o \tag{3.4}$$

although this convention may contribute to ambiguity in the definition of net spacecraft mass inasmuch as other structural components are already included in m_w and m_{ts}. It has been recommended that k_o be set equal to zero in order to avoid a double penalty, but to consider that m_n includes a spacecraft structural component (exclusive of integrating structure already included in m_{ps}).

For planet orbiter missions, the high-thrust chemical retro system is employed for the final capture maneuver at the target planet. This system consists of two parts: the propellant mass m_{pr}, and the retro stage or inert mass m_i which includes the engines and tankage. The inert mass is assumed to be proportional to the propellant. Hence,

$$m_r = (1 + k_r)\, m_{pr} \tag{3.5}$$

Net spacecraft mass m_n is the quantity that is usually optimized in low-thrust mission studies. In addition to the science payload m_{sci}, m_n would include such engineering subsystems as guidance, attitude control, communications, power (apart from the solar array), data processor, and supporting structure. Upon combining the above equations, net spacecraft mass may be expressed as

$$m_n = m_{sci} + m_{engr} = (1 - k_o)\, m_o - (1 + k_p)\, m_p - m_{ps} - (1 + k_r)\, m_{pr} \tag{3.6}$$

Using previous ballistic spacecraft experience, m_{sci} may be expected to be 10 to 20 percent of the net spacecraft mass. Properly, however, the exact fraction can only be determined after a careful analysis of the engineering subsystem requirements which are strongly dependent on the specific mission objectives.

3.2 Propulsion System Parameters

The solar panel output power varies as a function of the spacecraft distance from the Sun. Denoting G(R) as the normalized power variation and P_o as the power output at 1 a.u. available to the propulsion system, the propulsion power P_e may be expressed generally as

$$P_e = P_o\, G(R), \text{ watts} \tag{3.7}$$

where G(R) = 1 at R = 1 a.u. The quantity P_e is taken to be the electrical power supplied to the power conditioner. The kinetic jet power P_j developed by the thrusters is decreased by the power conditioning efficiency η_{pc} and the thruster efficiency η_t,

$$P_j = \eta P_e\, \sigma(t) \tag{3.8}$$

$$\eta = \eta_{pc}\, \eta_t(c) \tag{3.9}$$

where $\sigma(t)$ is included to indicate whether the thrusters are on or off;

$$\sigma(t) = \begin{cases} 1 & \text{during propulsion periods} \\ 0 & \text{during coast periods} \end{cases} \tag{3.10}$$

Equation (3.9) indicates that the thruster efficiency is a function of the effective jet velocity c.

In general, the thrusters are designed to operate at a constant value of jet velocity. Thruster specific impulse I_{sp} and jet velocity are often used interchangeably and are

related by the expression

$$c = g_o \, I_{sp} \ , \ m/sec \tag{3.11}$$

where $g_o = 9.80665 \ m/sec^2$ is the constant of Earth's surface gravity. Spacecraft mass is found from the differential equation

$$\frac{-dm}{dt} = \dot{m}_p = \frac{2P_j}{c^2} \ , \ kg/sec \tag{3.12}$$

where it is assumed that mass is decreased only by the propellant mass flow rate $\dot{m}_p$ during propulsion periods.

The basic link between the trajectory kinematic requirements and the spacecraft mass and propulsion parameters is provided by the thrust acceleration magnitude

$$a = \frac{F}{m} = \frac{2P_j}{mc} \ , \ m/sec^2 \ . \tag{3.13}$$

Using equations (3.7), (3.8) and (3.12), a(t) may also be written in the integral form

$$a(t) = \frac{a_o \, G[R(t)] \, \sigma(t)}{1 - \frac{a_o}{c} \int_o^t G[R(t)] \, \sigma(t) \, dt} \tag{3.14}$$

where a_o is the initial thrust acceleration at 1 a.u.,

$$a_o = \left(\frac{2\eta}{c}\right) \left(\frac{P_o}{m_o}\right) \ . \tag{3.15}$$

The denominator of (3.14) represents the instantaneous spacecraft mass relative to m_o. Hence the propellant mass ratio expended along a trajectory of flight time t_f could be written in the familiar form

$$\frac{m_p}{m_o} = 1 - e^{-\Delta V/c} \tag{3.16a}$$

where

$$\Delta V = \int_o^{t_f} a(t)dt = c\ln\left|1 - \frac{a_o}{c}\int_o^{t_f} G[R(t)]\ \sigma(t)\ dt\right| \qquad (3.16b)$$

The usefulness of (3.16) is, perhaps, more descriptive than it is functional since ΔV is neither easily computed nor is it independent of the spacecraft design parameters as in the case of ballistic trajectories.

3.3 Specific Mass

The specific mass of the propulsion system α_{ps} is a convenient figure of merit for describing electric propulsion technology. This quantity is defined as

$$\alpha_{ps} = \frac{m_{ps}}{P_o}\ ,\ \text{kg/kw}\ . \qquad (3.17)$$

A separate specific mass can be defined for the solar array subsystem and the thrust subsystem

$$\alpha_w = \frac{m_w}{P_I} \qquad (3.18)$$

$$\alpha_{ts} = \frac{m_{ts}}{P_o} \qquad (3.19)$$

where P_I is the installed power rating of the solar array at 1 a.u. In general, P_o will be less than P_I when one takes into account an auxiliary power drain ΔP_{aux} required for operating spacecraft subsystems, and a contingency factor ΔP_{cont} allowing for uncertainty in array performance and solar cell degradation due to possible solar flares. Also, in the case of inbound missions, the effective value of α_{ts} is increased by the ratio of the maximum power supplied to the thrust subsystem to that at 1 a.u. Introducing power factors f_w and f_{ts} defined by

$$f_w = \frac{P_I}{P_o} = \frac{P_I}{P_I - \Delta P_{aux} - \Delta P_{cont}} \tag{3.20a}$$

$$f_{ts} = \frac{P_{e,max}}{P_o} = G_{max} \tag{3.20b}$$

the overall propulsion system specific mass is then given by

$$\alpha_{ps} = f_w \alpha_w + f_{ts} \alpha_{ts} \quad . \tag{3.21}$$

Since the power and thrust subsystem specific masses may be dependent upon the operating power level, some care should be exercised when using these parameters in mission analysis. However, for solar-electric systems, the modular design of both the solar panels and the thruster array should result in an effective value of α_{ps} which is nearly constant over a range of overall power level P_o.

3.4 Trajectory Kinematics and Mission Classes

Denoting spacecraft velocity and position vectors by $\underline{V}$ and $\underline{R}$, the low-thrust trajectory is determined from the differential equations of motion

$$\dot{\underline{V}} = \underline{g} + a \hat{\underline{\lambda}} \tag{3.22}$$

$$\dot{\underline{R}} = \underline{V} \tag{3.23}$$

where $\hat{\underline{\lambda}}$ is a unit vector defining the thrust acceleration direction and $\underline{g}$ is the gravitational acceleration which is given by

$$\underline{g} = - \frac{\mu \underline{R}}{R^3} \tag{3.24}$$

in the oft-considered case of an inverse-square central force field. Associated with (3.22) and (3.23) are the initial conditions $\underline{V}(t_L) = \underline{V}_o$ and $\underline{R}(t_L) = \underline{R}_o$ where the trajectory time origin is the departure or launch time $t = t_L$. In the case

of interplanetary flight, it is assumed that the SEP spacecraft is launched from Earth on a hyperbolic escape trajectory characterized by some hyperbolic excess velocity V_{hL}. If low-thrust propulsion is initiated at a large distance from Earth, say near the sphere of influence, then the initial heliocentric velocity and position are given approximately by

$$\underline{V}_o = \underline{V}_e(t_L) + V_{hL}\,\hat{\underline{\lambda}}(t_L) \tag{3.25}$$

$$\underline{R}_o = \underline{R}_e(t_L) \tag{3.26}$$

where $\underline{V}_e$ and $\underline{R}_e$ are the heliocentric velocity and position vectors of Earth. It is noted that the effect of operating the electric thrusters for a short time in Earth's gravitational field can be accounted for by adding an appropriate velocity bias to (3.25) as described in the literature.[15] Generally, for the typically low level of thrust acceleration of interest here, this effect can be neglected in preliminary mission analyses.

To complete the statement of the trajectory kinematic problem, one requires the specification of terminal or end point boundary conditions which are appropriate to the particular mission. There are two general mission classes: (1) untargeted or area missions which include out-of-the-ecliptic flights, solar probes and asteroid belt fly-through, and (2) targeted missions to particular solar system bodies such as planets, asteroids or comets. Terminal conditions for untargeted missions are stated rather loosely and are time-independent; e.g., inclination, perihelion distance or aphelion distance. Targeted missions, on the other hand, require, at least, that the spacecraft position match that of the terminal body at the given arrival time $t = t_A$.

$$\underline{R}(t_A) = \underline{R}_p(t_A) \tag{3.27}$$

The velocity boundary condition depends on the type of targeted mission, i.e., flyby, rendezvous or orbiter. Rendezvous will be defined to mean an exact matching of orbits with a body of relatively small and irregular mass such as an asteroid or comet. An orbiter mission implies a planetary target and the use of a high-thrust chemical retro system to establish the desired orbit. The velocity boundary condition for each of these cases is given below:

Flyby Mission

$\underline{V}(t_A)$ is unspecified (free boundary condition)

Rendezvous Mission

$$\underline{V}(t_A) = \underline{V}_p(t_A) \tag{3.28}$$

Planet Orbiter Mission

$$\underline{V}(t_A) = \underline{V}_p(t_A) - V_{hp}\,\hat{\underline{\lambda}}(t_A) \tag{3.29}$$

where V_{hp} is the magnitude of the hyperbolic excess velocity at planet arrival. Assume that the desired orbit is specified by the periapse distance r_p and apoapse distance r_a and is coplanar with the planet approach trajectory. The velocity impulse required at periapse to establish this orbit is then given by the expression

$$\Delta V_r = \sqrt{V_{hp}^2 + \frac{2\mu_p}{r_p}} - \sqrt{\left(\frac{r_a}{r_p}\right)\left(\frac{2\mu_p}{r_a + r_p}\right)} \tag{3.30}$$

where μ_p is the planet's gravitational constant. The retro propellant mass fraction is

$$\rho = 1 - e^{-\frac{\Delta V_r}{I_{sc} g_o}} \tag{3.31}$$

where I_{sc} is the specific impulse of the chemical retro stage.

3.5 Trajectory and Payload Optimization

The problem of performance optimization arises because there is a multitude of solutions which will satisfy the trajectory kinematic conditions. In other words, the number of selectable parameters exceeds the number of kinematic conditions to be satisfied. The extra degrees of freedom may be used to maximize the net spacecraft mass. The mathematical formulation and details of the optimization theory applied to the two-point boundary value problem has been discussed extensively in the literature[3,15] and will not be repeated here. Rather, we will only summarize the mission parameters.

One optimization result has already been applied in expressing the velocity boundary conditions of equations (3.25) and (3.29). That is, the direction of the hyperbolic velocity must be colinear with the thrust acceleration direction $\hat{\underline{\lambda}}$. At Earth departure, V_{hL} is aligned in the direction defined by $\hat{\underline{\lambda}}(t_L)$. At planet arrival, in the case of orbiter missions, V_{hp} is aligned opposite to the direction defined by $\hat{\underline{\lambda}}(t_A)$. It is to be noted that the unit vector $\hat{\underline{\lambda}}(t)$, defined by a set of differential equations, is a continuous function of time and exists even during coast periods ($a = o$).

Table 3-1 summarizes the mission analysis parameters that have been described. The so-called input parameters are those which are generally held constant during the optimization process. Many of these are essentially fixed by the status of SEP technology, while others such as flight time, launch vehicle and orbit size can be varied as tradeoff parameters in a mission study. Ideally, the optimization parameters are those which are freely selectable so as to maximize the net spacecraft mass m_n. However, consideration of practical engineering design, reliability and cost could act to constrain certain parameters. Among the quantities most susceptable to constraint are the initial power level, the thrust direction

program, and the distribution and total duration of the propulsion periods. While recognizing the possible need for such constraints, generation of the optimum performance solution remains a very worthwhile exercise. The results so obtained provide a useful reference point for determining mission feasibility and for measuring the effects of off-optimum design performance.

4. TECHNOLOGY STATUS AND SPACECRAFT DESIGN CONSIDERATIONS

The intent of this section is to describe the developments in SEP component technology and conceptual spacecraft design as they relate to mission feasibility and performance. Solar cell array and thrust subsystems are discussed mainly in terms of realistic engineering design values for performance -- related parameters such as specific mass, power output function, and propulsion efficiency. Brief mention is made of the ongoing SERT II flight test as an example of the important step taken to demonstrate electric propulsion operation in the space environment. Several pre-Phase A studies of SEP spacecraft design for specific mission applications are reviewed. The final topic considered in this section is a weight comparison of SEP and ballistic spacecraft subsystems for an example Jupiter flyby mission.

4.1 Solar Cell Arrays

Development of a light-weight solar power source is paramount if the SEP concept is to show significant mission advantages over ballistic systems. The first large-scale effort in this regard was initiated in 1966 by the Boeing Company under a NASA-JPL contract. A design goal was established to demonstrate a 50 kw array having a specific mass of 23 kg/kw (50 lb/kw). The proposed concept is a modular foldout array employing a cable tie-down system providing structural integrity in the stowed position during launch. After the protecting shroud is released in orbit the four panel assemblies are deployed by an electrically driven cable system. Each of the large panels are made up of 13 (8 x 13 ft) subpanels hinged together. Silicon solar cells (2 x 2 cm) of 8 mil thickness are mounted on an epoxy fiberglass tape substrate supported by a bonded beryllium box-beam structure. Progress on this work has resulted in the fabrication and environmental testing of a full-scale subpanel array.[32] Successful tests have also

established confidence in the drive and hinge systems. More advanced foldout arrays utilizing an aluminum electroforming technique have been under investigation.[33] If successfully developed, this approach could possibly provide an array specific mass of 12 kg/kw.

Current efforts have been directed at the development of a rollout array design having a performance goal of 15 kg/kw (33 lb/kw) for a nominal 10 kw array. In the rollout or "window shade" concept the solar cells are mounted on a thin, flexible plastic sheet which is rolled around a storage drum in the stowed position. After launch, a deployable boom pulls out the array to its extended operational position. General Electric is under contract to NASA-JPL to develop the rollout array design and has reported excellent progress to date.[34] This technology is expected to achieve flight readiness in the early 1970's, and will probably find early use in the manned space station. The basic GE array design was adopted in two recent SEP spacecraft design studies for the Asteroid Belt mission.[27,28] Table 4-1 lists the technical characteristics of a 2.5 kw solar panel.

Solar array technology inputs to mission analysis may be summarized for the two basic design approaches:

Array Design	Specific Mass (α_w)	Specific Area
Foldout array	21 kg/kw	100 ft^2/kw
Rollout array	15 kg/kw	100 ft^2/kw

A contingency factor or power degradation of about 18 percent is usually applied to α_w in order to obtain a conservative estimate of mission performance. This would account for possible solar cell damage due to solar radiation (flare activity), micrometeoroid impacts, and array performance uncertainty.

A number of different models of solar array power output performance have been developed under varying assumptions about

Table 4-1

GE 2.5 kw ROLL-UP SOLAR ARRAY
TECHNICAL CHARACTERISTICS*

Specific Mass	14 kg/kw
Size	250 ft^2/panel (100 in. x 410 in.)
Mass	35 kg/panel
Electrical	
Voltage	100 volts
Power takeoff	Slip rings (Nimbus type)
Solar Cells	Conventional silicon (3 mil glass, 8 mil cell)
Materials	
Blankets	Kapton
Components	Beryllium
Cushioning	RTV 560
Bond	GE-SMRD 745
Resonant Frequency (deployed)	Above 0.04 Hz

*"Solar Electric Propulsion Asteroid Belt Mission Study", Final Report SD 70-21-2, Jan. 1970, North American Rockwell, Downey, California, JPL Contract 952566.

basic cell properties, equilibrium temperatures and array pointing. Figure 4-1 shows three typical curves of relative power output versus distance from the Sun. These curves, or slight modifications thereof, have been used for almost all SEP trajectory and mission analyses performed to date. The different power functions, G(R), obviously affect the trajectory calculations and will account, in some measure, for differences in reported results. This point should be kept in mind when reading the mission application discussion in Section 5. An attempt is made to identify a particular G(R) curve with each mission study reviewed in order to help explain apparent discrepancies in performance results.

4.2 Thrust Subsystem

The successful development program in ion engines has traditionally been the pacing element in electric propulsion technology. Demonstration of beam neutralization and thrust generation in the vacuum of space took place with the SERT I test flight in 1964. This was followed by an aggressive program of improved thruster design, fabrication and laboratory testing, and has culminated to date with the February 1970 launch of the SERT II Earth orbital test of a complete electric propulsion system. SERT II employs a mercury-fueled electron bombardment ion thruster 15 cm in diameter with a design power rating of about 1 kw. Larger thrusters of 30 cm and 2-3 kw power rating have been laboratory tested and are proposed as a suitable module size for space mission applications. Table 4-2 lists the operational and physical parameters of the 30 cm thruster.[27] The specific mass of a single thruster unit including feed system is about 2.4 kg/kw.

For purposes of mission analysis, the most important thruster parameter is its efficiency in converting electrical input power to kinetic beam power. This quantity is given by the product of thruster power efficiency and propellant

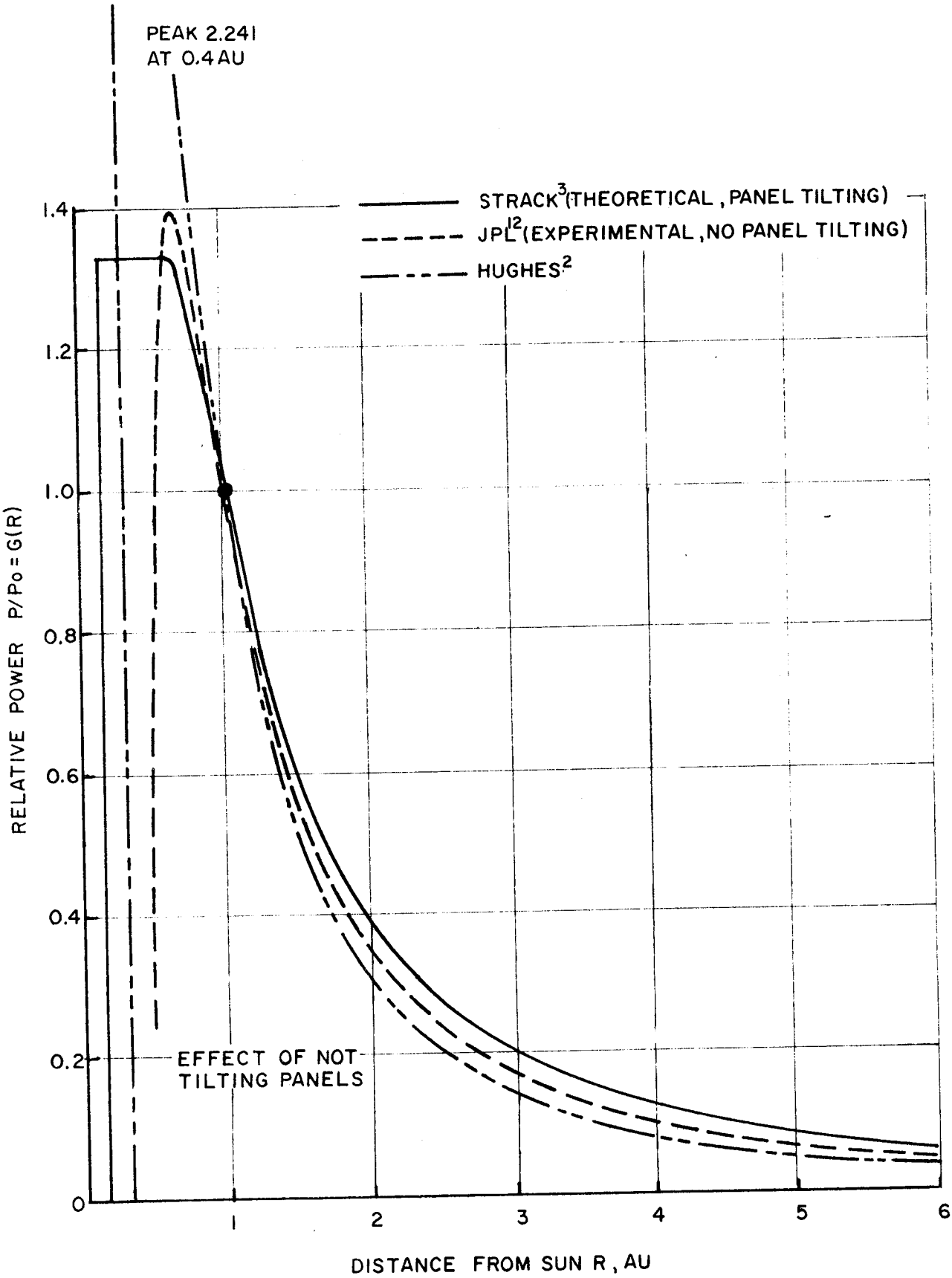

FIGURE 4-1. SOLAR CELL POWER PROFILE

Table 4-2

ELECTRON BOMBARDMENT THRUSTER CHARACTERISTICS*

Peak input power	2.25 kw
Thrust throttling range	3:1
Specific impulse	3200 sec
Propellant utilization efficiency	0.87
Power efficiency	0.79
Type of magnetic field	Electromagnet
Net accelerating voltage	1350 volts
Peak beam current	1.3 amps
Physical size	30 cm diameter, 30 cm length
Mass (including feed system and isolators)	5.4 kg
Maximum mean failure rate goal	1×10^{-5}/hour
Minimum operating life before burnout	7000 hours

*"Study of a Solar Electric Multi-Mission Spacecraft," Vol. 1B, Final Technical Report, TRW Systems Group, JPL Contract No. 952394, March 15, 1970.

utilization efficiency. Figure 4-2 shows three curves of thruster efficiency as a function of specific impulse. The lower curve represents the measured efficiency of the 1 kw thruster designated for the SERT II flight test. The middle curve gives the efficiency of the 30 cm thruster in the 2-3 kw range. At a typical specific impulse of 4000 seconds the efficiency is 75 percent. Most recent mission analyses have assumed this curve. The projected efficiency for the 2-3 kw thruster (early 1970's) is 90 percent at 4000 sec specific impulse.(25)

Another major technology component of the thrust subsystem is the power conditioning unit which must transform the low voltage power from the solar array into high dc voltages and low ac voltages required by the electric thruster and feed system. These supply voltages must be regulated for wide variations of solar array voltages due to varying temperature throughout the mission. Initial efforts to develop lightweight, efficient and reliable power conditioners began in 1965. One such effort conducted by Hughes Aircraft(2) under contract to JPL resulted in a 500 hr test of a 1 kw unit operating with a simulated solar array. Subsequent modifications were made in the design of a 2.5 kw unit having a specific mass of 6.4 kg/kw and an efficiency of 90 percent. Current technology goals for a unit of this size are a specific mass of 4 kg/kw, an efficiency of 90-95 percent, and a reliability of 96 percent for 10,000 hrs of operation. The design approach is based on modular power inverters (300-500 watts) connected together to provide the desired power rating. Each power conditioning panel provides a self-radiating capability. The functions of power matching controls and failure and switching logic are normally assigned to the power conditioning system.

The third major component of the thrust subsystem is the mechanical actuator required for thrust vector alignment during flight. As currently envisioned the thruster array

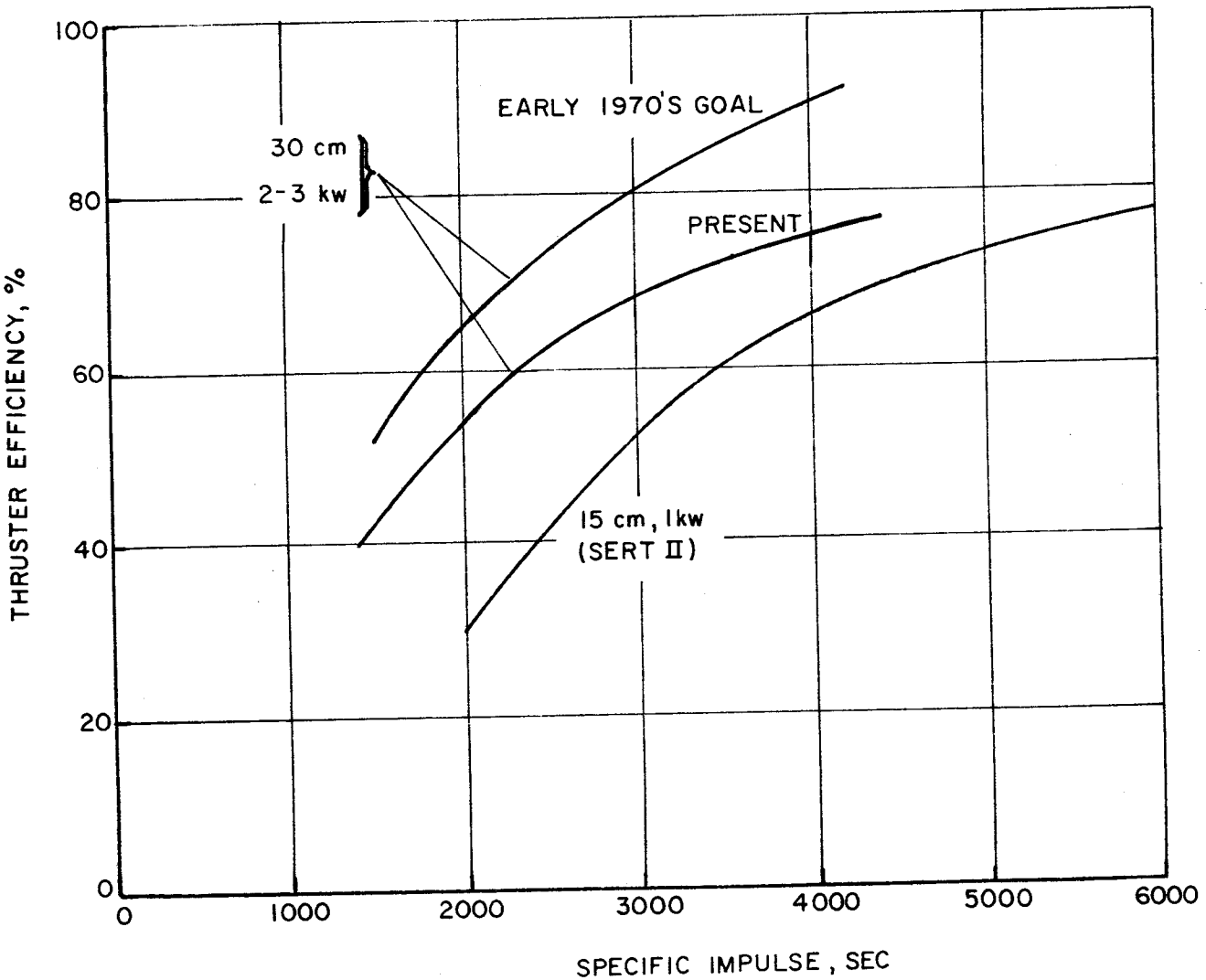

FIGURE 4-2. ELECTRON BOMBARDMENT THRUSTER EFFICIENCY.

would be translated in two perpendicular axes (up to 26 in. of motion), and gimballing of individual thrusters ($\pm$ 10°) would provide roll axis control. The gimbal-translator concept has been tested and flight-rated hardware is estimated to have a mass of about 1.5 kg/gimbal and 2.7 kg/translator.

Table 4-3 summarizes the propulsion system parameter values representative of 1970 technology status. A rollout solar array having a specific mass of 15 kg/kw is assumed. Thrust subsystem specific mass of 12 kg/kw is thought to be a conservative estimate. A typical specific mass breakdown of the thrust subsystem is 4.5 kg/kw for the power conditioners and 7.5 kg/kw for the thruster array including gimbal-translator and redundancy. It is emphasized, however that the values stated here are averages and that actual system specific masses are dependent upon the operating specific impulse and the particular design configuration. Assigning a 20 percent contingency factor to the power subsystem gives a total propulsion system specific mass of 30 kg/kw. Current tank design for mercury propellant gives a dry weight, including pressurization and expulsion systems, of only 3 percent of the propellant weight.

4.3 SERT II Flight Test

The objective of SERT II, launched in February 1970, is the evaluation of long-term (6 months) performance of an electron-bombardment ion thruster and its support subsystems in the space environment.[25] This test is viewed as an important milestone in the advancement of electric propulsion for actual mission applications. In addition to the thruster tests, important questions regarding RF interference, propellant deposition on spacecraft structures, and plasma and field effects on science experiments will be answered.

SERT II was launched from the Western Test Range by a Thorad-Agena vehicle into a near polar circular orbit of about

Table 4-3

SOLAR ELECTRIC PROPULSION PARAMETER VALUES*

1970 TECHNOLOGY STATUS

1.	Power subsystem specific mass, α_w (rollout solar array)	15 kg/kw
2.	Thrust subsystem specific mass, α_{ts} (includes power conditioner, thruster array, thrust vector control and redundancy)	12 kg/kw
3.	Effective propulsion system specific mass, α_{ps} (20% contingency factor on α_w for solar cell degradation, losses and auxiliary power requirement)	30 kg/kw
4.	Propulsion system efficiency, η (4000 sec)	68%
	Thruster efficiency at I_{sp} = 4000 sec 75%	
	Power conditioning efficiency 91%	
5.	Propellant tankage factor, k_p (percent of propellant mass)	3%

*2-3 kw thruster modules; 10-15 kw system power rating.

540 n. miles. The in-orbit configuration consists of the spent Agena stage to which is mounted a 1.5 kw solar array and the spacecraft and support unit. Gravity gradient stabilization and control moment gyros will provide 3-axis attitude control. Two 1 kw mercury bombardment thruster systems are to be operated sequentially to provide small changes in the orbital altitude. They are attached by separate gimbal mounts and are oriented to thrust radially toward the Earth with an offset of about 10°. Thrust level will be determined from measurements of spacecraft potential and electrical parameters of the thruster, in addition to direct acceleration measurements of the spacecraft.

Radio frequency noise induced by the ion thrusters are to be measured in the frequency bands: 300-700 MHz, 1680-1720 MHz, and 2909-2130 MHz. These frequency bands are scanned every 5 minutes in intervals of about 40 MHz bandwidths. Four small solar cell arrays operating at -80°C and +55°C are employed to measure surface contamination due to the ion beam.

As of March 10, 1970, the SERT II thrusters had logged 590 hours of successful operation. The thrust accelerometer, which worked during the initial period of flight but has since failed, produced an accurate corroboration of the estimated thrust level as measured by the electrical parameters.

4.4 SEPST Project

The objective of the Solar Electric Propulsion System Technology Project at the Jet Propulsion Laboratory is the demonstration by 1971 of a complete breadboard propulsion system incorporating all functional and performance requirements of a mission spacecraft system. This includes closed loop, variable power thruster operation; closed loop three-axis attitude control; and automatic failure detection and correction. The test system consists of three 2-1/2 kilowatt hollow cathode mercury bombardment ion engines, individually

gimbal mounted to a structure which translates in two dimensions. High precision translator and gimbal actuators allow extremely accurate positioning of the thrust vector. An analog computer, programmed to simulate the dynamic response of a spacecraft, will provide simulated spacecraft sensor signals to an electronic network which drives the translators and gimbals. The thrusters are connected to two power conditioners through a switching network which allows any thruster to be connected to either power conditioner. A small digital computer, simulating the functions of a spacecraft control computer and sequencer, contains a pre-stored thrust program which provides the single external command to the power conditioners required to vary the system thrust level. This computer also will survey the system status, and command thruster turn-off, system reconfiguration, and activation of standby units in the event of thruster or power conditioner failure.

4.5 Conceptual Spacecraft Design Studies

The engineering design of a fully integrated SEP spacecraft is as significant a step in this new technology area as the development of solar array and thrust subsystems. Ballistic spacecraft design techniques cannot be transferred directly and in toto to solar-electric spacecraft, although this experience is utilized to the fullest possible extent. For example, such support subsystems as data handling, communications, CC&S, cabling and attitude sensors may be treated essentially in the same manner for either flight mode. The science experiments and platform for the same mission objectives may also be nearly identical, although the possible interference of the electric thrusters on the experiments cannot be ignored in the design procedure. Design consideration areas which are, to varying degrees, different for SEP spacecraft include: (1) trajectory and payload optimization, (2) launch vehicle interface, (3) long-term thrust vector control, (4) navigation and guidance, (5) sensor field-of-view

and attitude dynamics in the presence of a large solar array, (6) thermal control, and (7) cost analysis.

A general exposition of each of these design areas is not within the scope of the present report. A discussion of items (2) through (6) above has been given by Mullin[16] and Bartz.[24] The area of trajectory and payload optimization and its interaction with mission and spacecraft design has also been treated in depth in the literature, e.g., Flandro[6] and Sauer.[15] The approach adopted in this report toward the subject of spacecraft design is to review three comprehensive studies conducted for specific mission applications. A summary of results and analysis techniques will serve to illustrate the developments in SEP mission design. The earliest study in this regard was reported in 1966 by Hughes[2] and treated the Mars orbiter mission in particular. The second study,[12] performed in-house by JPL, considered a Jupiter flyby mission. Finally, two parallel study efforts were performed in 1969-70 by North American Rockwell[27] and TRW Systems[28] under contract to JPL with particular emphasis on the Asteroid Belt mission.

4.5.1 Mars Orbiter Mission Study (Hughes)[2]

The three major phases of this study were mission analysis, hardware verification, and spacecraft system design. Low thrust trajectory and overall mission analysis verified that the SEP flight mode, assuming an effective propulsion system specific mass of 34 kg/kw, could deliver large payloads into a close orbit of Mars in reasonable flight times. Consideration of science objectives indicated that the mission payload should consist of a large array of orbital instruments plus a small lander capsule. Performance comparisons with all-chemical ballistic systems accomplishing the same mission showed that the major advantage provided by the SEP mode was

a smaller launch vehicle; the Titan III M as compared to a Saturn IB/Centaur.

The hardware phase of this study sought to verify experimentally the design goal of the ion propulsion system. This was accomplished by developing, integrating and testing an engine of the electron bombardment type with a matching power conditioner. It was concluded from results of this test that engine system components and support subsystems such as power conditioning were available as state-of-the-art technology, although advanced development feasibility indicated the probability of significantly improved performance.

Another important phase of this study was concerned with an in-depth reliability analysis of the power conditioning and control systems. The impact of this analysis is a weight-reliability tradeoff to determine the optimum number of propulsion system modules and standby units. Final choice of module size is determined by the power matching requirements of the mission. Results for the Mars orbiter mission indicated a suitable choice of 6 thrusters (2 in standby) and 4 power conditioning panels at a rated power of 2.2 kw. Baseline system reliability was specified at about 99 percent for a conservatively estimated unmodularized reliability of 80 percent.

Table 4-4 gives the subsystem weight breakdown of the SEP spacecraft design chosen for the Mars mission with a launch in 1973 and a 293 day flight time. A circular orbit of 5000 km altitude is specified. Foldout solar panels with an array power rating of 9.6 kw were chosen. The solar panels are deployed in a plane normal to the spacecraft longitudinal axis into four quadrants at the base of the spacecraft bus. The total array area is 1120 ft^2 broken down into 20 equal size rectangular subpanels (8 x 7 ft). The longitudinal axis is along the Sun-probe line and the solar cells are placed on the array surface opposite to the bus. The thruster array is

Table 4-4

SUBSYSTEM BREAKDOWN OF SOLAR-ELECTRIC MARS ORBITER AND LANDER (HUGHES)[2]

- o 1973 launch
- o Titan III M
- o 293 day flight
- o 5000 km altitude circular orbit
- o 9.6 kw solar array

	SUBSYSTEM & COMPONENTS	MASS, kg		% MASS FRACTION
1.	Thrust Subsystem		88	3.8
	Thrusters (6)	30		
	Structure & mechanisms	15		
	Power conditioners (4)	43		
2.	Power Subsystem	181	181	8.0
	(portion of solar array jettisoned)			
3.	Propellant Subsystem		149	6.6
	Propellant	124		
	Tankage	11		
	Feed system	14		
4.	Payload			
	a) Science		685	30.1
	(includes landing capsule, 42 kg)			
	b) Engineering		498	21.9
	Telecommunications	82		
	Guidance and control	43		
	Power (45 kg of original solar array)	122		
	Structure	206		
	Thermal control	18		
	Electrical harness	27		
5.	Retro Subsystem		670	29.6
TOTAL INJECTED MASS			2271	100.0

mounted external to the bus with the nominal thrust direction being fixed (not optimized) at 90° to the Sun line and parallel to the solar array plane.

A total injected mass of 2271 kg is provided by the Titan III M vehicle launched to a hyperbolic excess velocity of about 2.6 km/sec. The injected mass breaks down into 18.4 percent associated with electric propulsion functions, 29.6 percent for the chemical retro propulsion system used for Mars orbit insertion, 21.9 percent for engineering support subsystems, and 30.1 percent associated with the science instruments and lander capsule. It will be noted that the latter science weight proportion is unusually large relative to previous space mission experience.

Twenty percent of the installed solar array is taken into Mars orbit and provides a power capability of about 1 kw. The communications subsystem employs a 50 watt transmitter, a 7 x 7 ft planar high-gain antenna, and two low-gain omni-directional antennas for continuous coverage. Nitrogen resistojets are utilized for attitude control in addition to the method of thruster array translation during propulsion periods. An active thermal control system comprised of independent louver panels is specified to handle the large change in thermal energy balance throughout the mission.

4.5.2 Jupiter Flyby Mission Study (JPL)[12]

A flyby of the planet Jupiter with a launch in the 1975-76 time frame was investigated as an example mission for which to focus the application of mission analysis and spacecraft design techniques. The main purpose of this study was to demonstrate that feasible engineering solutions exist for SEP planetary missions. One of the study ground rules was the specification of a Mariner class payload and the choice of the Atlas/Centaur launch vehicle.

The first consideration in the area of mission analysis is the selection of trajectory type and nominal flight time. Figure 4-3 shows the variation of net spacecraft mass delivered to Jupiter over a range of flight times from 800 to 1500 days for both the direct and indirect flight modes. These results assume a value of 36.7 kg/kw for the specific mass α_{ps}, circular planetary orbits, optimization of the parameters V_{hL}, I_{sp}, and P_o, and a constant auxiliary power drain of 0.4 kw. It is noted that the cross-over point for the direct and indirect trajectories is around 900 days. Beyond this flight time the net mass does not increase very much for the direct trajectory, but increases significantly for the indirect trajectory. A 900 day flight was thought to be a reasonable upper limit for this mission and for comparison with equivalent ballistic missions. Table 4-5 compares the important system parameters of the two trajectories for the 900 day flight. A selection of the direct trajectory was made on the basis of the shorter propulsion time, smaller propellant and injected mass, smaller heliocentric transfer angle, and lower approach velocity. Each of these parameters impact on the spacecraft subsystem design; the choice of the direct trajectory leads to an overall spacecraft configuration and operation which is simpler to implement.

Having chosen the direct trajectory, the next step in the mission analysis was to determine the effect of system parameter variations and off-optimum design. Figure 4-4, for example, shows the variation of several spacecraft mass components as a function of solar panel output power and several values of thrust subsystem specific mass. Note that the optimum power increases somewhat as α_{ts} decreases. Figure 4-5 shows the optimized values of exhaust velocity ($=g_o I_{sp}$) and launch injection energy C_3 ($=V_{hL}^2$) as a function of output power. It is advantageous to design the vehicle around a lower than optimum value of power, although at some expense in payload.

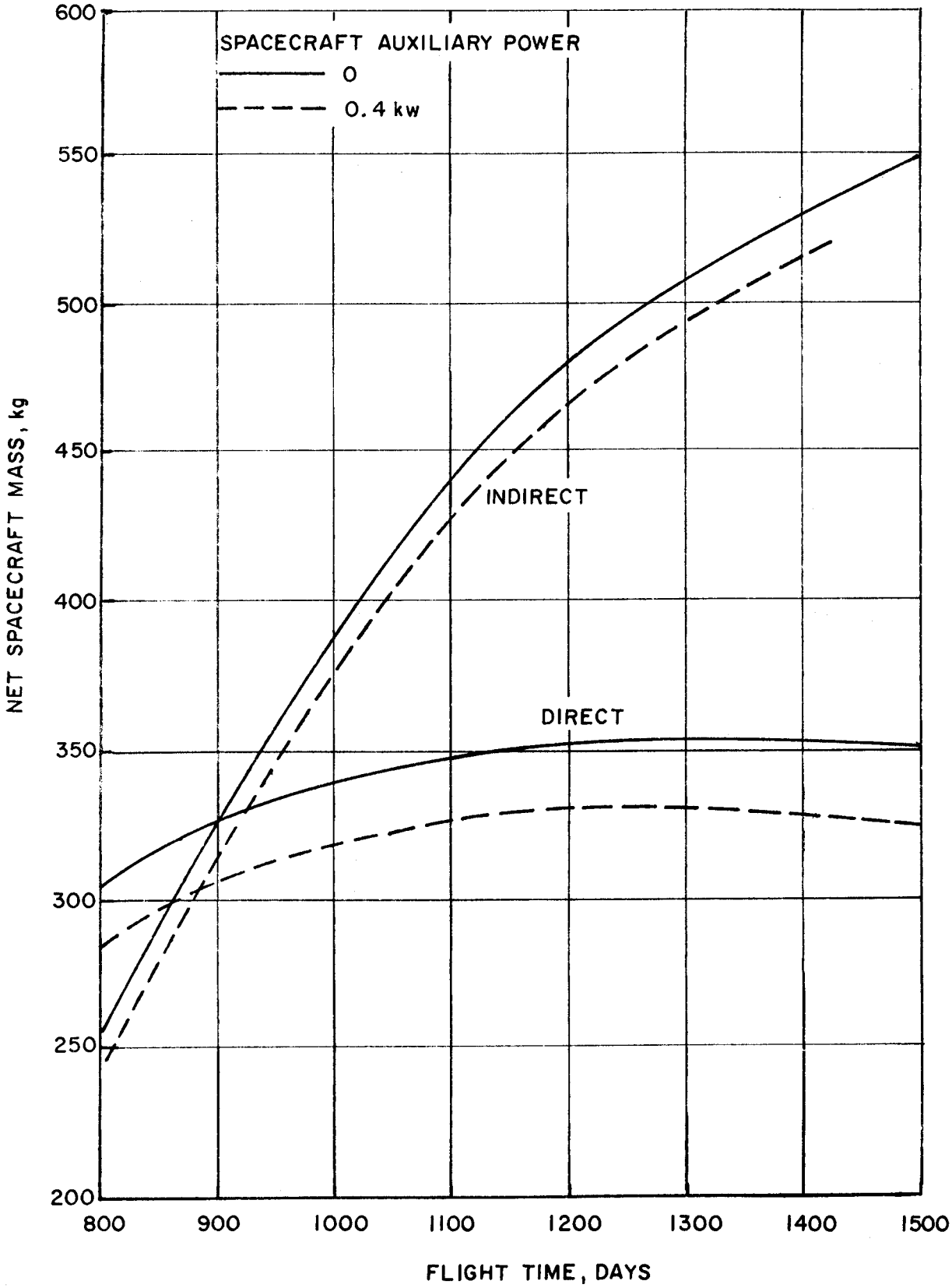

FIGURE 4-3. NET SPACECRAFT MASS VS. FLIGHT TIME FOR JUPITER FLYBY.

Table 4-5

COMPARISON OF 900 DAY DIRECT AND INDIRECT SEP TRAJECTORIES FOR JUPITER FLYBY MISSION*

Orbital Parameters	Direct Trajectory	Indirect Trajectory
Transfer angle, deg	240	480
Array power, kw	10.4	9.6
Specific impulse, sec	2640	3330
Hyperbolic velocity, km/sec	2.2	1.1
Propulsion time, days	430	620
Propellant mass, kg	290	430
Net mass, kg	305	315
Injected mass, kg	970	1090
Jupiter approach velocity, km/sec	6.0	12.8

* α_{ps} = 36.7 kg/kw
P_{aux} = 0.4 kw
Atlas(SLV3C)/Centaur

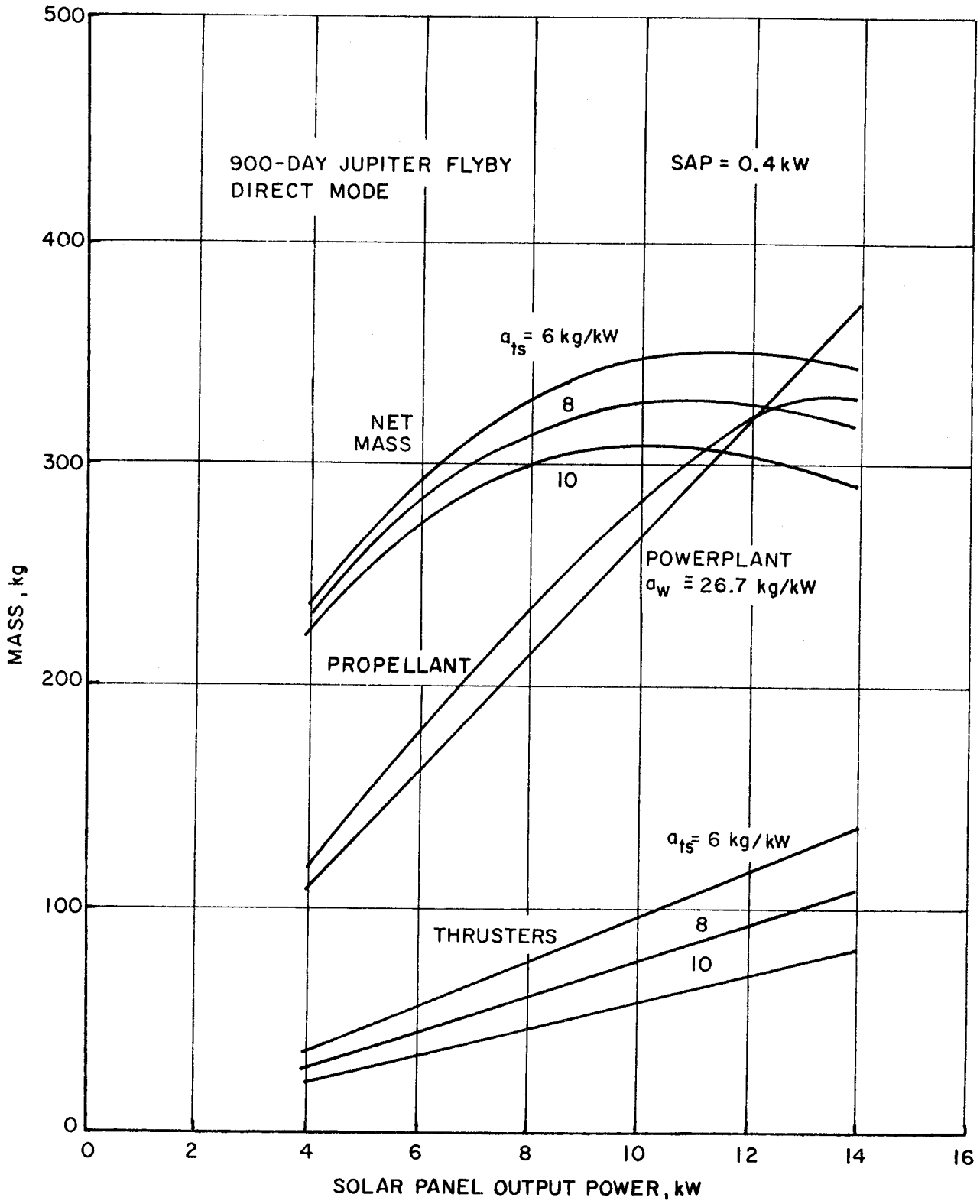

FIGURE 4-4. SOLAR PANEL OUTPUT POWER, kW (MASS VS. POWER)

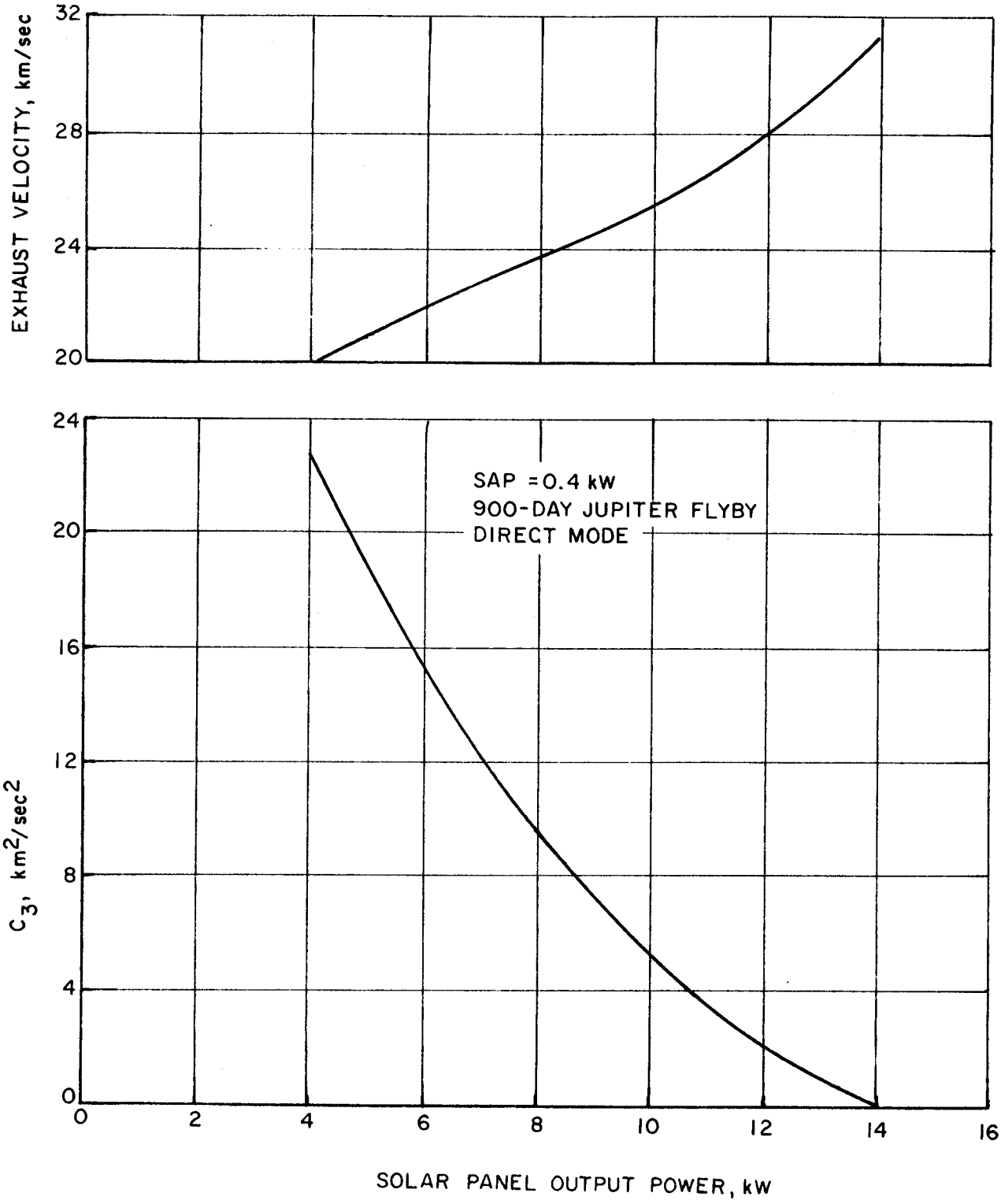

FIGURE 4-5. SOLAR PANEL OUTPUT POWER, kW (EXHAUST VELOCITY AND C_3 VS. POWER)

This requires an increase in launch energy and a decrease in exhaust velocity, assuming that these two parameters are reoptimized.

The aforementioned results are based on the simplifying assumption of coplanar, circular orbits for Earth and Jupiter. A more realistic estimate of vehicle performance requires the use of a more accurate planetary ephemeris and calculations as a function of launch date. For the 900 day direct trajectory, the optimum launch window occurs during the second quarter of 1976. Figure 4-6 shows the variation of net spacecraft mass over the launch window with the optimum solution being compared to that of fixed power and specific impulse. It is noted that use of a higher than optimum specific impulse results in a payload penalty of about 20 kg over a 30 day launch window, and a two week shift of the best launch date. Also, the propulsion on-time increases by about 100 days because the initial acceleration is correspondingly lower for the higher specific impulse.

Based on a final design iteration, the spacecraft propulsion parameters were fixed at the following values:

Power, P_o	11.1 kw
Specific impulse, I_{sp}	2700 sec
Net mass, m_n	295 kg

The method of off-loading propellant was chosen in order to maintain the above fixed net mass over the launch window. Figure 4-7 shows the variation of flight time, propellant and injection energy over the launch period, 4/10/76 to 5/20/76. Propellant loading is maximum at the start of the launch period and is thereafter off-loaded at the rate of 2.5 kg per day. The window closes shortly after 5/20/76 when the flight time rises above the 900 day constraint.

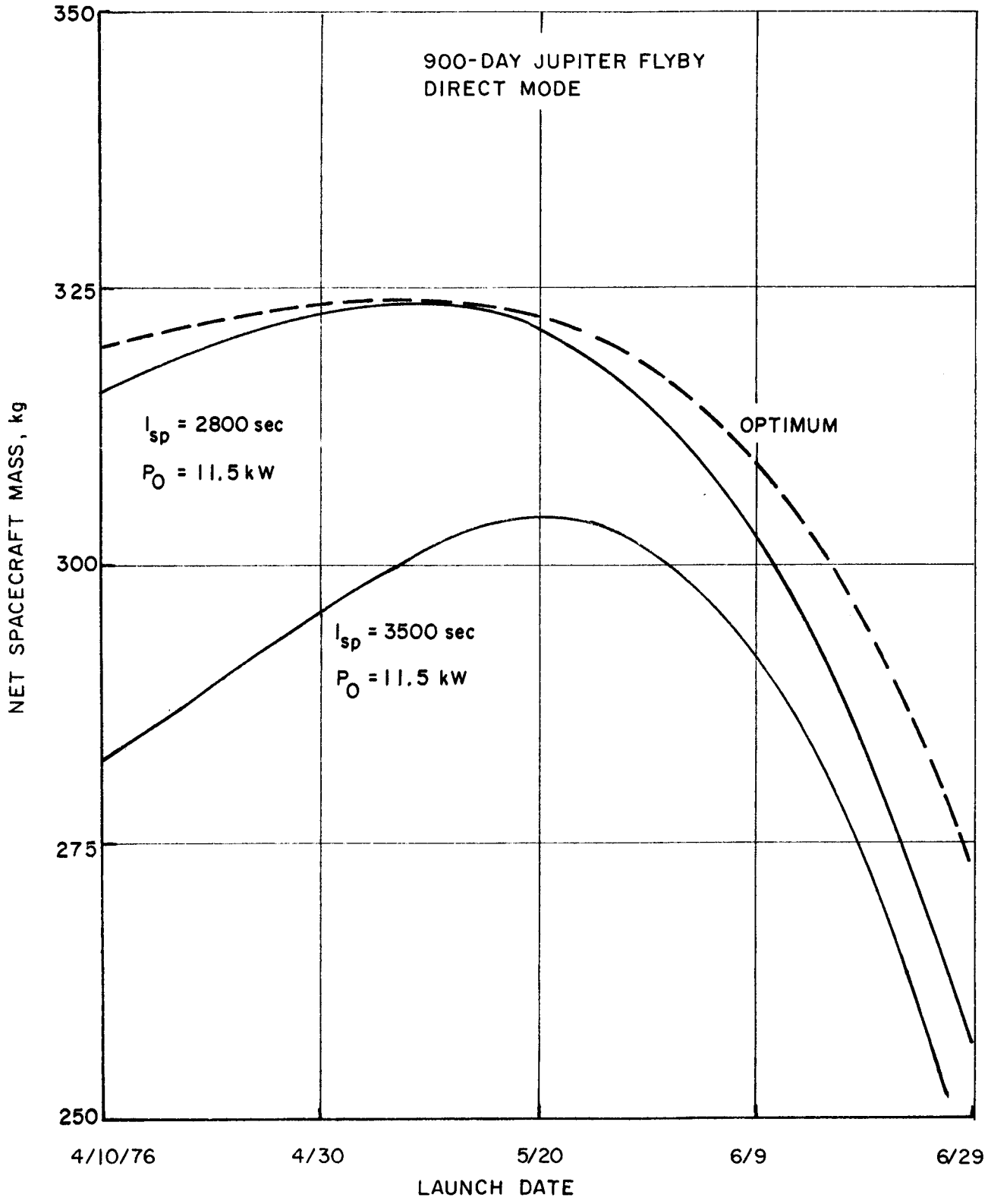

FIGURE 4-6. NET SPACECRAFT MASS VS. LAUNCH DATE.

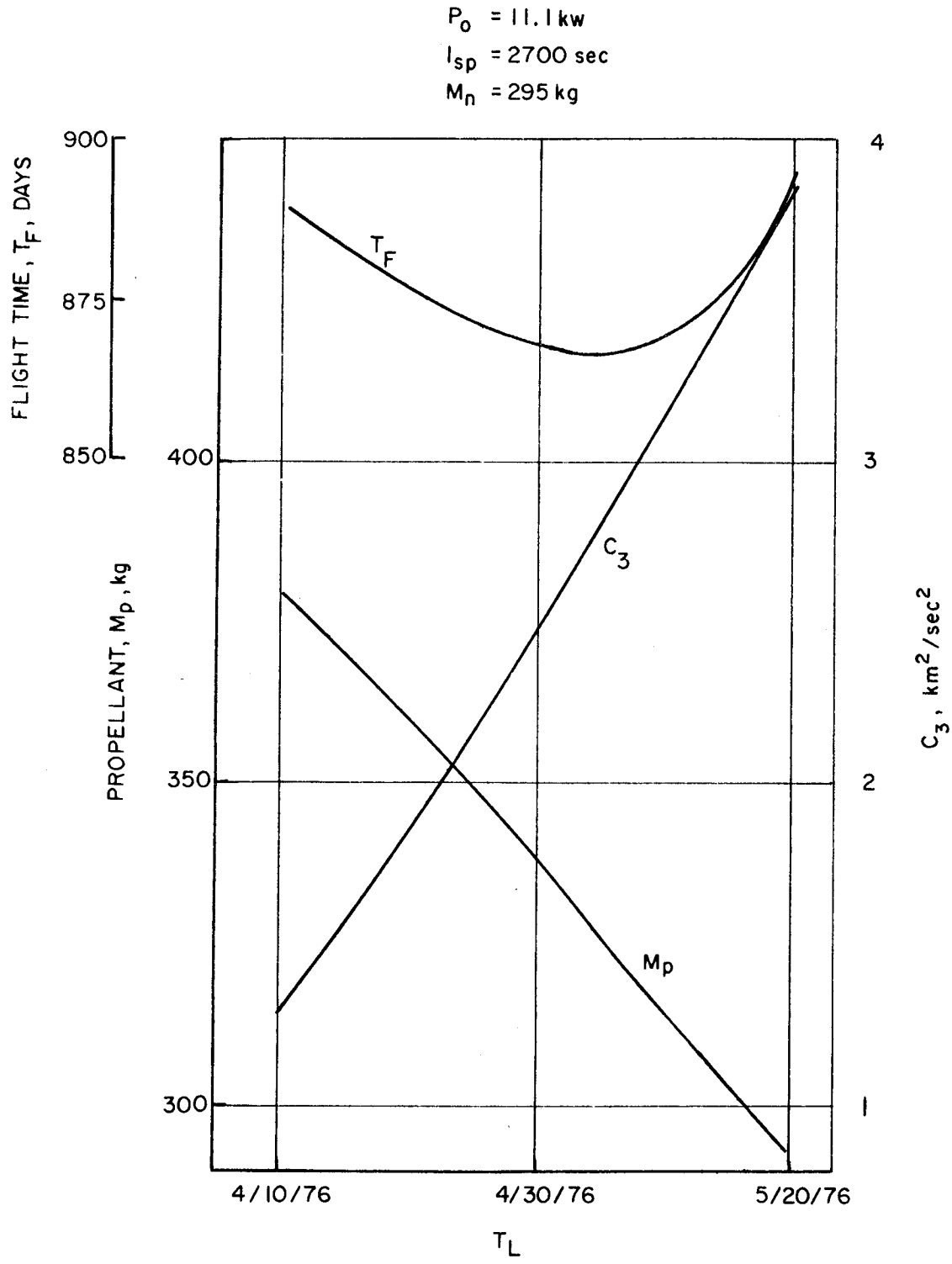

FIGURE 4-7. VARIATION OF PARAMETERS DURING LAUNCH WINDOW. JUPITER FLYBY, DIRECT MODE.

A subsystem mass breakdown is given in Table 4-6. The foldout solar panel power is 14 kw to which a contingency factor of 18 percent has been applied to account for potential power degradation. With this factor and the 400 watts of auxiliary power, the power input to the propulsion system is 11.1 kw. Five thrusters (one in standby) and four power conditioning panels are specified. Including the weight requirement of the thruster array translator and gimbals, the effective propulsion system specific mass is 35 kg/kw (77 lb/kw). The injected mass breaks down into 36.2 percent for the electric thruster and power subsystems, 36.9 percent for the propellant and tankage, and 26.9 percent for the science (33 kg) and engineering support subsystems (256 kg). Note that the mass designated as payload (289 kg) may be considered as being equivalent to that of a ballistic spacecraft.

The encounter trajectory chosen has a closest approach to Jupiter of 170,000 km with a one-sigma guidance error estimated to be 10,000 km. A closed-loop navigation and guidance procedure is required to achieve this encounter accuracy. Ground-based tracking (DSN) of the spacecraft at weekly intervals is required along with two updates of the nominal thrust program, the second update occurring near thrust termination.

An optimum thrust vector program is specified for this mission and is achieved by configuring the spacecraft such that the central bus (including the thruster array) rotates on an axis between pairs of solar array arms. A maximum of 180° rotation is allowed. The problem of power transmission from the solar array is solved without the use of slip rings by looping the cabling around the array central mast external to the spacecraft bus. This rotational configuration also allows complete orientation of the encounter science platform without slewing the entire spacecraft from the Sun-Canopus reference system. It may be noted in this regard that the entire solar

Table 4-6

SUBSYSTEM BREAKDOWN OF SOLAR-ELECTRIC JUPITER FLYBY (JPL)[12]

- o 1976 launch
- o Atlas(SLV3C)/Centaur
- o 900 day flight, direct mode

	SUBSYSTEM & COMPONENTS	MASS, kg		% MASS FRACTION
1.	Thrust Subsystem		82	7.6
	Thrusters (5)	25		
	Gimbals and actuators	5		
	Translator	7		
	Power conditioners (4) (11.1 kw at 4.08 kg/kw)	45		
2.	Power Subsystem		306	28.6
	Solar panels, 14 kw at 21.9 kg/kw 1476 ft^2 at 9.5 watts/ft^2			
3.	Propellant Subsystem		394	36.9
	Propellant	383		
	Tankage & plumbing (3%)	11		
4.	Payload		289	26.9
	a) Science	(33)		(11.5%)
	Cruise science	11		
	Encounter (TV, IR spec)	17		
	Scan platform	4		
	Planet sensors	1		
	b) Engineering	(256)		(88.5%)
	Telecommunications	63		
	Guidance & control	64		
	Power	38		
	Structure	55		
	Thermal control	12		
	Electrical cabling	16		
	Pyrotechnic	6		
	Actuators	2		
TOTAL INJECTED MASS			1071	100.0

array is kept during Jupiter encounter and provides a power capability of about 600-800 watts.

Attitude control is provided by the electric thruster system during the powered flight phase and by a Mariner type cold gas system during the coast phase. The large attitude system requirement is unique to the SEP spacecraft in that the moments of inertia are about 15,000 slug-ft^2 in pitch/yaw and 30,000 slug-ft^2 in roll. Another unique characteristic is that upon deployment of the solar array the inertia increases by a ratio of 60 to 1. This requires that the gas system have a large dynamic range.

Finally, Figure 4-8 shows the power profile of the Jupiter mission and the thruster switching characteristic. Initially, four 2.5 kw thrusters are operating. Thrusters are switched off, one at a time, at 125 days, 200 days, 325 days, and 470 days. A variable propellant flow rate provides power matching between switching times.

4.5.3 Asteroid Belt Mission Study (NAR[27] and TRW [28])

A recent review and presentation[29] to NASA-OSSA on the results of these two parallel studies will be used here as source material. Basic study objectives included: (1) SEP mission prototype concept primarily for asteroid belt exploration but also consideration of multimission capability, (2) low cost and state-of-the-art spacecraft design, (3) program development plan, and (4) program cost estimates. The trajectory profile for the asteroid belt fly-through is shown in Figure 4-9. This belt extends from about 2 a.u. to 4 a.u. from the Sun with the heaviest concentration of meteoroid particles and larger objects occurring near 2.5 a.u. Particle orbits about the Sun are largely circular. The diagram shows the flux direction relative to the spacecraft at various points along the trajectory. An aphelion distance of 3.5 a.u. was found to result in maximum cumulative flux and, hence, optimum

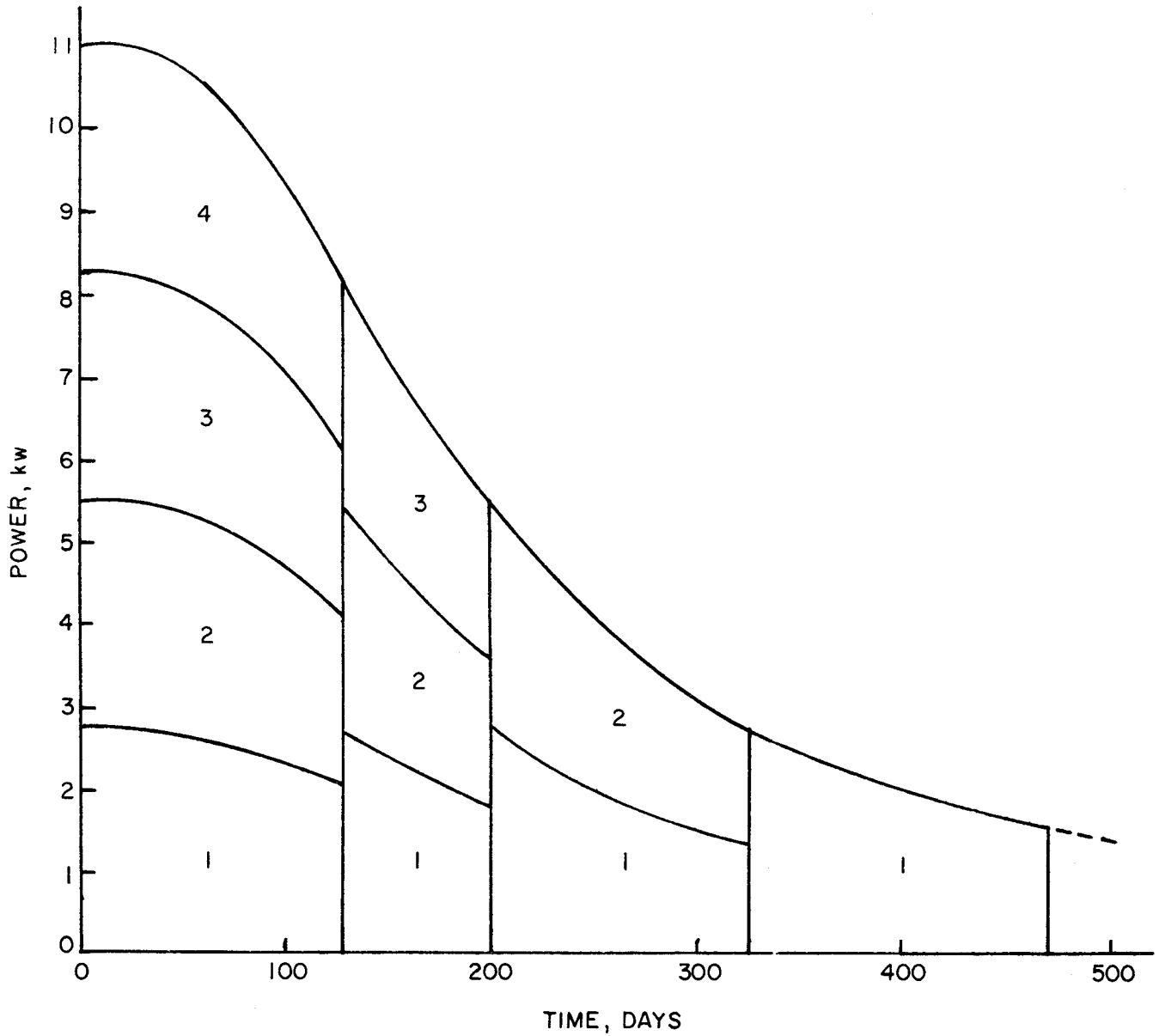

FIGURE 4-8. POWER-TIME HISTORY FOR JUPITER FLYBY SHOWING THRUSTERS IN OPERATION.

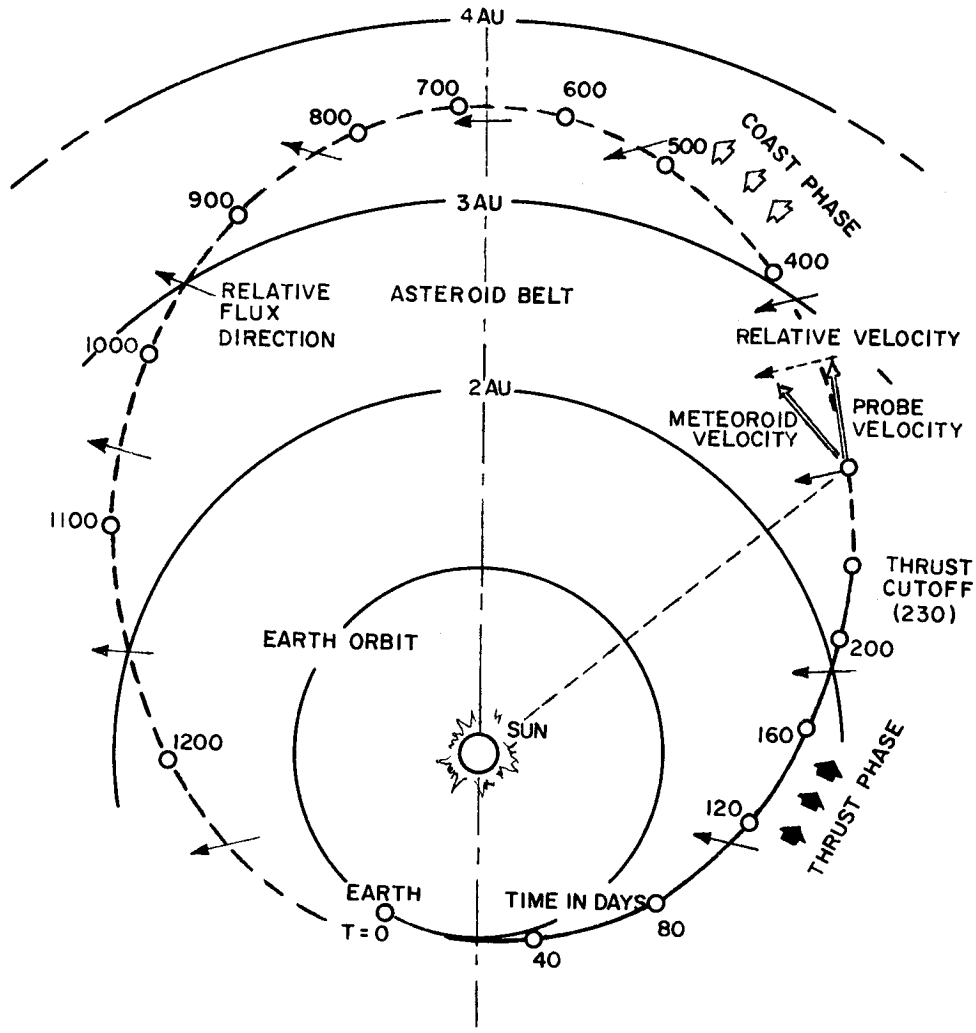

FIGURE 4-9. SPACECRAFT TRAJECTORY AND RELATIVE FLUX ORIENTATION FOR ASTEROID BELT MISSION.

data return. Thrust cutoff occurs near 2 a.u. about 230 days after launch, the aphelion distance is reached in about 700 days, and the spacecraft then coasts back in toward 2 a.u. for a total flight time of about 1200 days.

Table 4-7 lists the baseline design choices which are common to both the NAR and TRW studies. The Atlas(SLV3C)/Centaur launch vehicle is specified for the asteroid belt mission, although the Titan IIIC is also considered for purposes of improved performance capability. Additional choices common to both studies are rollout solar arrays, 3-axis attitude control, Hg bombardment thruster, and a thrust vector program fixed with respect to spacecraft orientation (i.e., not completely optimum). Table 4-8 compares the different design parameters which resulted from each study. Installed solar array power is 6.4 kw in the TRW design and 10 kw in the NAR design. Specific impulse choices are 3200 sec and 3500 sec, respectively. An effective array degradation factor of 24 percent is applied in the TRW design and 15 percent in the NAR design. The larger allowance in the former case is a result of choosing pressure cell meteoroid impact sensors which are mounted to the array; the capacitor sensors in the latter case were not thought to cause significant degradation. With reference to the comment on optimum power, it may be noted that an array of 13 kw is near optimum for the Titan IIIC vehicle and the missions considered. Science payload, including the impact sensors, is on the order of 100 kg.

Table 4-9 gives a detailed breakdown of spacecraft mass, design characteristics and technology status corresponding to each study (for the asteroid mission). It is noted that the excess capability of the Atlas/Centaur over the required spacecraft injected mass in each case is about 20 kg. Both contractors have chosen subsystem designs which are similar in many respects. Mass differences may be accounted for largely by differences in array power and total injected mass. The rather significant

Table 4-7

ASTEROID MISSION/SPACECRAFT BASELINE DESIGN*

CHOICES COMMON TO BOTH STUDIES (TRW SYSTEMS, NORTH AMERICAN ROCKWELL)

LAUNCH VEHICLE	ATLAS/CENTAUR
ASTEROID MISSION TRAJECTORY	THRUST TO ABOUT 2 A.U., COAST TO 3.5 A.U.
DURATION BEYOND 2 A.U.	ABOUT 1000 DAYS
SOLAR ARRAY TYPE	ROLLOUT -- SINGLE BOOM
SPACECRAFT STABILIZATION	3 AXIS
THRUSTER TYPE	MERCURY BOMBARDMENT ION
BEAM CLEARANCE	HEMISPHERICAL
THRUST ANGLE WITH RESPECT TO S/C	FIXED
THRUST VECTOR ADJUSTMENT	TRANSLATION, GIMBAL

*Comparison data summary by JPL.

Table 4-8

ASTEROID MISSION/SPACECRAFT BASELINE DESIGN CHOICES

Item	TRW	NAR
Mission emphasis	Multimission	Asteroid fly-through
Power selection	About 1/2 optimum, 6.4 kw	About 3/4 optimum, 10 kw
Reason	Minimize cost	Maximize capability
C_3, km^2/sec^2	20	12
Gross (injected) S/C mass, kg	581	728
Net S/C mass, kg	325	375
Science payload, kg	110	80
Technology payload, kg	23	--
Science payload - particles & fields	5 expts. - 14 kg	5 expts. - 17 kg
Science payload - meteoroid	$30m^2$, 80 kg pres. cells Sisyphus, TV, TOF	$70m^2$, 31 kg capacitors Sisyphus, EBP
Technology payload	E field, beam, surface, radio	--
Coast phase data gather rate	Up to 49 bps	About 10 bps
Coast phase data trans. rate	64 bps, 10 hr, each 1.6 da.	40 bps, 6.6 hr, daily

*Comparison data summary by JPL.

Table 4-9

ASTEROID BELT MISSION STUDY SUBSYSTEM BASELINE DESIGN CHOICES*

Subsystem	TRW SYSTEMS Kg	Type	Status	NORTH AMERICAN ROCKWELL Kg	Type	Status
CC&S	8	Magnetic core	Use MM'69	10	Magnetic core	Use MM'69
Data Handling	26	2-PCM encoders	Enlarge existing	22	Convolution encoder	Pioneer IX
		2-mag. tapes	Extend life "		Tape recorder	Use MM'71
Communications		2.5m-parab. ant.	Pioneer F tech.		1.47m-parab. ant.	Use Viking
	33	2-Watkins 25w TWT	Use SIV-B	39	20w TWT	Use MM'71
		Receiver, exciter, SW	Use MM'69		Receiver, exciter, SW	Use MM'69
Attitude Control		Star sensor	Use MM'69		4-star sensors	Use MM'69
	39	Tracker-rotate, gimbal	Modify 777	77	Fixed tracker	Use MM'69
		N_2 resistojet RCS			Cold N_2 RCS	Standard
Structure, mechs.	52	Be sandwich panel box	New design	77	Open truss box	New design
Thermal Control	14	Louvers, heaters, ins.	Modify OGO	15	Louvers, heaters, ins.	New design
Power	106	2-3.2 kw rollouts	Modify GE design	155	4-2.5 kw rollouts	Use GE design
	29	1200 WH AgZn batt.	Use MM'69	29	1200 WH AgZn batt.	Use MM'69
		regulators, inverters	Modify MM'69, 777		regulator, inverter	Use MM'69
Elect. Distrib.	20	Shielded harness	Std-new design	54	Shielded harness	Std-new design
Thrust		3-2.25 kw Hg ion	SERT II, SEPST		3-3.6 kw Hg ion	SEPST tech.
	50	2-transistor PCU's	SEPST tech.	63	2-transistor PCU's	SEPST tech.
		TVC-trans. gimbal	SEPST tech.		TVC-trans. gimbal	SEPST tech.
Total Subsystem	377			541		
Hg Propellant	71			107		
Sci/Tech. payload	133			80		
S/C Gross Mass	581			728		
Atlas/Centaur Capability	601	at C_3 = 20 km^2/sec^3		751	at C_3 = 12 km^2/sec^2	

*Comparison data summary by JPL.

difference in attitude control system mass is due to the difference in attitude control propulsion and also to NAR's choice of four separate star trackers and TRW's choice of a single tracking device with multi-star viewing capability.

Table 4-10 lists the performance characteristics for TRW's multimission spacecraft. The two added missions are a Jupiter flyby and a 35° out-of-the-ecliptic flight. It will be noted that the Titan IIIC has been chosen for these additional missions; the science payload is 115 kg for the Jupiter flyby and 87 kg for the extra-ecliptic flight.

Finally, a cost estimate for the asteroid belt spacecraft is given in Table 4-11. Science payload, launch vehicle and DSN operational costs are not included here, so these estimates do not reflect the total mission costs. Both contractors estimated nearly equal spacecraft costs for a one-flight operation - $54M (TRW) and $59M (NAR). It is noted here that the purchased solar array specific cost (General Electric estimate) is one-half million dollars per kilowatt. Hence, the solar array cost is not a major element of the total spacecraft cost. A relatively small cost increment is added when a two spacecraft/flight operation is considered. In this case the two-spacecraft cost estimates are $63.5M (TRW) and $74.5M (NAR).

4.6 Comparison of Solar-Electric and Ballistic Mission

The final item considered in this section is a simplified performance comparison of the solar-electric and ballistic flight modes for an equivalent mission-a flyby of the planet Jupiter. Current estimates of SEP technology parameters are assumed for this purpose (see Table 4-3). The main objective

Table 4-10

ELECTRIC PROPULSION PERFORMANCE OF MULTIMISSION SPACECRAFT (TRW SYSTEMS)

	Asteroid Belt	Jupiter Flyby	Out-of-Ecliptic
Injection energy (km^2/sec^2), $C_3 = V_{hL}^2$	20	29	21.3
Launch Vehicle	Atlas/Centaur	Titan IIIC	Titan IIIC
Total launch vehicle capability (kg)	601.2	603.5	820.3
Total injected spacecraft mass (kg)	580.6	580.8	797.6
Gross solar array power at 1 a.u. (kw)	6.4	6.4	6.4
Solar array degradation (%)	24**	15	15
Net solar array power* (kw)	4.85	5.45	5.45
Thruster input power* (kw)	3.97	4.46	4.46
Thrust force* (milli-lbs)	39.3	44.1	44.1
Propellant ratio	0.123	0.169	0.40
Propellant mass (kg)	71.4	98.2	318
Total thrust time (days)	243	280	550
Destination	3.5 a.u.	5.2 a.u.	35 deg

*At Earth departure.

**Includes 11 percent due to micrometeoroid sensors.

Table 4-11

ESTIMATED ASTEROID MISSION SPACECRAFT COSTS

- One or Two Spacecraft Flights Launched July-December 1975
- Costs of Science Payload, Launch Vehicle and DSN not included
- 1969-70 Dollars

Items Covered	Contractor Cost in Millions of Dollars			
	TRW Systems[28]		North American Rockwell[27]	
	One Flight	Two Flights	One Flight	Two Flights
Spacecraft Design Development Production Testing Flight Operations Project Management	54.0	63.5	59.0	74.5

here is to examine the question of ballistic vs SEP "payload;" i.e., what are the various subsystem differences in terms of mass and what impact do these differences have on a performance comparison?

To assess the worth of a proposed solar electric mission as compared to a ballistic mission, a common basis for comparison is required. Since a prime mission objective is to acquire scientific information, one truly relevant basis for comparison would be on the content of the scientific data returned. This is, therefore, the standard for comparison used in this section.

Having selected a basis for comparison, two alternative approaches are available: (1) mission parameters such as launch vehicle and flight time can be held constant and the value of the science data return varied, (2) the science data return can be held constant and other mission parameters varied. The former alternative presents a difficult problem in that a relative assessment of the value of the data returned is highly subjective. The latter alternative eliminates the subjective problem and allows one to compare missions on the basis of different flight times and/or launch vehicles. Consequently, the latter method is chosen as the comparison method for this section.

To provide an example of how the comparison method can be applied, the following proposed mission was considered:

Jupiter flyby (ballistic), 1974 launch
952 kg spacecraft, 20 day launch window
Titan IIIX(1205)/Centaur/BII
600 day flight time

To use the comparison method one needs to determine the launch vehicle and/or flight time requirements associated with a solar electric mission providing the same science data return as the proposed ballistic mission. This can be accomplished by first

considering the proposed ballistic spacecraft on a subsystem basis and then estimating the modifications required to make the spacecraft compatible as a solar electric payload. Of course, only those modifications which will not alter the science data return of the mission are acceptable. The mass of the modified spacecraft can then be considered as the net spacecraft mass for a solar electric mission.

A subsystem mass breakdown for the proposed ballistic spacecraft and the corresponding estimated mass for a solar electric spacecraft are shown in Table 4-12. Here the 952 kg ballistic spacecraft has been modified so that it can be considered as having a net spacecraft mass of 787 kg for a solar electric mission. The science data return of the modified spacecraft would be the same as for the initial ballistic spacecraft.

In modifying the ballistic spacecraft, the following subsystems were left unchanged:

Science package
Data handling
Communications
Power conditioning
Central computer & sequencer
Platforms & booms
Cabling
Structure

The remaining subsystems were modified for the following reasons:

*Power Source -- The proposed ballistic payload used an RTG power source which supplied 540 watts of electrical power. A solar electric spacecraft would have approximately 1 kw of electrical power available at Jupiter.

---

*This subsystem will account for the largest part of the difference between ballistic and SEP systems, and is very much mission dependent.

Table 4-12

BALLISTIC PAYLOAD AND CORRESPONDING ADJUSTED PAYLOAD SUBSYSTEMS FOR SEP JUPITER FLYBY MISSION

Subsystem	Ballistic Payload Subsystem Mass (kg)	* Ballistic Payload Subsystem Mass Adjusted for SEP Mission (kg)	Δ
Science package	184	184	
Data handling	41	41	
Communications	66	66	
Power conditioning	12	12	
CC&S	18	18	
Platforms/booms	92	92	
Power source	121	18	(-103)
Cabling	60	60	
Structural	77	77	
Guidance & control	43	19	(-24)
Midcourse prop. (dry)	8	--	(-8)
ACS propulsion (dry)	9	25	(+16)
Contingency (10% dry mass)	81	61	(-20)
ACS propellant	6	9	(+3)
Midcourse propellant	6	--	(-6)
Adapter (5% gross mass)	41	34	(-7)
Growth allowance (10% gross mass)	87	71	(-16)
TOTAL	952	787	(-165)

*PD69-151, Space Division, North American Rockwell, Outer Planet Exploration Missions, Study Report, October 1969.

The residual solar electric power was therefore considered adequate for operating the spacecraft. An 18 kg battery was considered necessary to provide one source of electrical power which would be independent of the solar panel power.

Guidance and Control -- The guidance and attitude control sensors and the attitude control propellant for the ballistic spacecraft were removed. Subsystems estimated in JPL study[12] were substituted. This study made allowance for a solar electric spacecraft having an overall mass similar to the adjusted spacecraft overall mass. It was therefore considered that the JPL estimates would be adequate for these subsystems since the larger moment of inertia factors were taken into account.

Midcourse Propellant -- The midcourse propellant mass was omitted from the adjusted spacecraft since its function would be performed on a continual basis by the solar electric propulsion system.

Contingency, Adapter and Growth Allowance -- The percentage allowance for these factors were the same for the adjusted spacecraft as for the ballistic spacecraft.

The solar electric mission performance curves for the Titan IIIC and Titan IIIX(1205)/Centaur are illustrated in Figure 4-10. These curves are based on assuming circular planetary orbits and a zero launch window for the SEP mission but this should have small effect on the comparison. The ballistic payload and the adjusted payload mass are shown to illustrate the different results that can be obtained depending upon whether or not the ballistic spacecraft mass is adjusted.

Table 4-13 summarizes the results of the comparison. It is seen that the difference in flight time between the cases

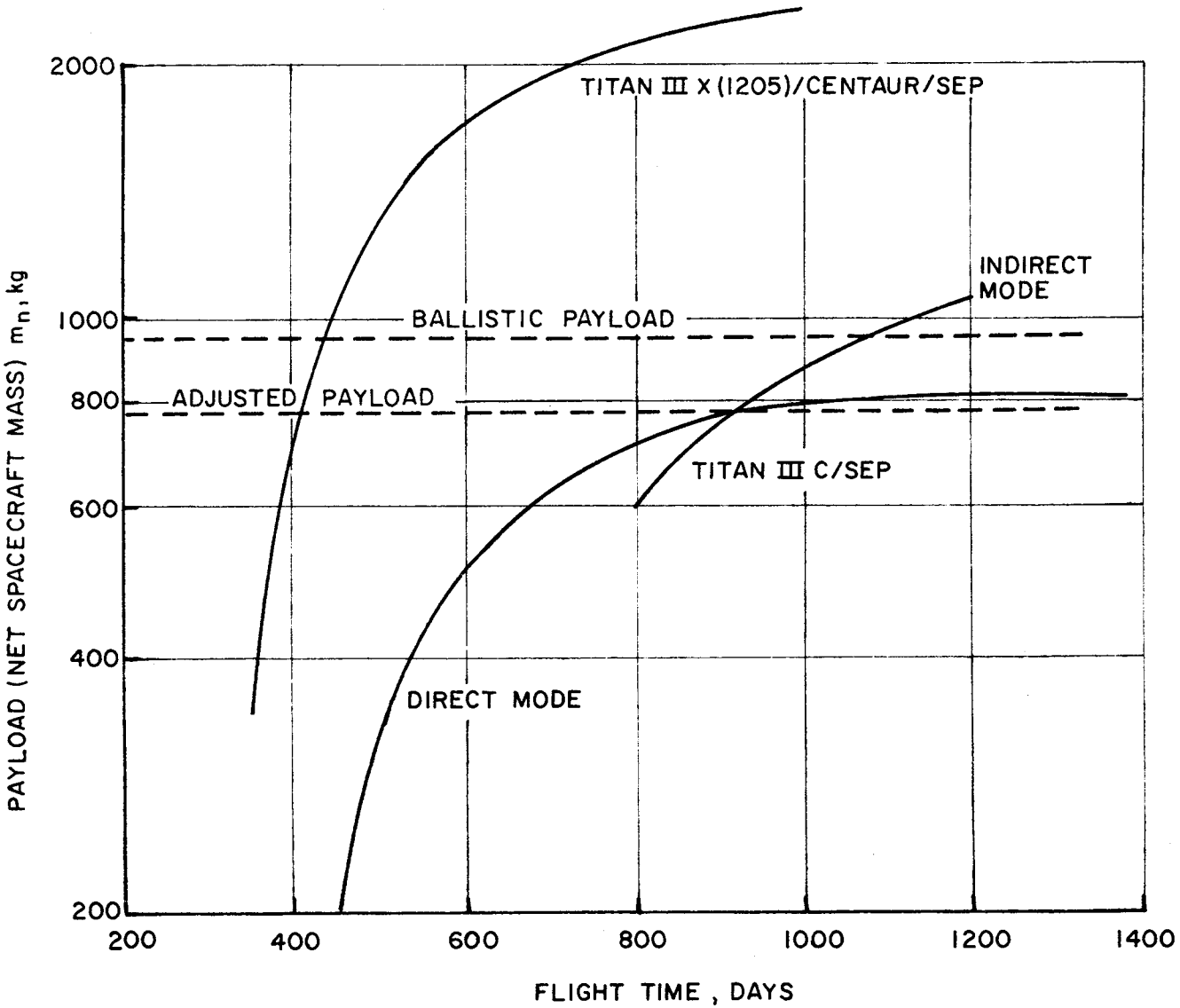

FIGURE 4-10. PAYLOAD VERSUS FLIGHT TIME FOR JUPITER FLYBY MISSION WITH SOLAR ELECTRIC PROPULSION.

Table 4-13

TRADEOFFS FOR FIXED SCIENCE PAYLOAD FOR A BALLISTIC AND SEP FLYBY MISSION TO JUPITER

Mission	Launch Vehicle	Flight Time
Ballistic	Titan IIIX(1205)/Cent/BII	600 days
SEP (Adjusted payload)	Titan IIIC	880 days
SEP (Adjusted payload)	Titan IIIX(1205)/Cent	410 days
SEP (Ballistic payload)	Titan IIIC	1080 days
SEP (Ballistic payload)	Titan IIIX(1205)/Cent	440 days

of adjusted and unadjusted payload is not very significant when the Titan/Centaur launch vehicle is assumed. For the Titan IIIC, this difference is 200 days or about 20 percent. It may be mentioned that the easier comparison approach of not adjusting the payload between ballistic and SEP spacecraft would normally result in a conservative estimate of SEP performance. This approach is adopted in the following section on SEP capability for total solar system exploration.

5. MISSION APPLICATION STUDY RESULTS

The purpose of this section is threefold: (1) to compare results of different studies of the same mission in order to ascertain the level of agreement between independent analyses, (2) to present an overall picture of SEP capability for solar system missions on the basis of a self-consistent set of input parameter assumptions, and (3) to compare SEP and ballistic flight mode performance for these missions. Results utilized for this purpose were obtained from the extensive data base reported in the current literature. Table 5-1 presents a synoptic description of the various mission studies surveyed.

5.1 The Use of Scaling in Performance Analysis

One of the objectives of the present survey study was to formulate a set of scaling laws and to validate their accuracy. By "scaling laws," we mean a relatively simple, algebraic, noniterative formula which allows one to transform performance (net spacecraft mass) results from one set of input parameter assumptions to another. Clearly, the motivation for doing so is to circumvent the need for computer reoptimization which is both expensive and time consuming. Some type of simple scaling was needed in order to easily compare results obtained from previous studies. Secondly, the use of scaling, if valid, would be of significant advantage in future mission application studies.

Appendix A describes the scaling law development task, presents the resultant formulas, and gives supporting data on validity checks. The reader is referred to this appendix since only a skeleton summary is given here. The assumption of trajectory invariance (relative to different input parameters) is invoked in deriving the scaling formulas. This is not a particularly new concept and has been applied, in one form or another, in previous analyses of nuclear-electric propulsion. Trajectory invariance is, of course, never satisfied in the

TABLE 5.1 MISSION APPLICATION STUDIES - COMPARISON OF PARAMETER ASSUMPTIONS

REFERENCE STUDY	MISSION APPLICATION	LAUNCH VEHICLE	SOLAR POWER CURVE G (R)	PROPULSION SYSTEM EFFICIENCY η (4000 sec)	PROPULSION SYSTEM SPECIFIC MASS α_{ps} (kg/kw)	TANKAGE FACTOR kp	STRUCTURE FACTOR ko	RETRO SPECIFIC IMPULSE I_{sc} (sec)	RETRO INERTS kr	PLANET ORBIT SIZE (RADII)	TRAJECTORY MODEL	LAUNCH OPPORTUNITY	INITIAL POWER P_o (kw)	SPECIFIC IMPULSE I_{sp} (sec)	LAUNCH VELOCITY V_{hl}	ARRIVAL VELOCITY V_{hp}	THRUST VECTOR PROGRAM $\hat{\Delta}(t)$	PROPULSION PERIODS $\sigma(t)$
MOLITER, ET AL[1]	MARS ORBITER	SATURN 1B/CENTAUR	HUGHES	0.60	28	0.065	0	310	0.111	NOT GIVEN	3D	1971	48	4000	OPTIMIZED	OPTIMIZED	FIXED	OPTIMIZED
HUGHES[2]	MARS ORBITER JUPITER FLYBY	SEVERAL	HUGHES	0.60	30-34	0.06-0.10	0	310	0.111	SEVERAL	3D	1973	9.6-17	3500-4000	OPTIMIZED	OPTIMIZED	FIXED	OPTIMIZED
JPL[12]	JUPITER FLYBY	SLV3C/CENTAUR	JPL	0.68	35	0.03	0	-	-	-	3D	1975-76 *	OPTIMIZED	OPTIMIZED	OPTIMIZED	OPTIMIZED	OPTIMIZED	OPTIMIZED
FLANDRO, BARBER[6]	JUPITER FLYBY	SLV3X/CENTAUR	HUGHES	0.60	30	0	0	-	-	-	3D	1975 *	OPTIMIZED	OPTIMIZED	OPTIMIZED	OPTIMIZED	OPTIMIZED	OPTIMIZED
FLANDRO[11]	JUPITER SWINGBY	SEVERAL	JPL	0.60	30	0	0	-	-	-	3D	1976-80 *	- - - - - - - - - - OPTIMIZED FOR JUPITER FLYBY - - - - - - - - - -					
PRINCETON[14]	JUPITER FLYBY ASTEROID REND.	SEVERAL	HUGHES	0.60	20-30	0.06	0.08	-	-	-	2D	OPEN	OPTIMIZED	OPTIMIZED	OPTIMIZED	-	OPTIMIZED	OPTIMIZED
SAUER[15]	MARS ORBITER	TITAN III C	JPL	0.68	34-35	0.03	~0.09	300	0.15	1.3 X 4	3D	1971 *	OPTIMIZED	3500	OPTIMIZED	OPTIMIZED	OPTIMIZED	OPTIMIZED
STRACK, ZOLA[8]	PLANET FLYBY AND ORBITER	SEVERAL	STRACK	0.67	34	0.10	0.10	300	0.20	2 X 200	2D	OPEN	OPTIMIZED	OPTIMIZED	OPTIMIZED	OPTIMIZED	OPTIMIZED	OPTIMIZED
ZOLA (1968)[10]	OUTER PLANET FLYBY, ORBITER	SLV3C/CENTAUR	STRACK	0.60	31	0.10	0.10	300	0.20	2 X 200	2D	OPEN	11.1	4500	OPTIMIZED	OPTIMIZED	OPTIMIZED	< 800 DAYS
ZOLA (1969)[20]	PLANET FLYBY AND ORBITER	SLV3C/CENTAUR	STRACK	0.68	34	0.10	0.10	300	0.20	2 X 200	2D	OPEN	OPTIMIZED	OPTIMIZED	OPTIMIZED	OPTIMIZED	OPTIMIZED	OPTIMIZED
HORSEWOOD[19]	PLANET FLYBY AND ORBITER	SEVERAL	JPL	0.68	30	0.03	0	300	0.111	2 X 38	2D	OPEN	OPTIMIZED	OPTIMIZED	OPTIMIZED	OPTIMIZED	OPTIMIZED	OPTIMIZED
MEISSINGER, PARK[5]	AREA MISSIONS	ATLAS/BII	HUGHES	0.57	34	0	0	-	-	-	2D, 3D	OPEN	3	4500	OPTIMIZED	-	FIXED	CONSTRAINED
STRACK[3]	SOLAR PROBE	SATURN 1B/CENTAUR	STRACK	0.66	34	0.10	0.10	-	-	-	2D	OPEN	OPTIMIZED	OPTIMIZED	OPTIMIZED	-	OPTIMIZED	OPTIMIZED
TRW (1967)[7]	OUT-OF-ECLIPTIC	-	CONSTANT	0.62	-	0	0	-	-	-	3D	OPEN	PARAMETRIC	PARAMETRIC	PARAMETRIC	-	FIXED	PARAMETRIC
RAMLER[4]	EARTH ORBIT RAISING	-	CONSTANT	-	-	0	0	-	-	-	3D	OPEN *	ACCELERATION PARAMETRIC		-	-	FIXED	CONTINUOUS
READER, REGETZ[21]	SYNCHRONOUS SATELLITE	TAT/DELTA	CONSTANT	0.80	30	0	0	-	-	EARTH SYNCHRONOUS	3D	1975 (OPEN)	9.0	3000	-	-	FIXED	< 200 DAYS
MEISSINGER, GREENSTADT[9]	GEOMAGNETIC TAIL REGION	ATLAS/BII	CONSTANT	0.65	33	0	0	-	-	2 X 200	2D	OPEN	2.3	3500	NEAR-ESCAPE	-	FIXED	APOGEE COAST
NAR[27]	ASTEROID BELT	SLV3C/CENTAUR	JPL	0.69	28	0	0	-	-	-	2D	1975 (OPEN)*	7.8	3500	OPTIMIZED	-	NEAR-OPTIMUM	210 DAYS
TRW (1970)[28]	MULTI-MISSION	SLV3C/CENTAUR	JPL	0.69	30-32	0	0	-	-	-	2D	1975 (OPEN)*	5.1	3200	OPTIMIZED	-	NEAR-OPTIMUM	< 550 DAYS
IITRI[23]	COMET RENDEZVOUS	TITAN CLASS	STRACK	0.68	30	0.06	0	-	-	-	3D	SEVERAL *	NEAR-OPTIMUM	NEAR-OPTIMUM	NEAR-OPTIMUM	0	OPTIMIZED	OPTIMIZED

* LAUNCH WINDOW CONSIDERATIONS

the exact sense. Details of the optimum trajectory profiles, for different input parameters, are not identical. However, for the purpose of estimating near-optimum values of net spacecraft mass, it turns out that there are many situations of interest where this assumption is justified for the accuracy needed.

Input parameters for which scaling is provided include: launch vehicle selection, propulsion system specific mass and efficiency, tankage and structure factors, and, in the case of planet orbiter missions, orbit size and retro system specific impulse and inert fraction. Of these inputs, the most significant ones for parametric mission analysis are launch vehicle, specific mass and orbit size. This implies that these quantities are most subject to selection variations or technology changes.

In the case of launch vehicle scaling alone, the scaling law (A→ B) for net mass m_n and power P_o is simply

$$\frac{m_{nB}}{m_{nA}} = \frac{P_{oB}}{P_{oA}} = \frac{m_{oB}}{m_{oA}}$$

where the subscripts A and B refer to the two different vehicles. In determining m_{oB}, it must be assumed that the same value of launch hyperbolic velocity applies to both cases, i.e., $V_{hL,B} = V_{hL,A}$. Hence scaling accuracy depends upon the condition that both launch vehicle trajectories would optimize at the same value of velocity, or nearly so. This condition is substantially true in the case of indirect trajectories so that even the Atlas/Centaur and Titan IIIX/Centaur vehicles could be scaled with fair results. However, for direct trajectories, the Titan IIIX/Centaur mission would actually optimize at a significantly higher value of V_{hL} than would the Atlas/Centaur. The scaling results would therefore be largely inaccurate; i.e., the scaled value of m_{nB} would be much less than the

optimum m_{nB}. Appendix A presents further details on the conditions required for accurate launch vehicle scaling.

Scaling of specific mass is found to be valid providing that the change in α_{ps} is within $\pm$ 25 percent. Orbit size scaling is found to be surprisingly accurate over a very wide range of periapse and apoapse distances.

5.2 Comparison of Multiple Study Results

A number of different studies have reported SEP performance results for outer planet missions, particularly Jupiter missions. This data will be used here for purposes of comparison. The scaling laws given in Appendix A are used to transform the diverse input parameter assumptions to the common parameter set:

Titan IIIC

$\alpha_{ps} = 30$ kg/kw

$k_p = 0.03$

$k_o = 0$

$\eta = \dfrac{0.769}{1+\left(\dfrac{14.3}{c}\right)^2}$; $c = g_o I_{sp}$, km/sec

Orbiter

$r_p = 2$ planet radii

$r_a = 38$ planet radii

$I_{sc} = 300$ sec

$k_r = 0.111$

This parameter set is employed in the recent AMA study[19] which reports the largest data base for SEP planetary missions that is available in the literature. Also, the parameter values are thought to be representative of current technology. A point of clarification is in order here before discussing the comparison of results. When other studies do not agree

with the AMA results it should not be implied that these other results are wrong or necessarily less accurate. It must be remembered firstly that scaling is not perfectly accurate, and secondly that scaling cannot account for certain parameter differences (e.g., solar power curve). Our purpose in this section will be served if several study results are shown to be in general agreement ($\pm$ 10%), or if reasons for certain differences can be explained.

Figure 5-1 compares the results of five independent trajectory analyses of the Jupiter flyby mission. Table 5-1 may be referred to for the original parameter conditions assumed in each study. The comparison shows excellent agreement between the AMA[19] and JPL[12] data, and generally good agreement between each of the different studies. The two LeRC[10] data points at a flight time of 1000 days are based on a propulsion time constraint that was imposed in that study. A somewhat lower value of net mass would be expected. The largest differences are associated with the Princeton[14] and Hughes[2] data. Both of these studies employed the same solar power curve and propulsion efficiency curve. With reference to Figure 4-1, it is noted that the Hughes power curve is, relatively, the most conservative of the three. This difference is significant enough to account for the apparent discrepancies shown in Figure 5-1. Also, a specific launch year is assumed in the Hughes study rather than circular, coplanar orbits.

Figure 5-2 compares the AMA and LeRC[20] data for flyby missions to the outer planets. No propulsion time constraint was imposed in this LeRC study. In general, the two studies would have to be said to be in good agreement. Differences may be attributed to inexact scaling and different solar power curves. It is not clearly understood, however, why the LeRC data point for the 2000 day Saturn flyby lies above the reference curve. These two studies are also compared in Figure 5-3 for outer planet orbiter missions.

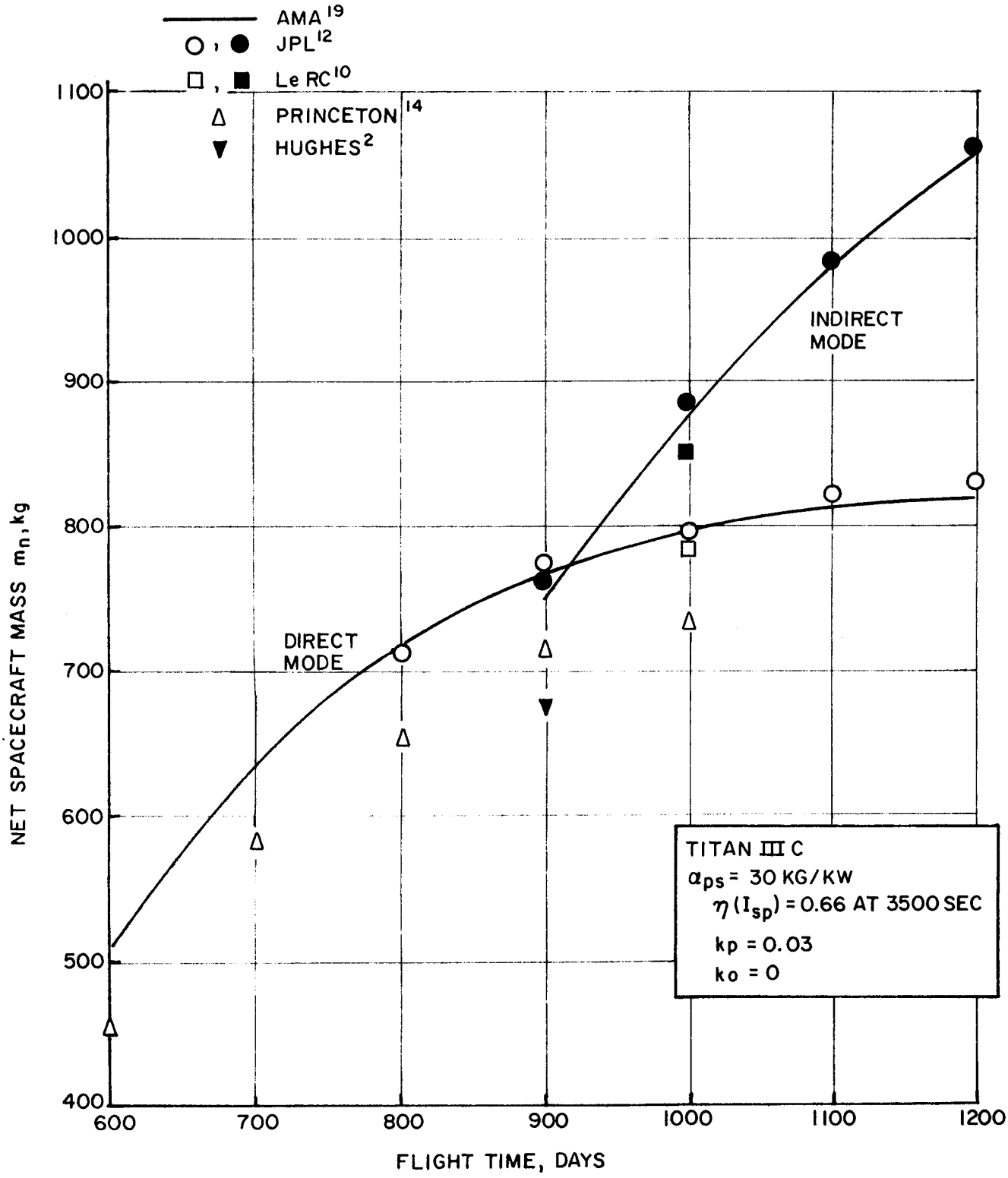

FIGURE 5-1. COMPARISON OF SEP JUPITER FLYBY DATA SCALED TO REFERENCE(AMA)INPUT PARAMETERS.

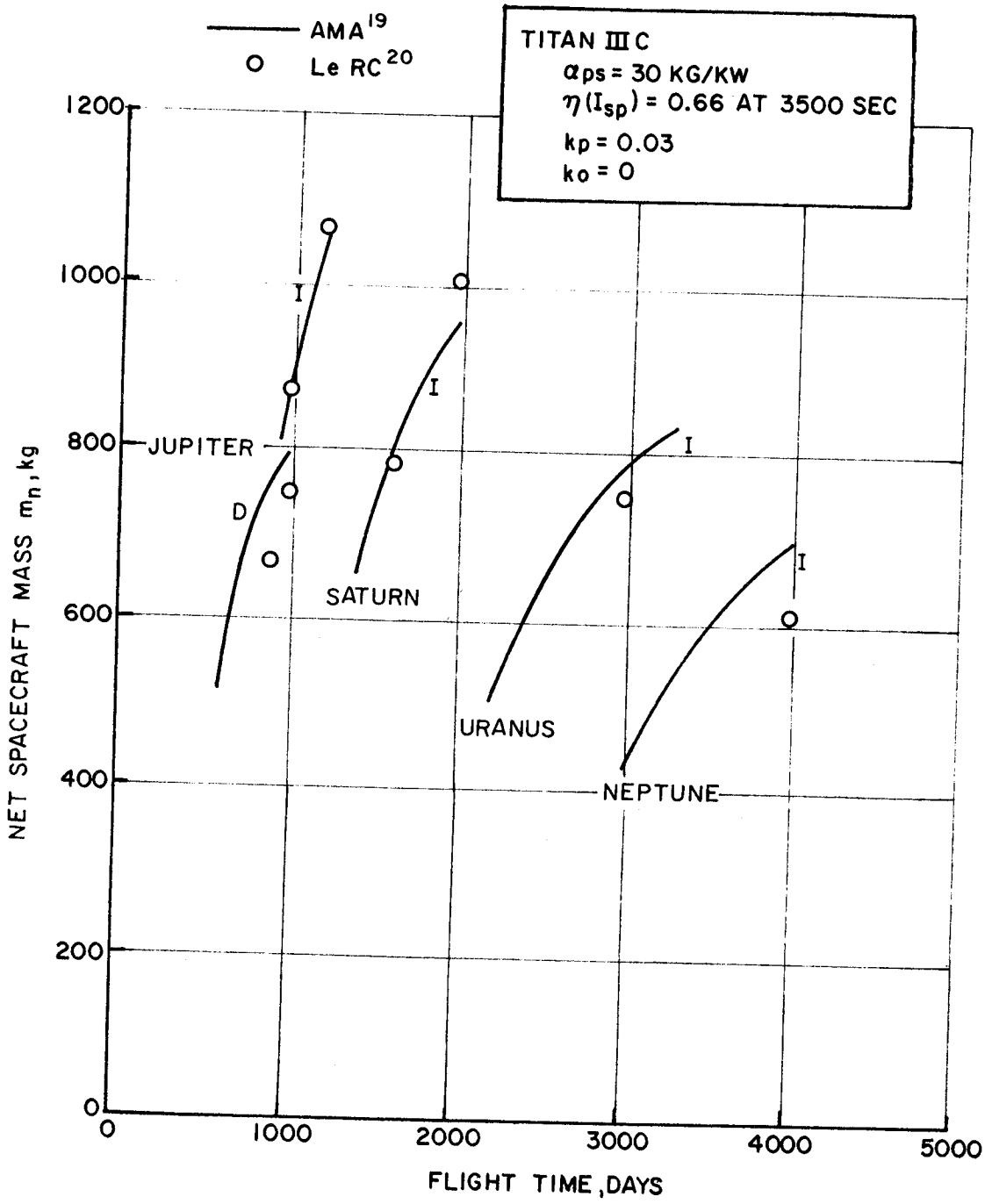

FIGURE 5-2. COMPARISON OF SEP OUTER PLANET FLYBY DATA SCALED TO REFERENCE (AMA) INPUT PARAMETERS.

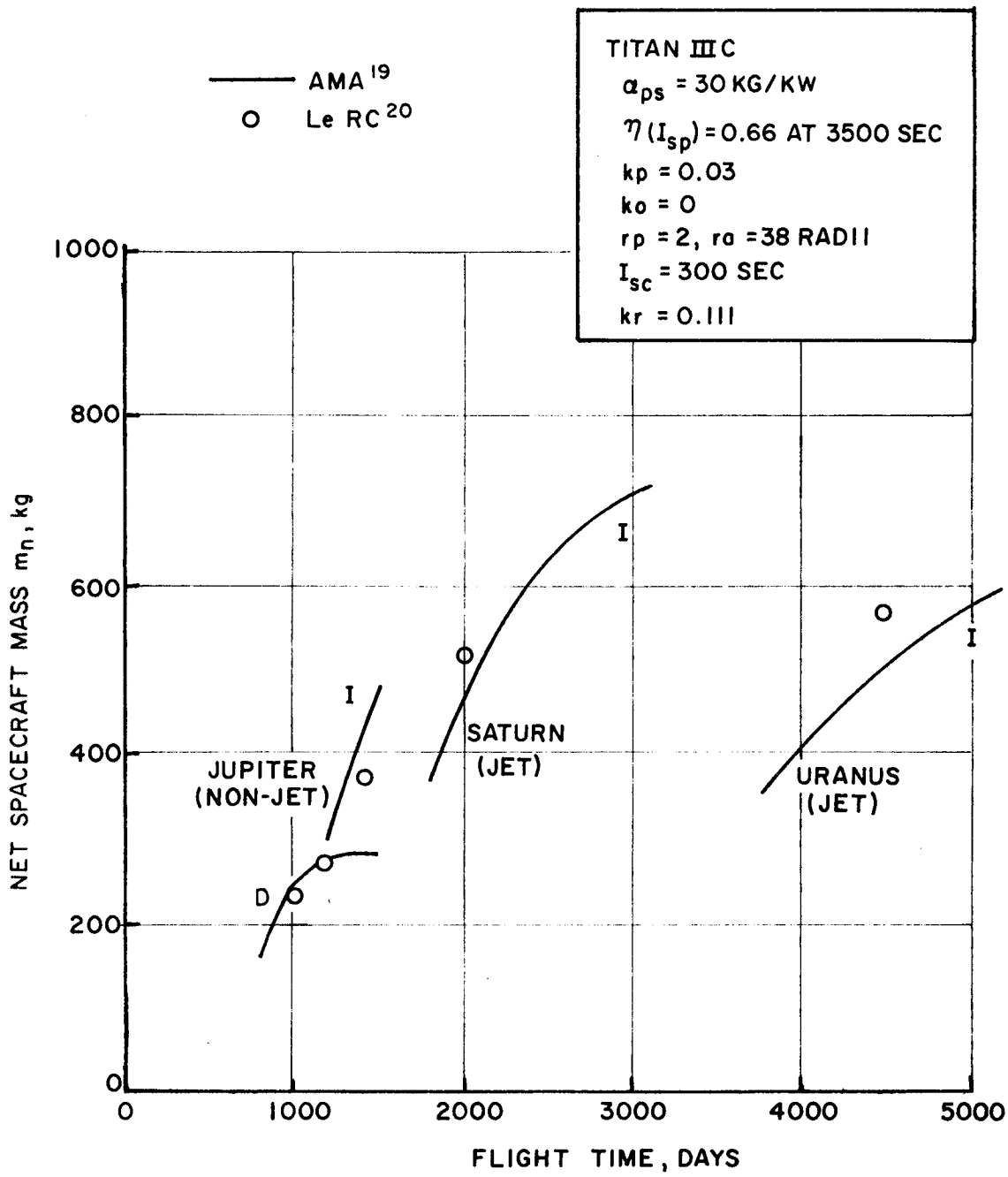

FIGURE 5-3. COMPARISON OF SEP OUTER PLANET ORBITER DATA SCALED TO REFERENCE (AMA) INPUT PARAMETERS.

A final comparison is made with data recently computed by Sauer* for a Jupiter orbiter mission, direct mode, with propulsion system jettisoning, and employing the Titan IIIX(1205)/Centaur launch vehicle. The original orbit size in Sauer's data is 4 x 38 planet radii; otherwise the input parameter set is the same as listed above. This example of orbit size scaling gives the following comparative results:

t_f	m_n (AMA)	m_n (Sauer, scaled)
800 days	1096 kg	1094
900	1204	1204
1000	1265	1264
1200	1304	1305
1400	1291	1284

Two conclusions are apparent from this comparison exercise. First, it is evident that a number of different organizations involved in SEP mission analysis have independent trajectory computer programs which, essentially, check one another and provide accurate results. Secondly, when published results of previous studies appear not to agree, the explanation usually lies with the fact that different study ground rules or input parameters were assumed. The performance scaling laws presented in this report are found to be helpful in understanding these apparent discrepancies.

5.3 SEP Capabilities for Solar System Missions

This section presents extensive graphical performance data for SEP missions to the planets, asteroids, comets and other solar system regions. This data is given in the form of net spacecraft mass versus flight time for several launch vehicle candidates. Unless otherwise stated, the input parameter set given in Section 5.2 has been used consistently.

*C. Sauer, JPL, private communication.

Also, unless otherwise noted, the results correspond to a complete optimization of trajectory and propulsion system parameters. The trajectory model assumed is two dimensional except in the case of out-of-the-ecliptic and comet rendezvous missions. Ballistic and SEP flight modes are compared for each of the mission applications. One basis for comparison is the same launch vehicle assumption for both ballistic and SEP flight modes. The currently planned Burner II (2300) is used as the ballistic upper stage example. In some cases a smaller launch vehicle is also shown for the SEP application. It should be noted that launch vehicle performance is based on the 1969 OSSA Estimating Factors Handbook. Launch vehicle size is generally limited here to the currently programmed Titan IIIX(1205)/Centaur (5 segment solid strapons). Net spacecraft mass in the ballistic case is equivalent to the entire ballistic spacecraft delivered to the target, whereas in the SEP case net mass does not include the power or thrust subsystems. Also, a zero launch window is assumed. Each of the above factors in the comparison tends to give a relative performance advantage to the ballistic flight mode.

5.3.1 Planet Flyby Missions

SEP capability for planet flybys is shown in Figure 5-4 and Figure 5-5, respectively, for the Titan IIIC and Titan IIIX(1205)/Centaur launch vehicles. The asteroid Ceres, at a mean distance of 2.77 a.u., is also included but no data is given for Pluto. Both the direct and indirect flight modes are shown where applicable (outer planets). Supporting data on the optimum power P_o for each of the mission examples is given in Figures 5-6 and 5-7. In general, P_o increases with flight time for the direct mode and decreases for the indirect mode. The payload capability of smaller launch vehicles for outer planet missions is improved significantly by using the indirect flight mode. For example, the

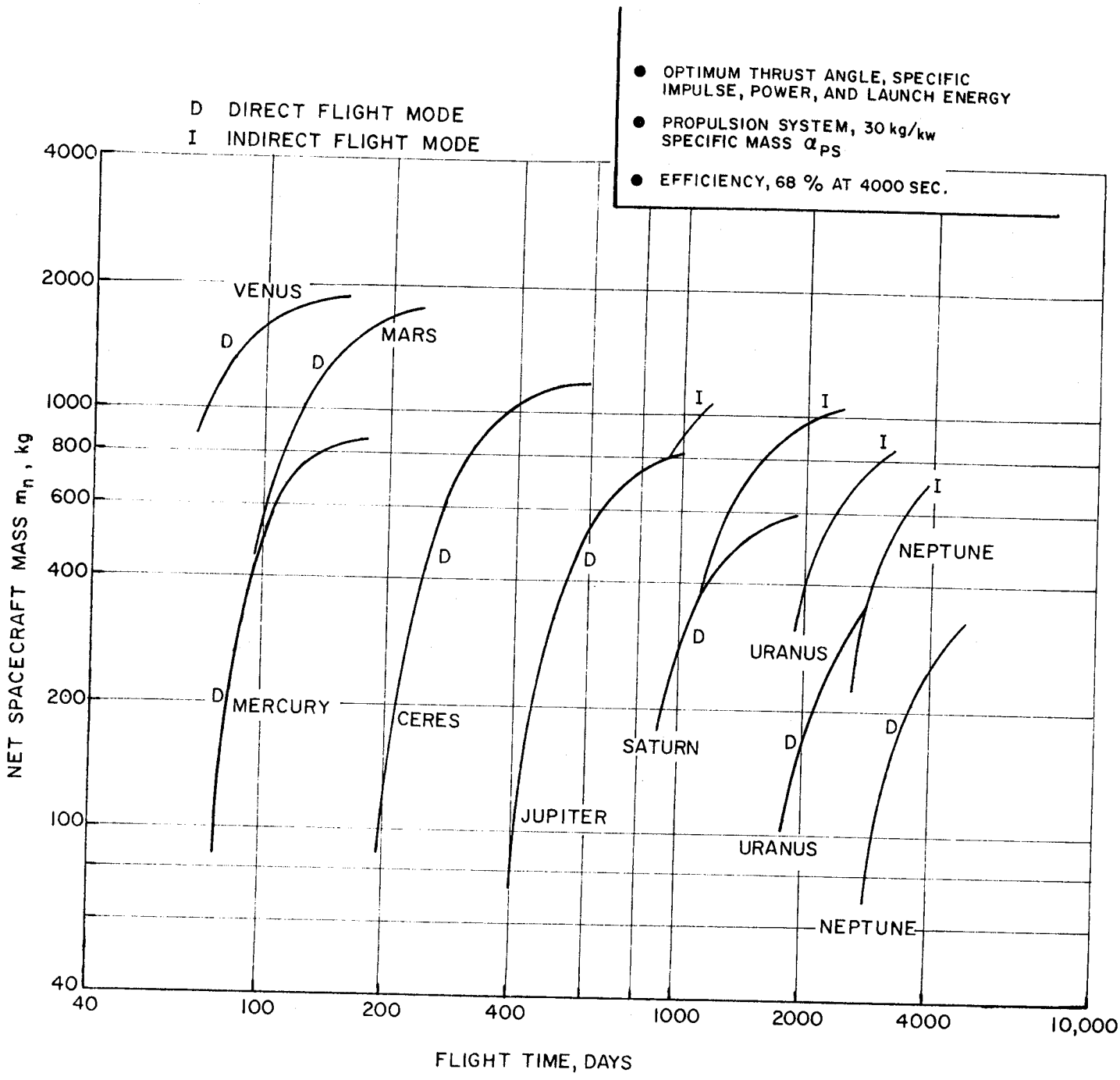

FIGURE 5-4. SOLAR-ELECTRIC PROPULSION CAPABILITY FOR PLANET FLYBYS, TITAN III C LAUNCH VEHICLE. (DATA FROM HORSEWOOD[19])

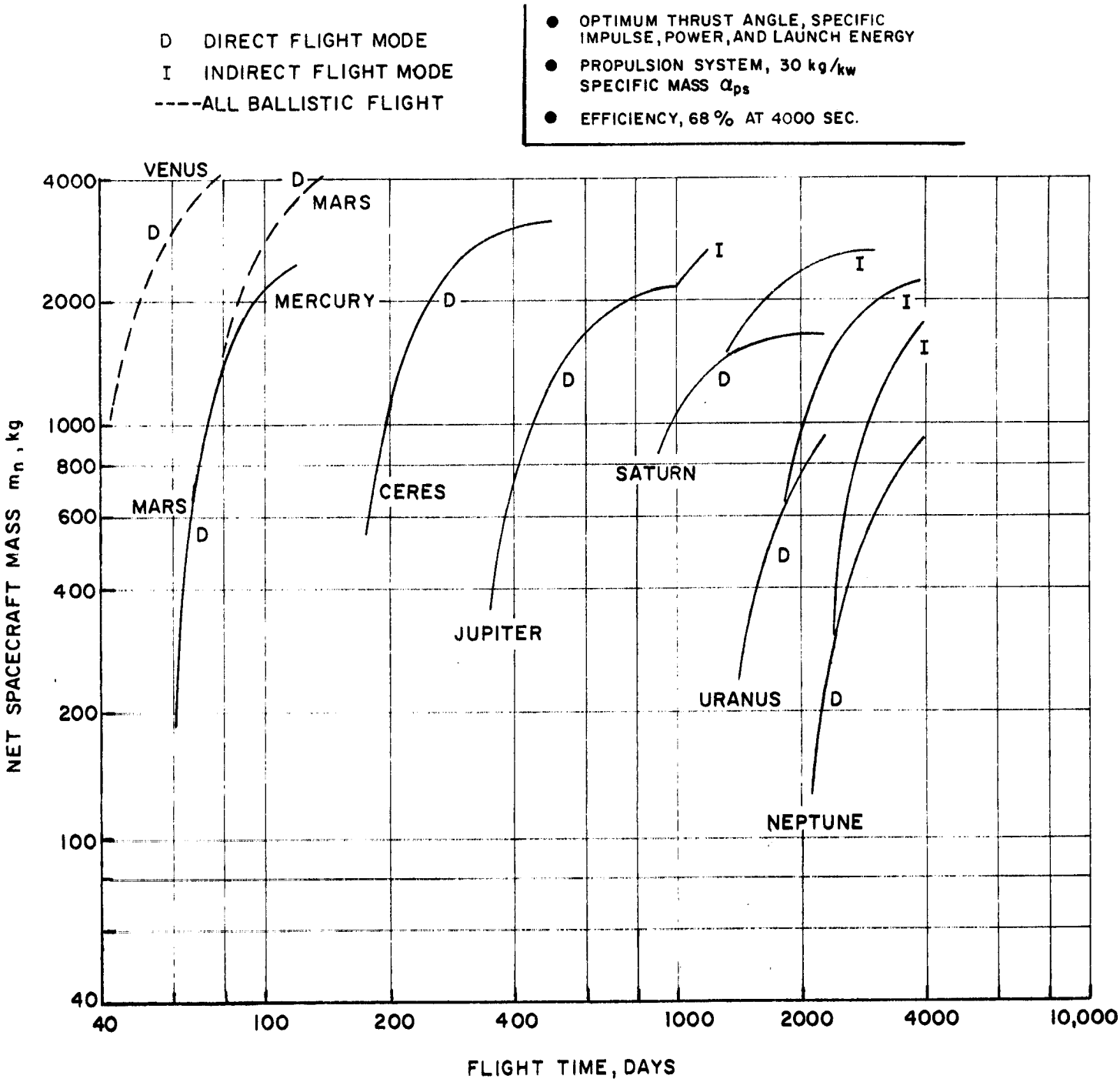

FIGURE 5-5. SOLAR-ELECTRIC PROPULSION CAPABILITY FOR PLANET FLYBYS, TITAN III X (1205)/ CENTAUR LAUNCH VEHICLE. (DATA FROM HORSEWOOD[19]).

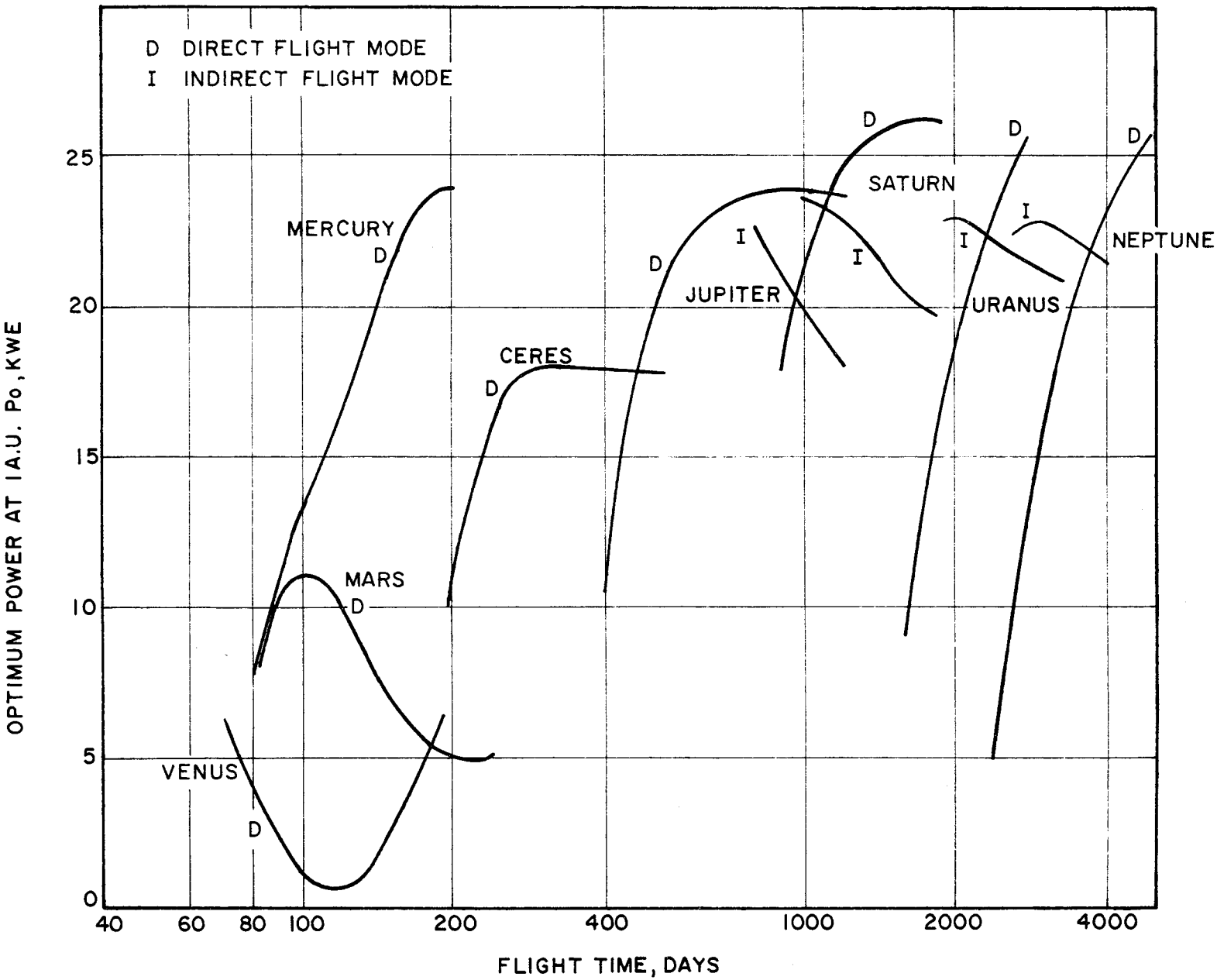

FIGURE 5-6. OPTIMUM POWER FOR SOLAR-ELECTRIC PLANET FLYBYS, TITAN IIIC LAUNCH VEHICLE. (DATA FROM HORSEWOOD[19])

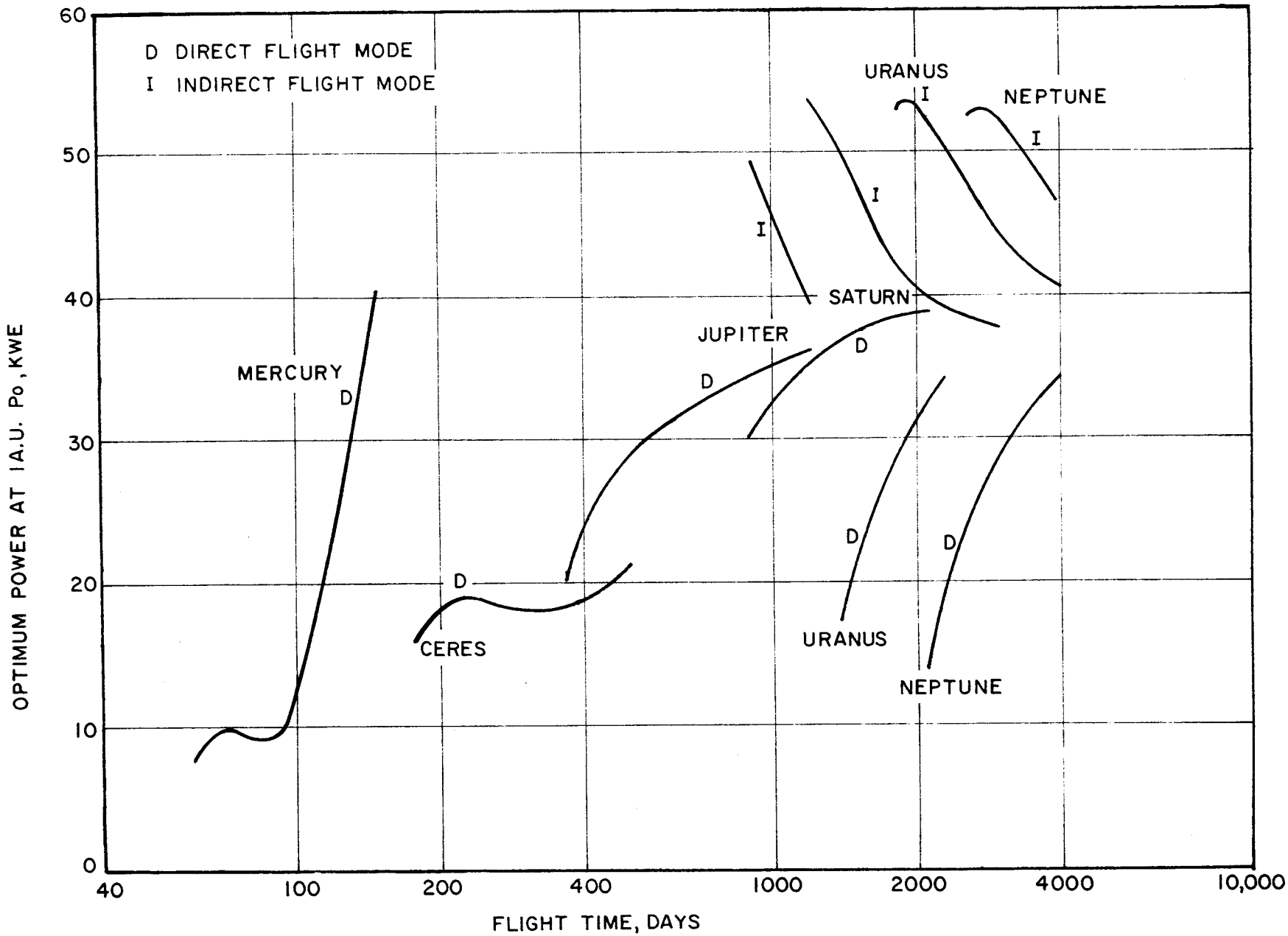

FIGURE 5-7. OPTIMUM POWER FOR SOLAR-ELECTRIC PLANET FLYBYS, TITAN IIIX(1205)/CENTAUR LAUNCH VEHICLE. (DATA FROM HORSEWOOD[19])

Titan IIIC can deliver 500 kg to Uranus and Neptune in flight times of 2200 days and 3200 days, respectively.

Figure 5-8 compares ballistic and SEP performance for outer planet flyby missions. Considering a payload capability of at least 450 kg, the SEP flight mode is found to give significantly shorter flight times for missions to Uranus and Neptune but less so for missions to Jupiter and Saturn. The ballistic mode is, of course, preferable for flybys of the inner planets. SEP flyby missions to the outer planets utilizing a Jupiter swingby (gravity-assist) have been investigated by Flandro.[11] It was shown that the Titan IIIX(1205)/Centaur/SEP could deliver substantially higher payloads than the ballistic mode (Burner II upper stage), or the same payload in greatly reduced flight time. For example, taking a 650 kg spacecraft delivered on the Earth-Jupiter-Saturn-Pluto Grand Tour in 1977, the SEP flight time is only 6 years whereas the all-ballistic flight time is 8.5 years.

5.3.2 Planet Orbiter Missions

Presented in Figures 5-9 to 5-12 is the SEP capability for performing planet orbiter missions, again based on the two Titan class launch vehicles. The orbit size assumed is 2 x 38 planet radii (except for Ceres rendezvous), and the chemical retro system is representative of current (Earth-storable propellant) technology. The solar power source is taken into orbit about the inner planets because of its obvious utility at close distances to the Sun. It may also be used at Jupiter, but doubtfully at Saturn or beyond. In terms of net spacecraft mass, there is a clear advantage to jettisoning the entire electric propulsion system prior to orbit insertion. This is the only case considered for Uranus and Neptune orbiters. It will be noted that for the shorter flights to Venus and Mars there is no advantage to adding the SEP upper stage to the launch vehicle; i.e., $P_o = 0$ is optimum. The

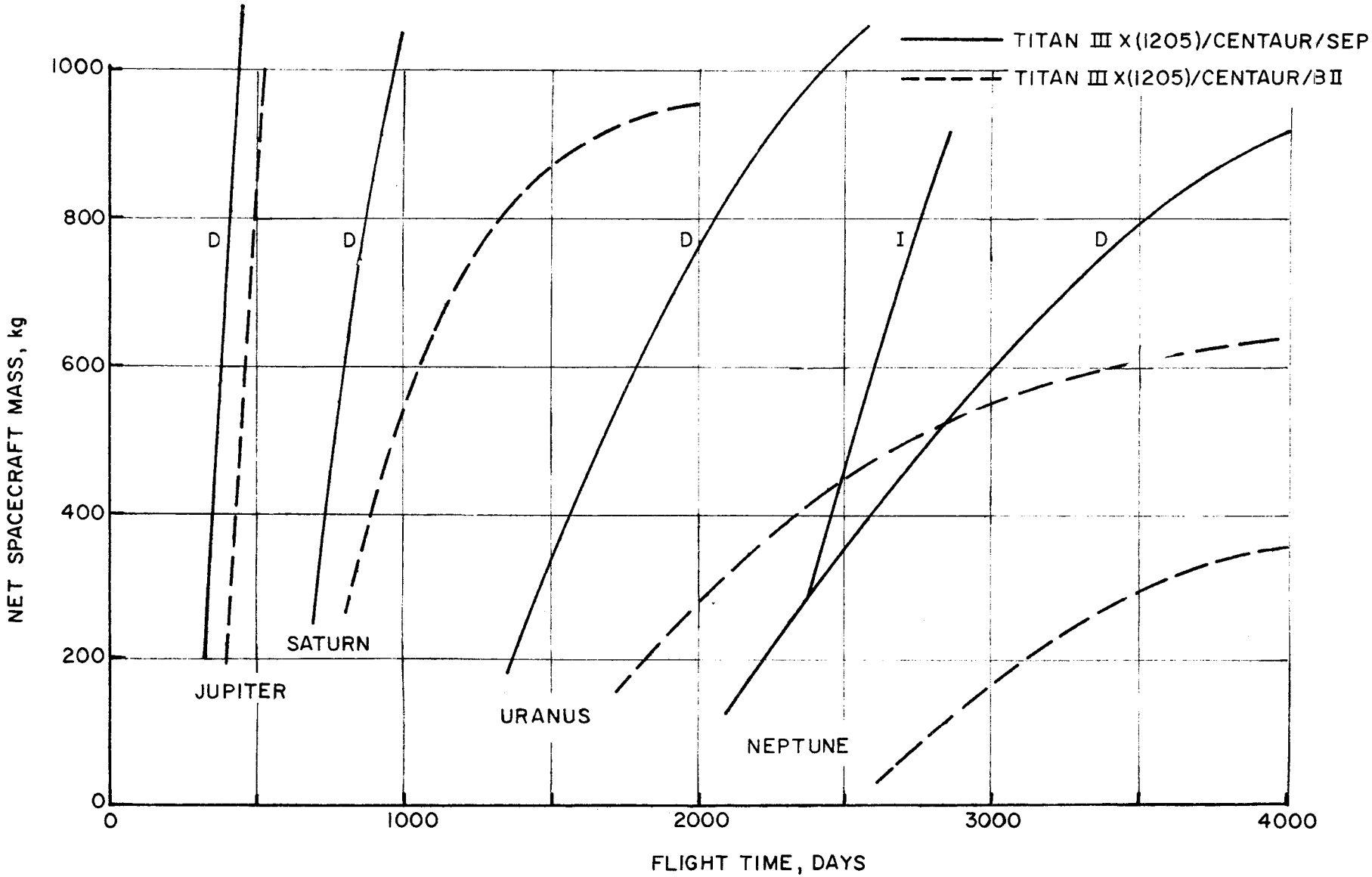

FIGURE 5-8. PERFORMANCE COMPARISON OF BALLISTIC AND SEP FLIGHT MODES FOR OUTER PLANET FLYBYS.

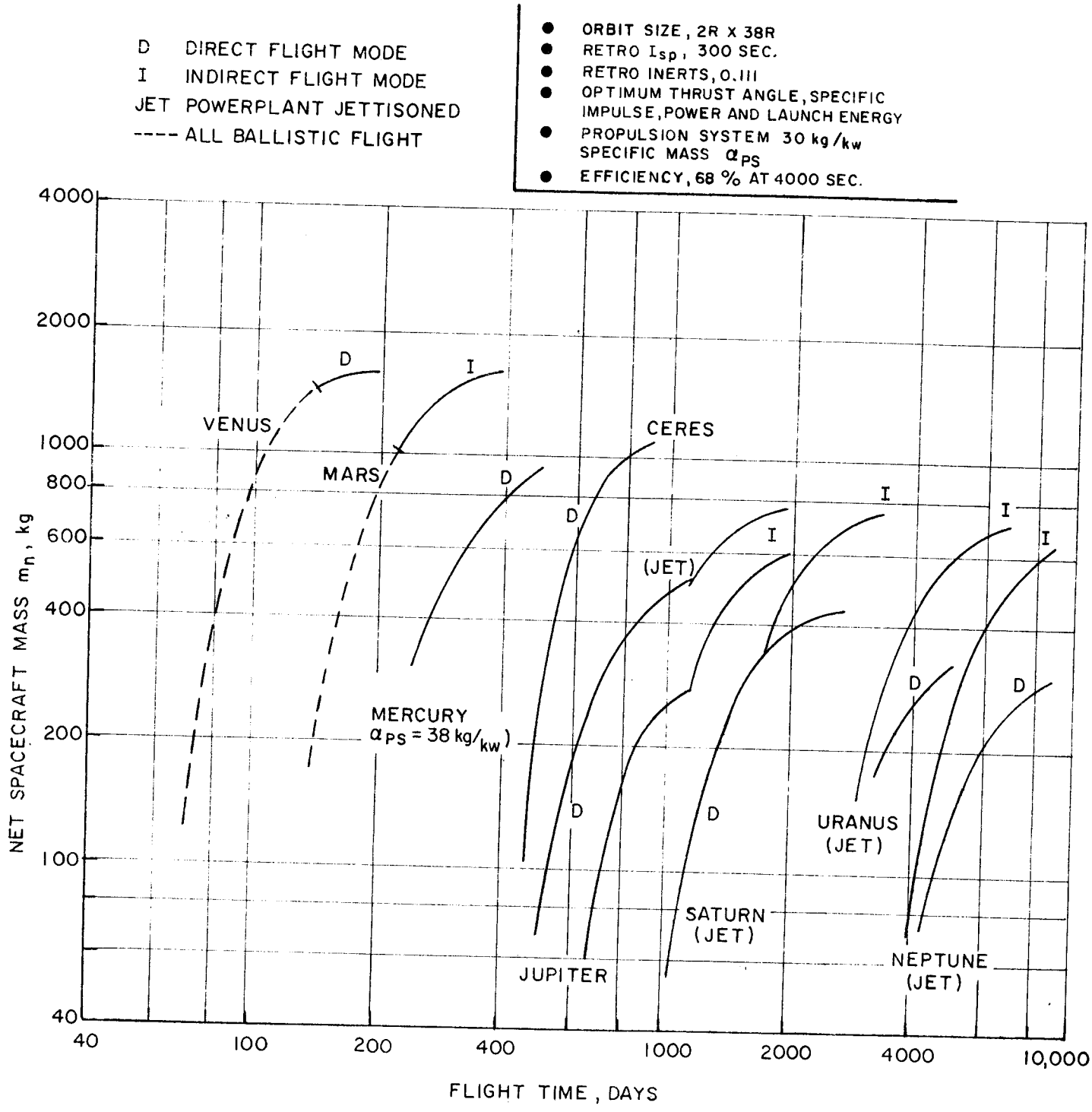

FIGURE 5-9. SOLAR-ELECTRIC PROPULSION CAPABILITY FOR PLANET ORBITERS, TITAN III C LAUNCH VEHICLE. (DATA FROM HORSEWOOD[19]).

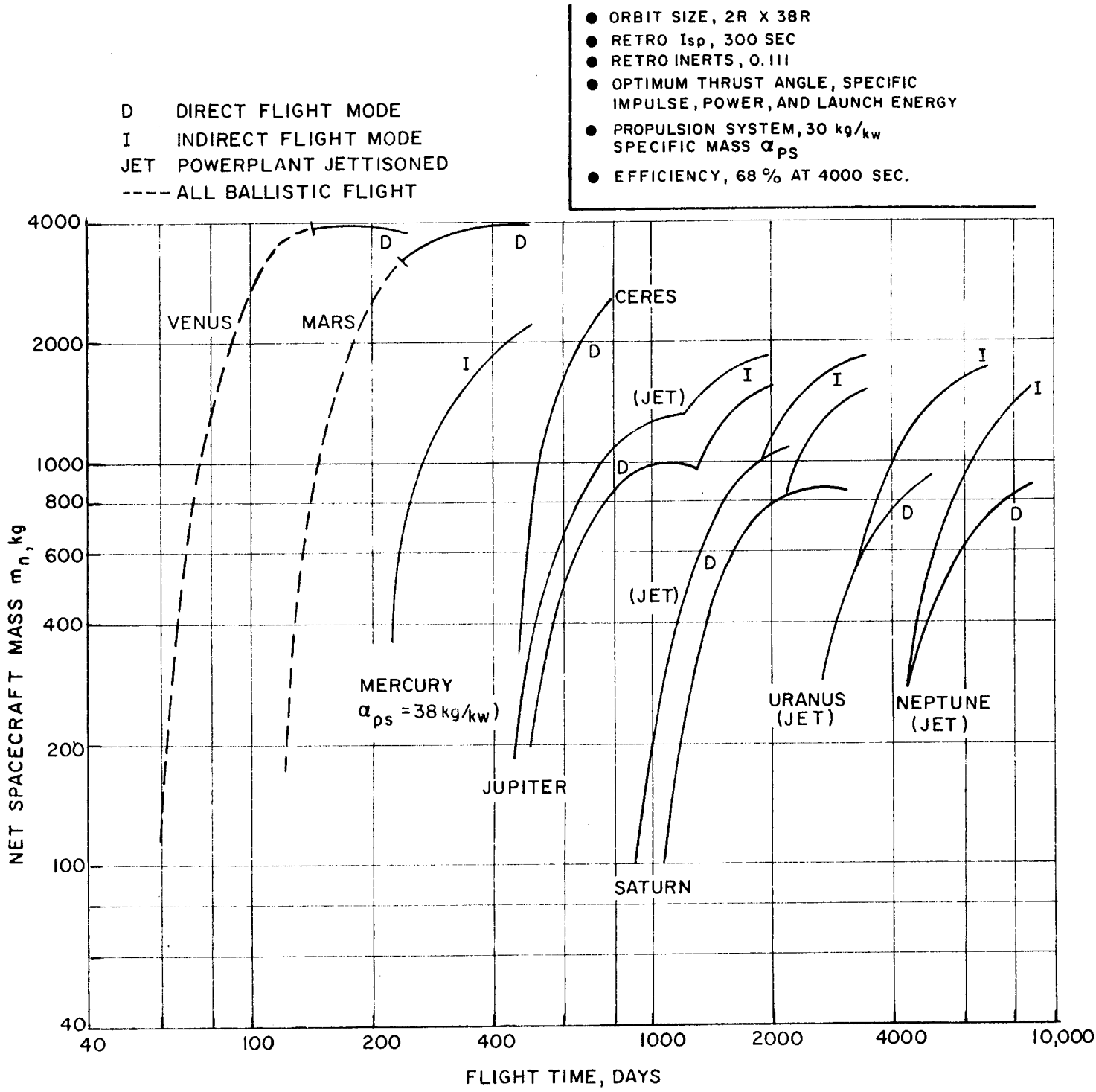

FIGURE 5-10. SOLAR-ELECTRIC PROPULSION CAPABILITY FOR PLANET ORBITERS, TITAN IIIX(1205)/CENTAUR LAUNCH VEHICLE. (DATA FROM HORSEWOOD[19]).

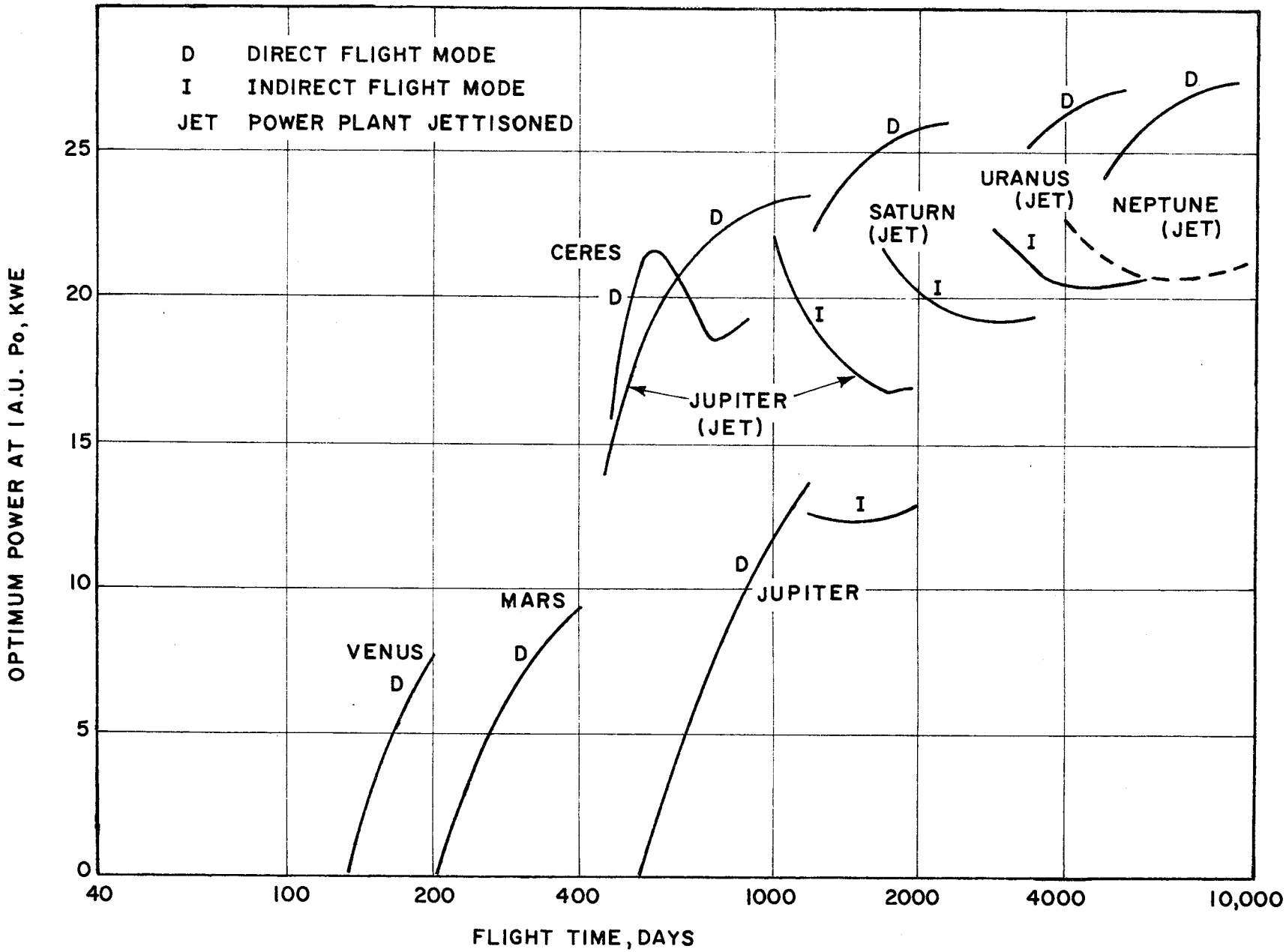

FIGURE 5-11. OPTIMUM POWER FOR SOLAR-ELECTRIC PLANET ORBITERS, TITAN III C LAUNCH VEHICLE. (DATA FROM HORSEWOOD[19])

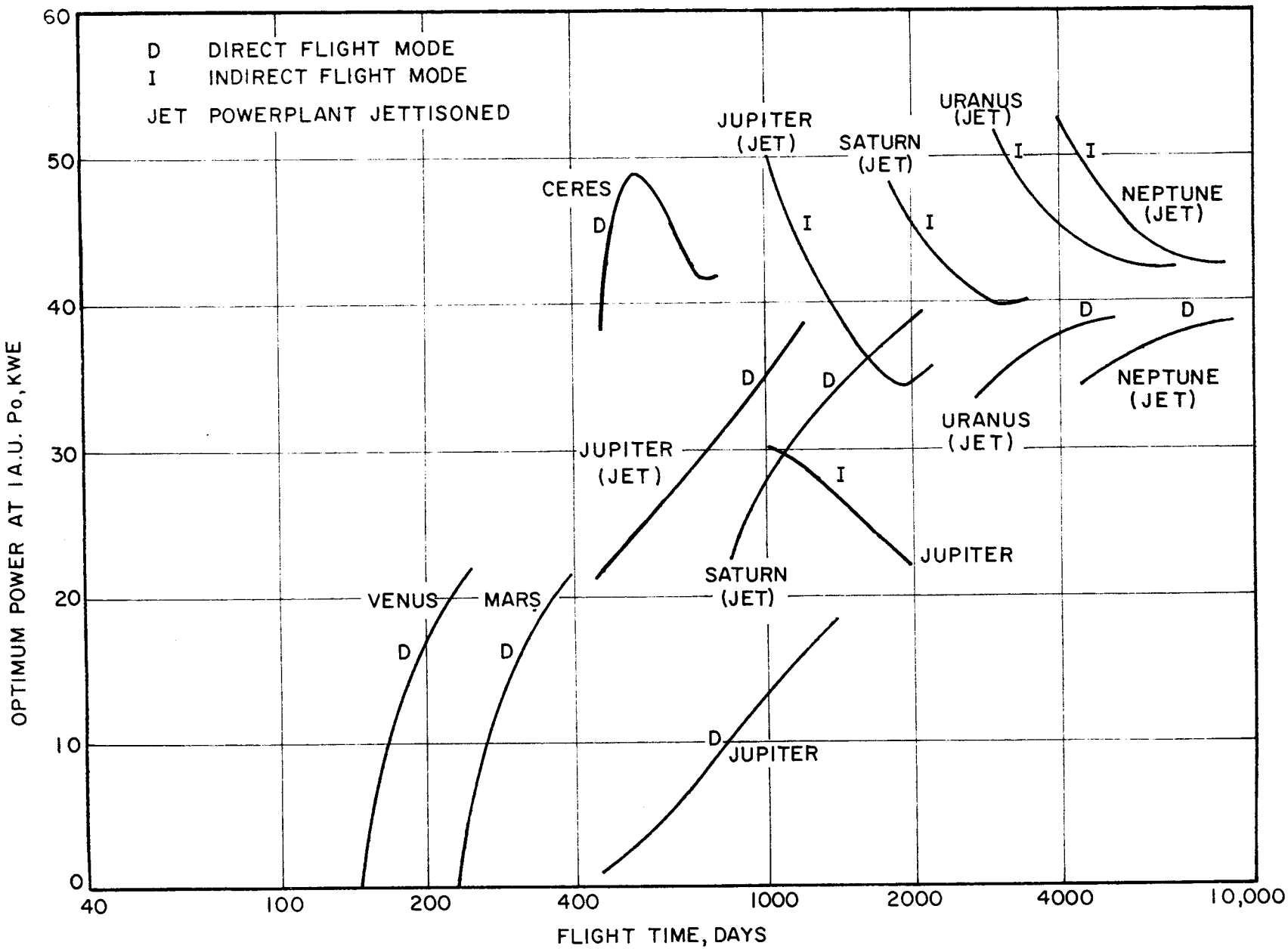

FIGURE 5-12. OPTIMUM POWER FOR SOLAR-ELECTRIC PLANET ORBITERS, TITAN III X (1205)/CENTAUR LAUNCH VEHICLE. (DATA FROM HORSEWOOD[19])

specific mass is increased to 38 kg/kw in the case of Mercury orbiters because of the required increase in thruster power rating (above that at 1 a.u.) for operations at close solar distances. Also, additional solar array mass is needed to handle the thermal control problem. The solar array is assumed to be taken into orbit about Mercury. Substantial amounts of power would be available in theory. However, the effect of high temperatures on the solar array may seriously limit the power availability in Mercury orbit. This question will have to be given careful attention in any future SEP spacecraft design study for this mission application.

A comparison of ballistic and SEP orbiters of Venus and Mars is shown in Figure 5-13. The Titan IIIC/BII is assumed for the ballistic mission and compared to the Titan IIIC/SEP capability. An orbiting spacecraft of 1000-1500 kg is probably a reasonable requirement for high data-rate mapping missions. The SEP mode offers no particular advantage in the case of the nominal 2 x 38 orbit. However, its utility for these missions might be increased if tighter orbits are specified or if extensive orbit maneuvers such as plane changes are desired. The Mercury mission is not shown in this graph because there is no reasonable basis for comparison. It has been shown that the Saturn V/Centaur ballistic mission can only deliver about 100 kg to Mercury orbit in the Hohmann flight time of about 100 days. This is a consequence of the high Mercury inclination, high ballistic approach velocities, and little help from the small gravitational field of Mercury. The solar-electric mission does not suffer from these limitations because the trajectory can be shaped to arrive in-plane with very low approach velocities.

Figure 5-14 compares ballistic and SEP orbiter missions to the outer planets assuming the Titan IIIX(1205)/Centaur launch vehicle. Selecting 600 kg as a minimal orbiter design point, it is seen that only at Jupiter would the ballistic

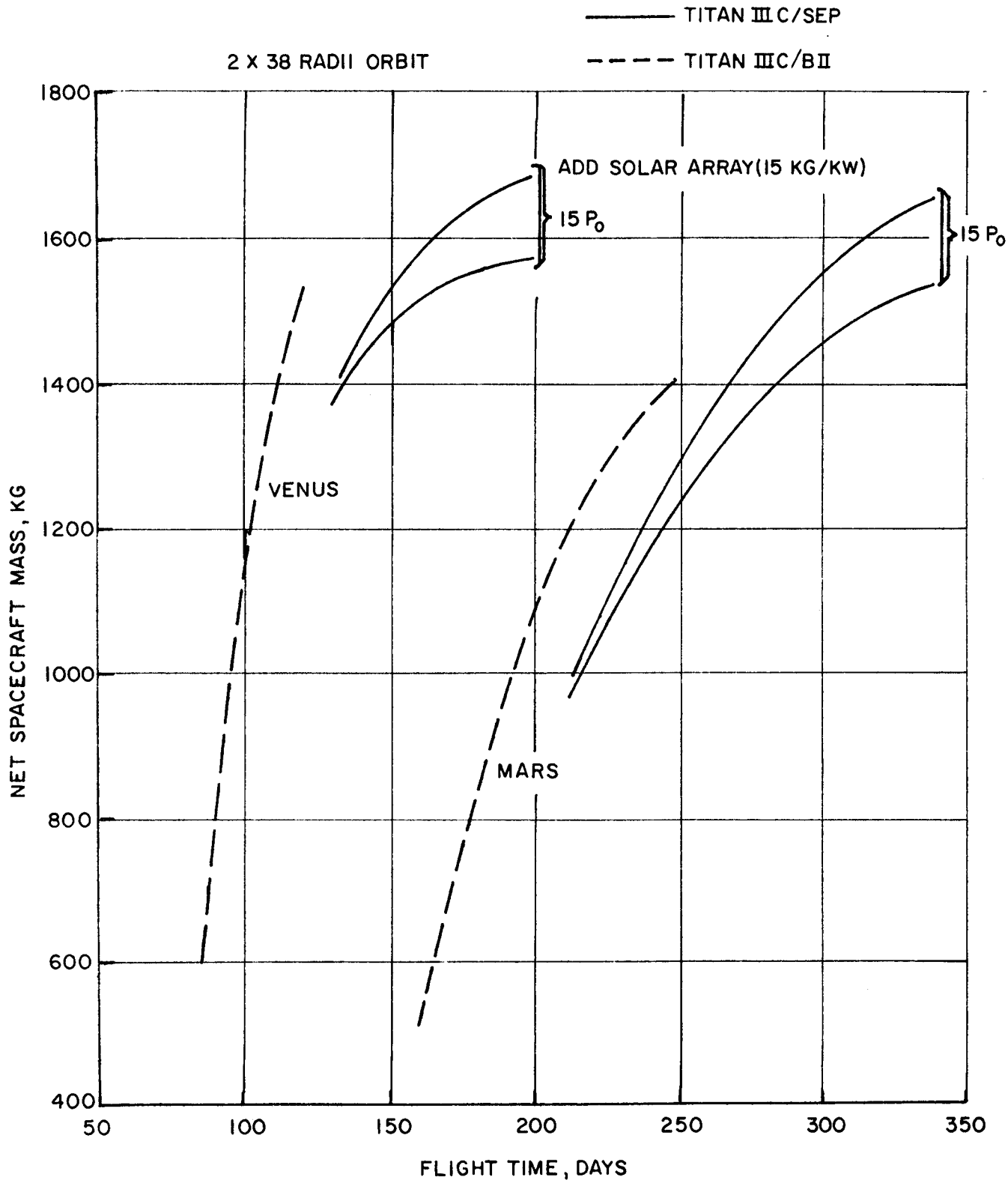

FIGURE 5-13. PERFORMANCE COMPARISON OF BALLISTIC AND SEP FLIGHT MODES FOR ORBITERS OF VENUS AND MARS.

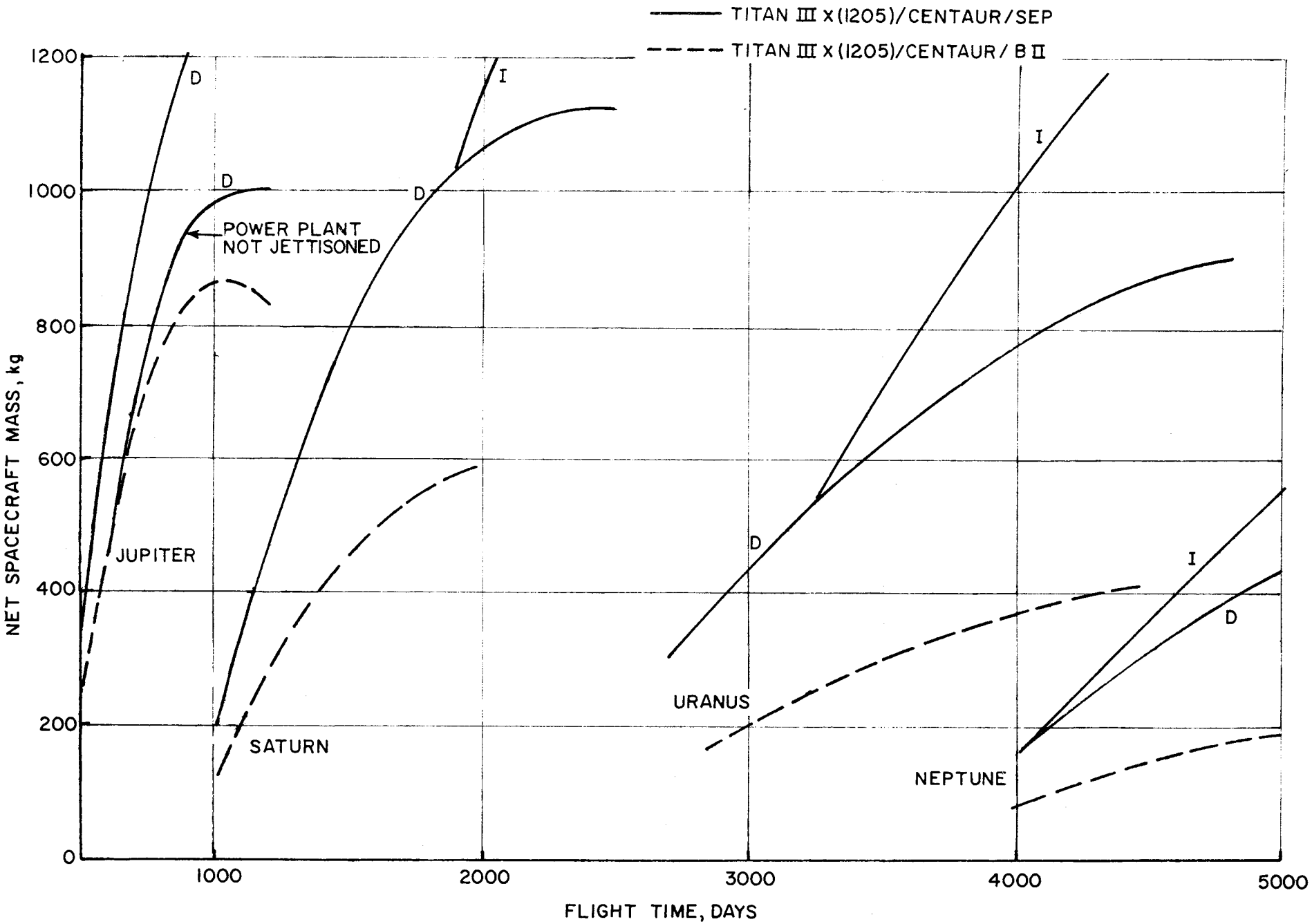

FIGURE 5-14. PERFORMANCE COMPARISON OF BALLISTIC AND SEP FLIGHT MODES FOR OUTER PLANET ORBITERS (2 X 38 PLANET RADII).

approach be adequate without stepping up to a larger launch vehicle. If the Titan IIIX(1207)/Centaur/BII were available, then the 600 kg ballistic missions to Saturn and Uranus could be accomplished in 1400 days and 4200 days, respectively. The SEP mission to Uranus utilizing the (1205) launch vehicle requires a flight time of about 3400 days. The optimum propulsion time for this example is 1930 days, although about one-half of this time is spent thrusting at negligible power levels. Zola[10] has found that a propulsion time constraint of 800-1000 days could be imposed with a resultant payload (net mass) penalty of about 15-20 percent for the Uranus mission. Such a constraint would probably be necessary in order to satisfy thruster lifetime limitations.

Figure 5-15 illustrates the effect of off-optimum power operation for several examples of Jupiter orbiter missions. It has been mentioned that designing for a lower than optimum power level results in a smaller spacecraft configuration and a lower cost. In the case of direct trajectories, the power rating may be reduced to one-half of optimum power with a payload penalty of only 6 percent. For indirect trajectories the payload penalty increases to about 19 percent. These results assume reoptimization of both I_{sp} and V_{hL} for each value of power. This is dictated by the requirement to maintain the thrust acceleration at a near-optimum level. The most sensitive parameter here is V_{hL} which determines the initial spacecraft mass. If I_{sp} were fixed at the value corresponding to $P_{o,opt.}$ a small additional payload penalty would be incurred. The off-optimum power characteristic described for the Jupiter mission applies generally to other missions as well, although the payload penalty will vary somewhat. Typically, the more energetic missions incur a larger payload penalty.

5.3.3 Asteroid Rendezvous

The example of rendezvous with the asteroid Ceres was included in the results of Figures 5-9 and 5-10. In

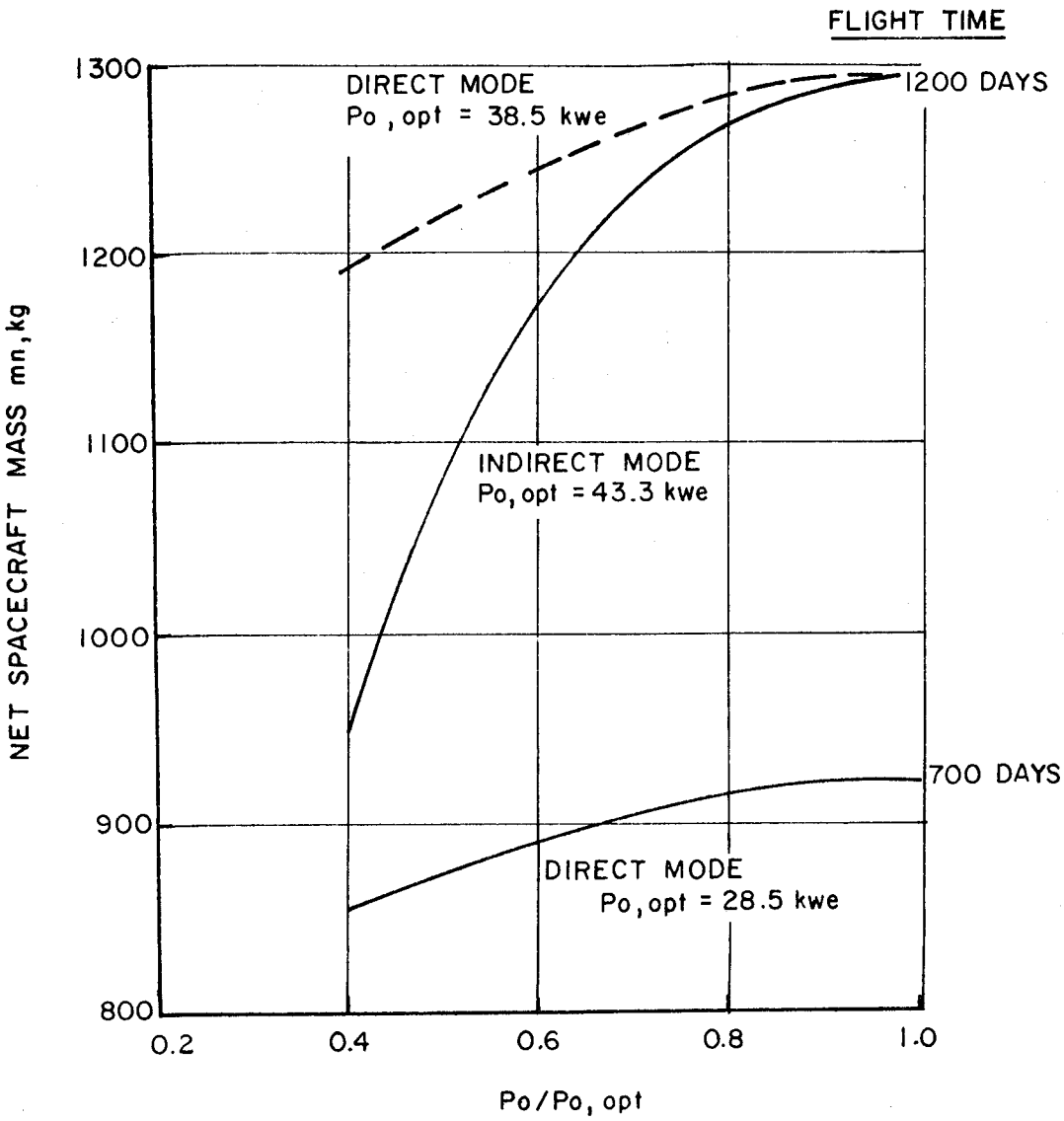

FIGURE 5.15. PAYLOAD LOSS DUE TO OFF-OPTIMUM POWER OPERATION, JUPITER ORBITER (2 X 38 RADII), TITAN III X(1205)/CENTAUR/SEP, PROPULSION SYSTEM JETTISONED.

Figure 5-16 a comparison is made with an equivalent ballistic mission requiring the Titan IIIX(1205)/Centaur/BII. On the basis of flight time alone, the ballistic mission would be adequate if a net spacecraft mass of 420 kg or less were acceptable. The advantage of SEP for this mission would depend upon the need to deliver a larger payload than the maximum ballistic capability.

5.3.4 Comet Rendezvous

The difficulty of comet rendezvous lies in the fact that most periodic comets have high inclination and eccentricity. This results in a high total ΔV requirement if the mission is performed ballistically. A recent study[23] by IIT Research Institute has investigated the feasibility of such missions considering a group of 16 comet rendezvous opportunities in the time period 1975-95. The well known Halley's Comet, due to appear next in 1985-86, is included in this group. Trajectory and payload calculations were performed for both ballistic and low-thrust flight modes. The ballistic mode included 3-impulse direct transfers and Jupiter gravity-assist transfers when applicable. Solar-electric and nuclear-electric low thrust flights were investigated for mission opportunities to four selected comets. Results of this study have demonstrated the superior performance potential of electric propulsion spacecraft for comet rendezvous missions. Advantages include significantly shorter flight times, smaller launch vehicles and/or larger payloads.

Table 5-2 presents a comparison of the different flight modes in terms of launch vehicle and flight time requirements. Payload capability is approximately 450 kg in each case except where noted otherwise. Gravity-assist opportunities are not available for the Encke/80 and Kopff/83 missions, and the 3-impulse mode is not appropriate for the Halley mission because of the excessive velocity requirements. Nuclear-electric results

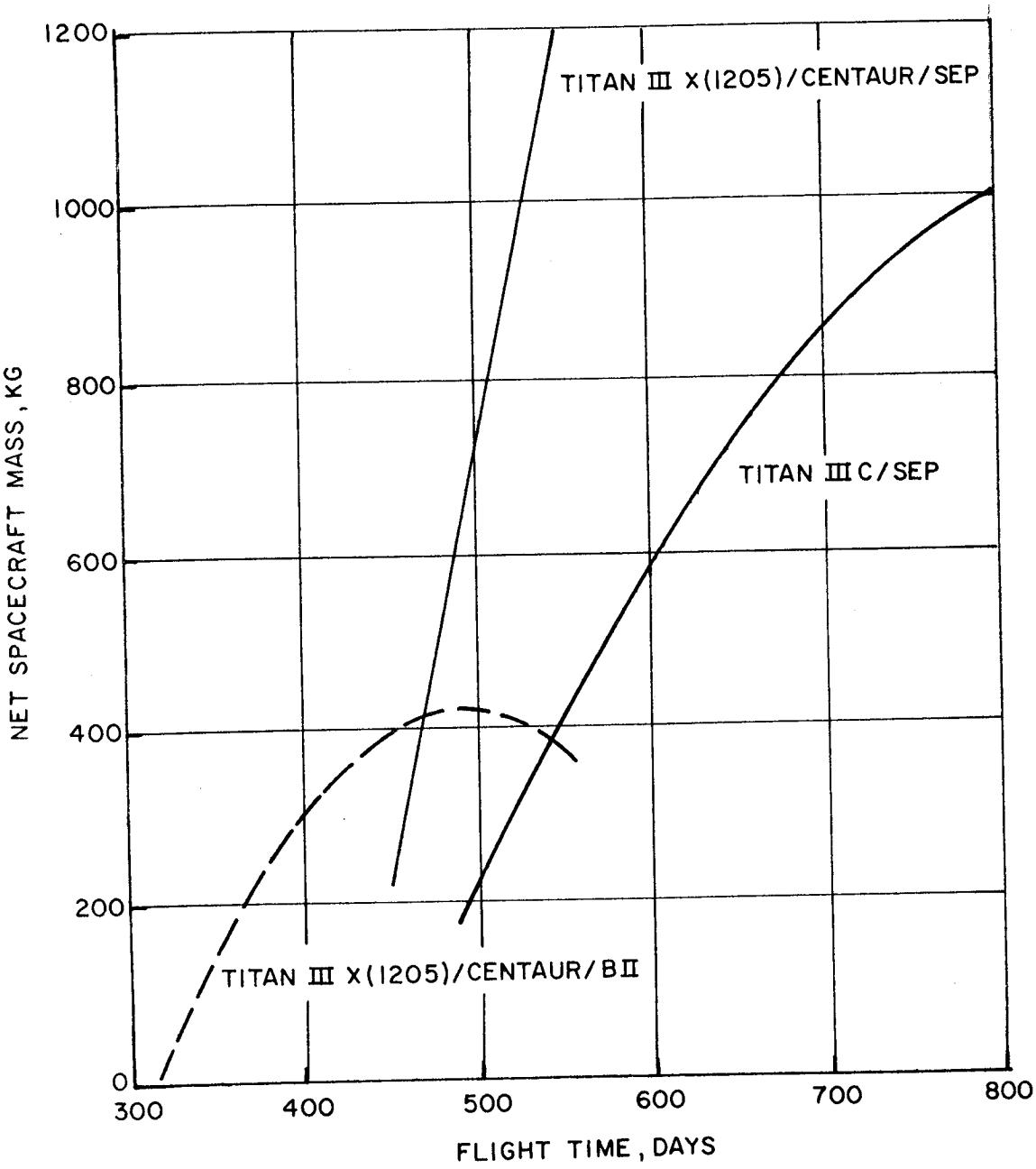

FIGURE 5-16. PERFORMANCE COMPARISON OF BALLISTIC AND SEP FLIGHT MODES FOR ASTEROID (CERES) RENDEZVOUS AT 2.77 A.U.

Table 5-2

COMET RENDEZVOUS - FLIGHT MODE COMPARISONS

450 kg Net Spacecraft Delivered to Rendezvous

	Ballistic Mode		Low Thrust Mode	
	3-Impulse	Gravity-Assist	Solar-Electric	Nuclear-Electric
ENCKE/80 Launch vehicle Flight time	Titan IIIX(1207)/ Centaur 3.3 yrs		Titan IIIC 2.5 yrs	Titan IIIX(1207)/ Centaur 1.4 yrs (1990 passage)
D'ARREST/82	Titan IIIX(1207)/ Centaur 4.8 yrs (300 kg)	Titan IIIX(1205)/ Centaur/BII 4.7 yrs	Titan IIIC 1.9 yrs	
KOPFF/83	Titan IIIX(1205)/ Centaur 3.7 yrs		Titan IIIC 1.9 yrs	
HALLEY/86		Saturn V/Centaur	Titan IIIX(1207)/ Centaur 7.5 yrs (190 kg)	Titan IIIX(1207)/ Centaur 2.6 yrs

were not generated for rendezvous opportunities before the mid-1980's. Of the 3-impulse ballistic missions studied, comets Encke and Kopff are the best opportunities in that the flight times are not excessively long (less than 4 years). The Titan IIIX(1207)/Centaur is required to perform the Encke mission, but the Kopff mission could be accomplished with the smaller Titan IIIX(1205)/Centaur. A ballistic rendezvous with D'Arrest/82 is better accomplished by utilizing a Jupiter gravity assist rather than the direct 3-impulse mode. Solar-electric propulsion offers the best performance potential for each of the missions to Encke/80, D'Arrest/82 and Kopff/83. Employing the Titan IIIC launch vehicle, SEP flights reduce the flight time requirement to only 2-2.5 years. Constant power, nuclear-electric flights allow still greater reductions in flight time. For example, the Encke mission (1990 passage) requires a flight time of only 1.4 years. The Halley mission is ideally suited to nuclear-electric propulsion, this being the only way of obtaining a relatively short flight time. To accomplish the Halley rendezvous ballistically would require a launch vehicle commitment of the Saturn V plus upper stages and a flight duration of almost 8 years. This mission does not appear to be attractive for SEP application. The Titan IIIX(1207)/Centaur provides a marginal payload of under 200 kg, the power rating is high (50 kw), and the flight time is over 7 years with the propulsion on-time being a large fraction of the mission duration. One possibility yet to be explored is the matching of SEP with a solar concentrator system so that the power level can be maintained at high levels even at large solar distances. Halley's orbit is highly retrograde, and the efficient change from posigrade to retrograde motion must be made at large distances from the Sun (> 3.5 a.u.).

SEP trajectory profiles are shown in Figures 5-17 and 5-18 for the D'Arrest/82 and Halley/86 mission opportunities. In the D'Arrest example the spacecraft traverses nearly a full

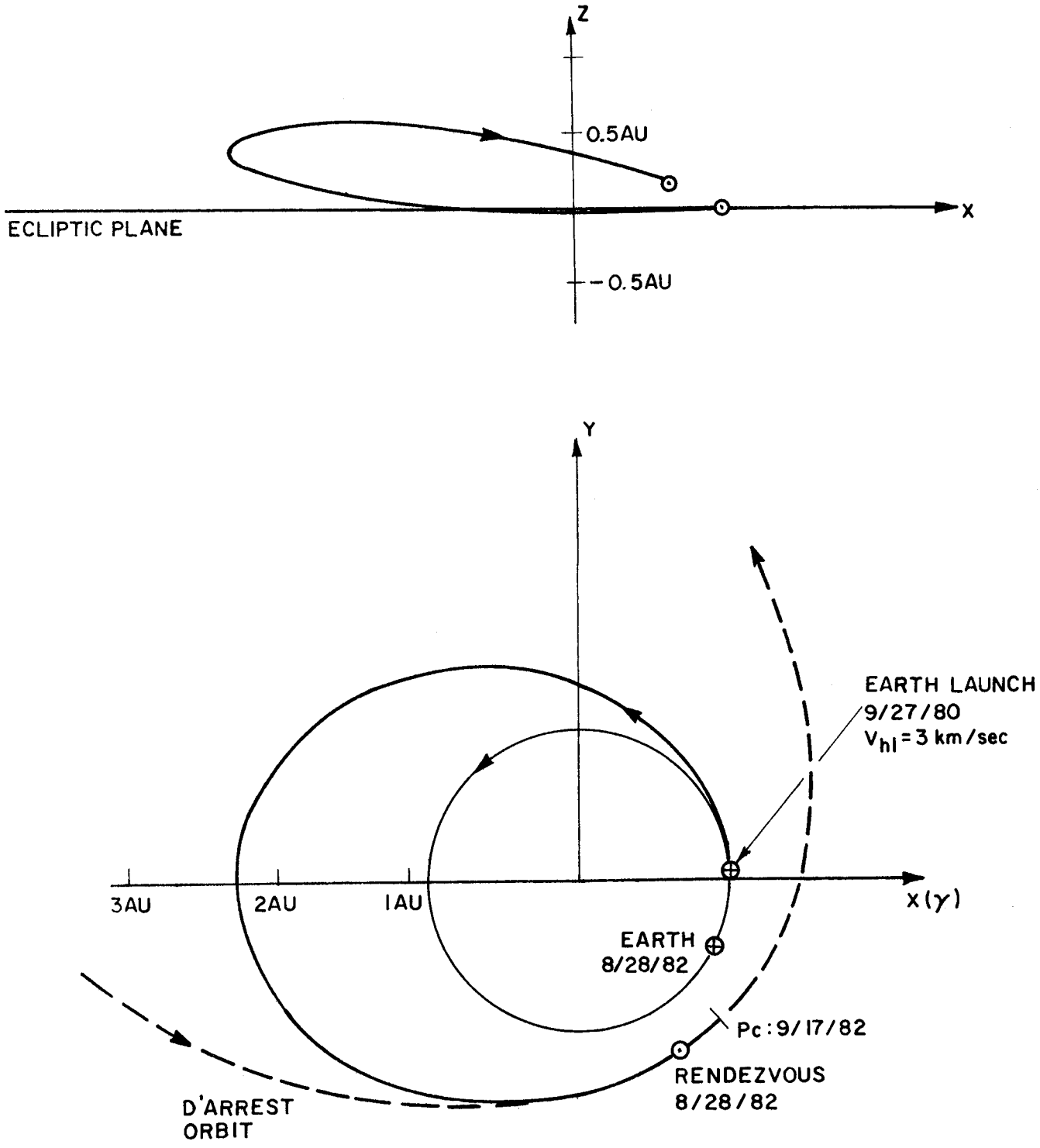

FIGURE 5-17. 700 DAY SOLAR-ELECTRIC RENDEZVOUS WITH COMET D'ARREST/82

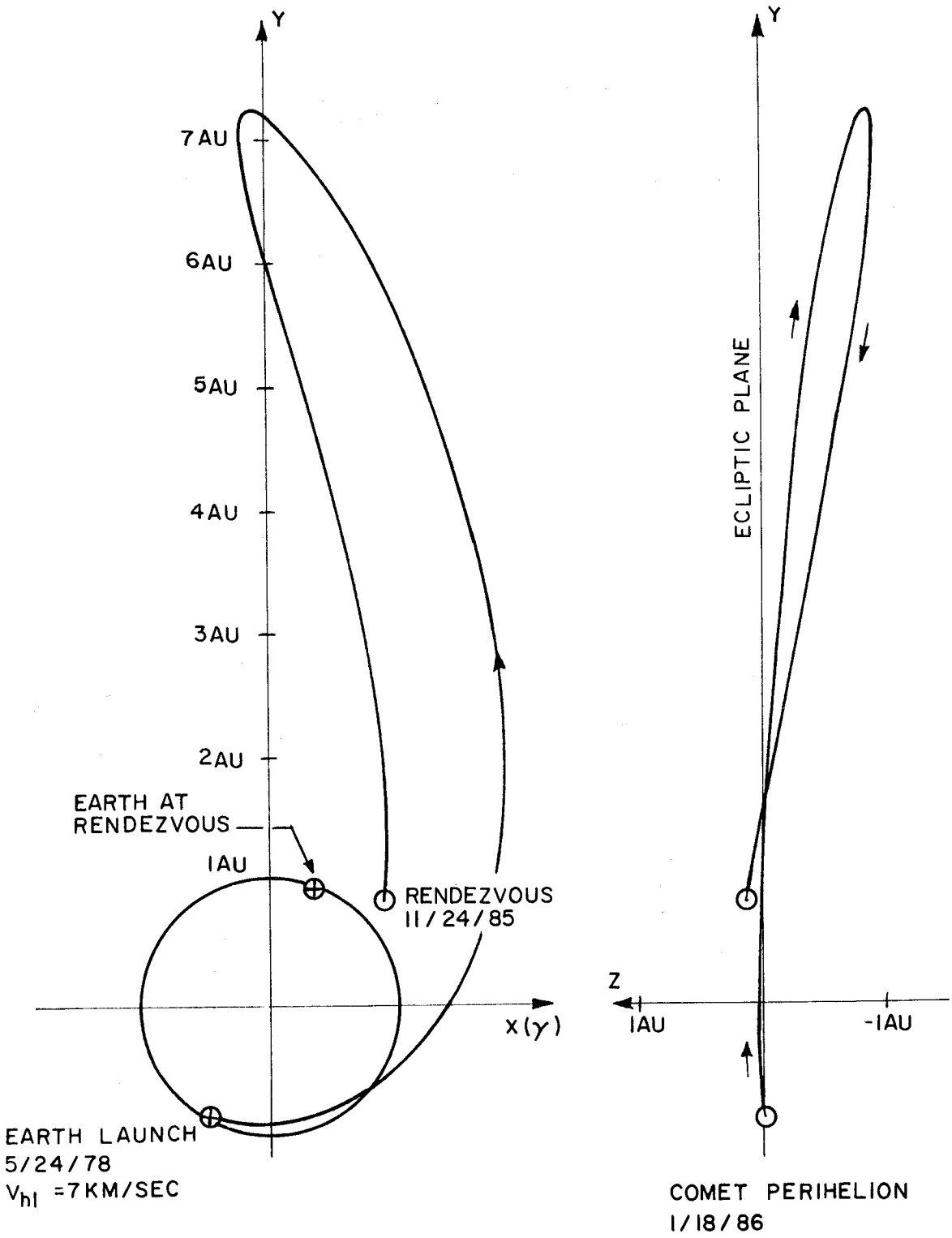

FIGURE 5-18. 2740 DAY SOLAR-ELECTRIC RENDEZVOUS WITH HALLEY'S COMET

revolution about the Sun, reaches a maximum solar distance of about 2.4 a.u., and an out-of-plane distance of about 0.6 a.u. With the Titan IIIC and a specific impulse of 3500 sec, the optimum power and propulsion time are about 20 kw and 616 days, respectively. The SEP trajectory to Halley's Comet has an aphelion distance of 7.3 a.u. at which point the momentum reversal begins. The power output here is only 2 kw (P_o = 50 kw). However, this low output provides sufficient thrust acceleration to change the trajectory because of the slow motion near aphelion. This example trajectory requires nearly continuous propulsion over the 7.5 year trip duration.

Characteristics of net spacecraft mass as a function of power rating are shown in Figures 5-19 to 5-21 for the Encke/80, D'Arrest/82 and Kopff/83 missions. The Titan IIIX(1205)/Centaur is considered in addition to the Titan IIIC in order to ascertain whether or not significant payloads can be delivered utilizing relatively small solar arrays. For example, suppose P_o were limited to 15 kw which is a lower than optimum power for both launch vehicles -- very much so for the Titan IIIX(1205)/Centaur. The net mass capability of these two vehicles at P_o = 15 kw are compared below:

Mission	Titan IIIC	Titan IIIX(1205)/Centaur
Encke/80	420 kg	600 kg
D'Arrest/82	375 kg	460 kg
Kopff/83	300 kg	$<$ 300 kg

The larger launch vehicle offers a fair improvement in payload for the Encke and D'Arrest missions, but none at all for the Kopff mission. These numbers are only illustrative of the tradeoff that can be made in mission design studies. A final design selection would depend upon many factors including science payload requirements and launch vehicle and spacecraft costs.

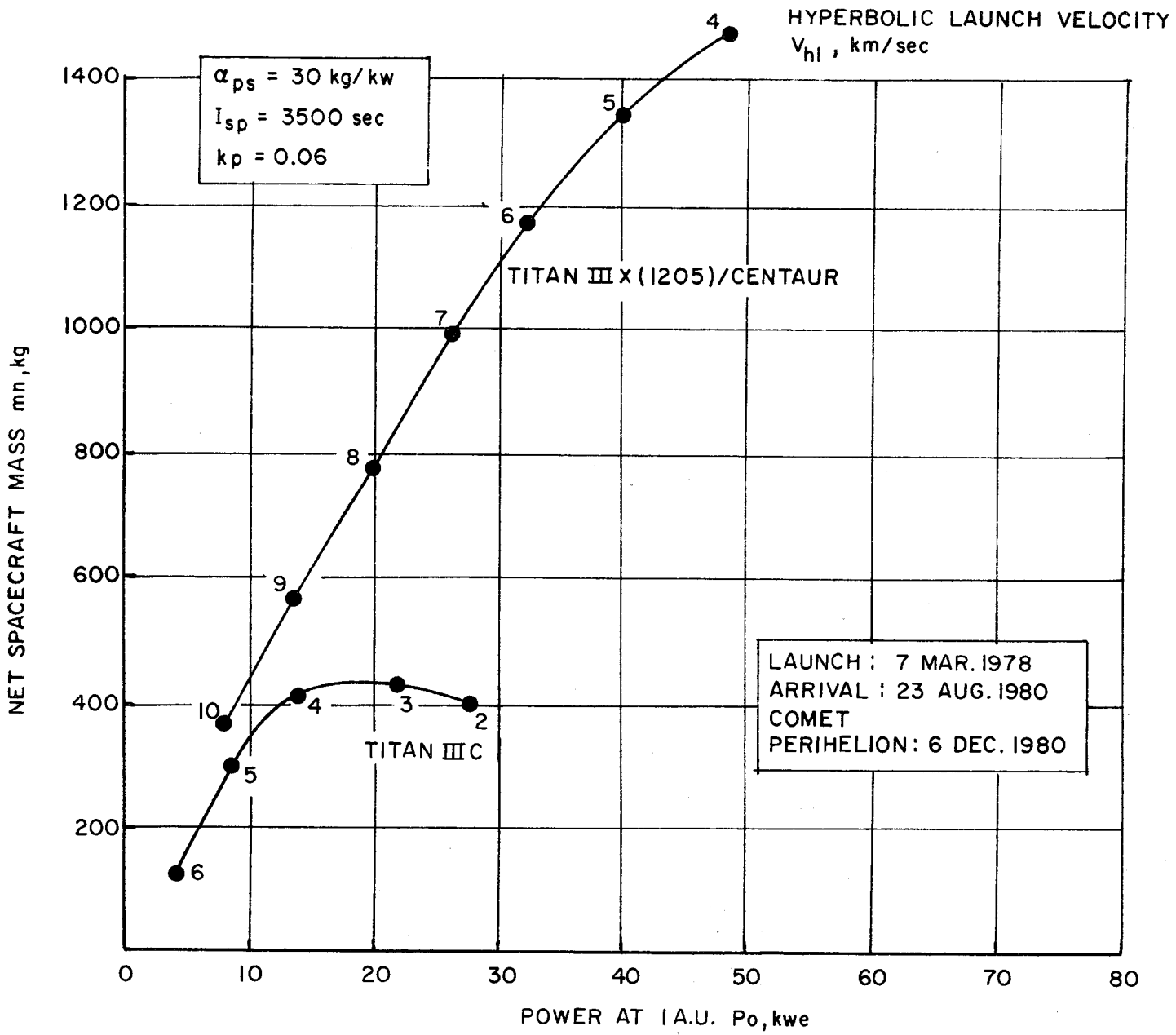

FIGURE 5-19. SOLAR-ELECTRIC PAYLOAD CAPABILITY FOR 900 DAY RENDEZVOUS TRAJECTORY TO COMET ENCKE/80.

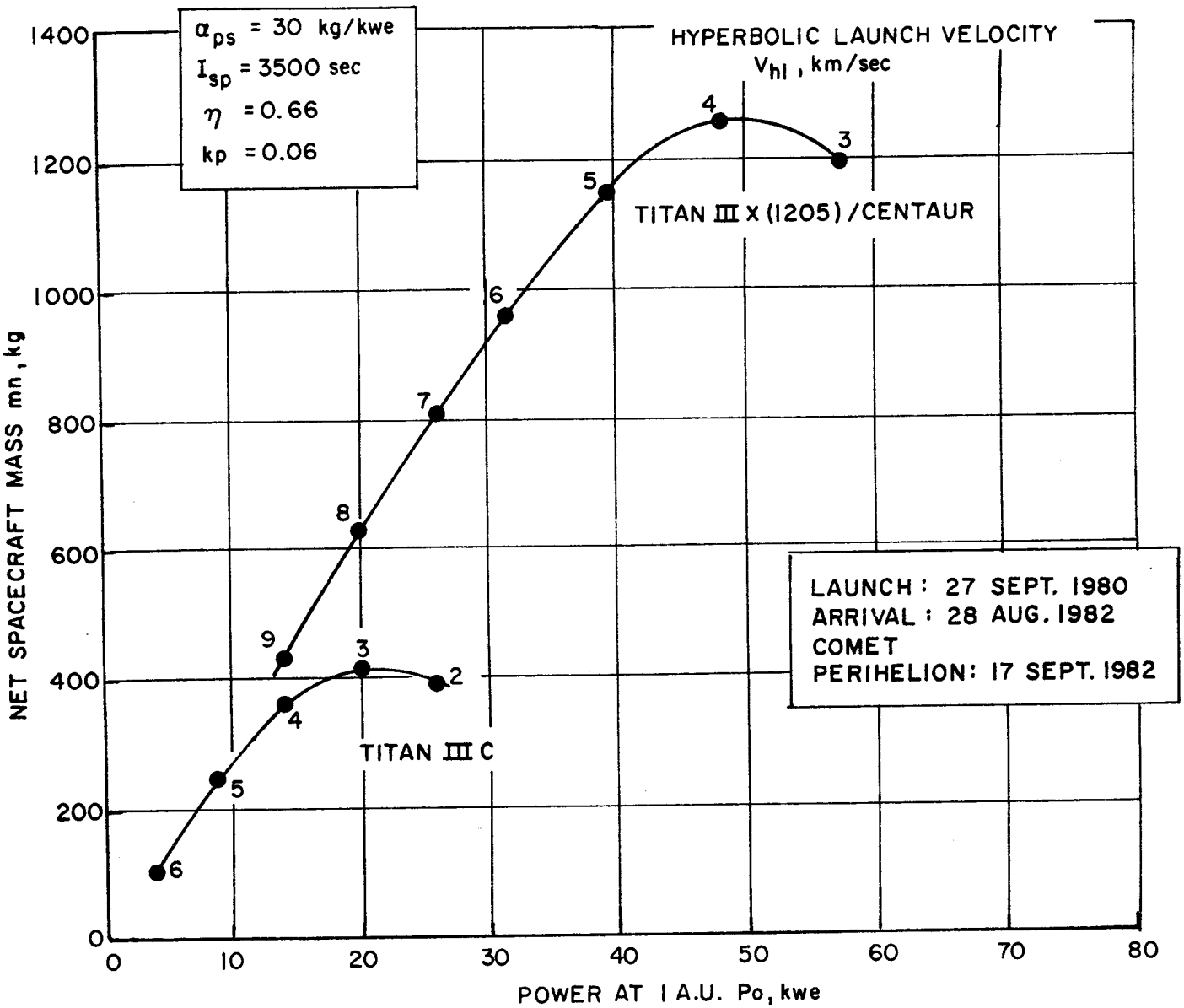

FIGURE 5-20. SOLAR-ELECTRIC PAYLOAD CAPABILITY FOR 700-DAY RENDEZVOUS TRAJECTORY TO COMET D'ARREST /82.

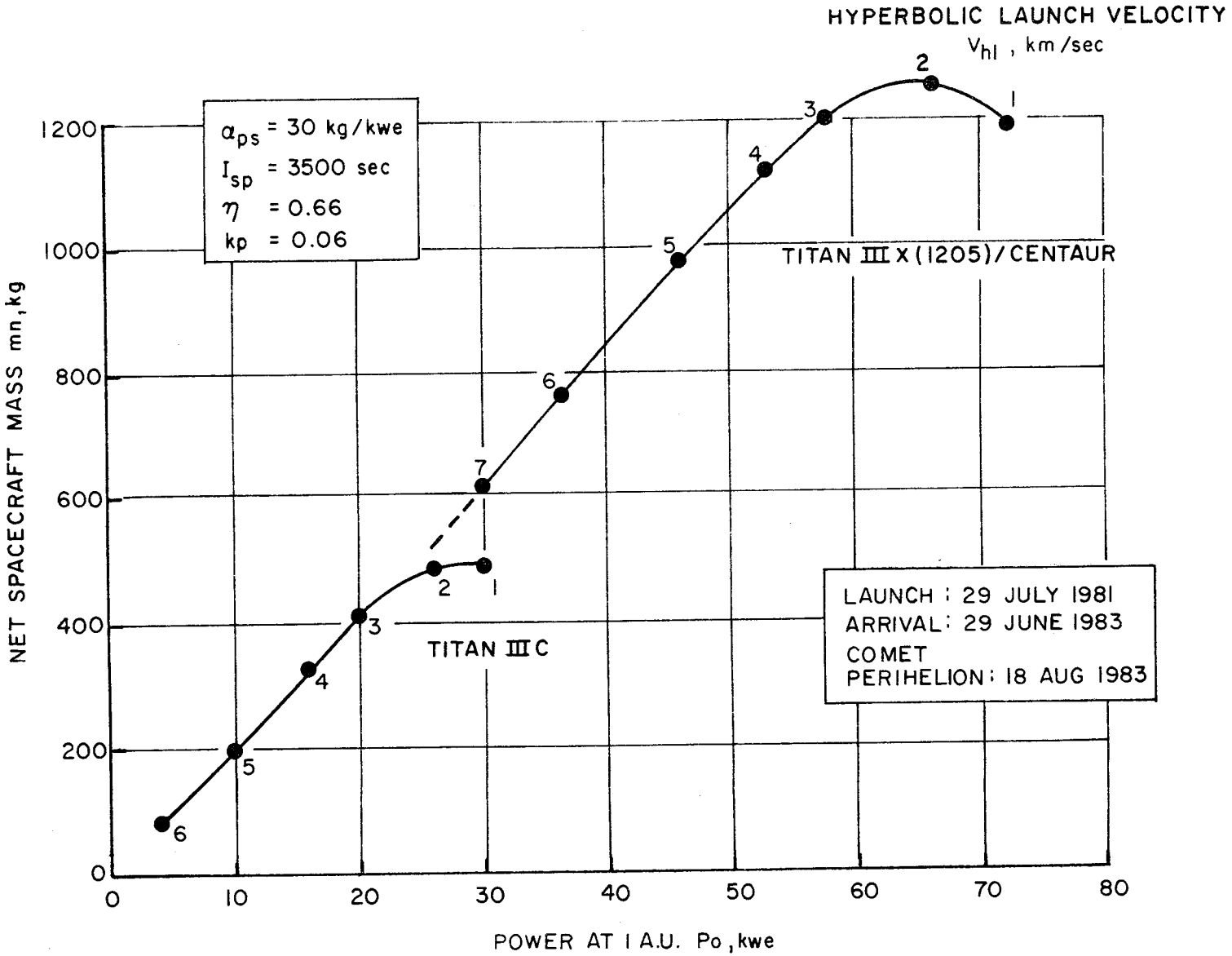

FIGURE 5-21. SOLAR-ELECTRIC PAYLOAD CAPABILITY FOR 700-DAY RENDEZVOUS TRAJECTORY TO COMET KOPFF/83.

5.3.5 Area Missions

This mission category refers to non-specific targets such as out-of-ecliptic regions, close solar regions and asteroid belt regions. The latter mission example has been discussed in Section 4.5.3. Ballistic and SEP capabilities for out-of-ecliptic missions are compared in Figure 5-22. Direct ballistic flights are limited in out-of-plane angle to about 25°, but the flight times are very short. The example shown is a 25° flight employing the Titan IIIX(1205)/Centaur/BII which delivers a net mass of 360 kg in 95 days. At the other extreme, very large payloads are possible for 45° and 60° flights if the ballistic Jupiter swingby mode is employed. The penalty in this case is long flight times of about 1400 days. SEP capability appears to lie in the middle region between the ballistic mode extremes. This region is characterized by out-of-ecliptic angles between 25° and 45°, payloads between 300 and 800 kg, and flight times between 400 and 800 days. An additional advantage of SEP flights is the inherently longer observational periods that would be available through the entire range of celestial latitudes up to the desired destination angle.

Ballistic and SEP capabilities for performing close solar probe missions are compared in Figure 5-23. Assuming that the ballistic launch vehicle is limited to the Titan IIIX(1205)/Centaur/BII, the Jupiter swingby mode is necessary to achieve the 0.1 a.u. solar mission. Ballistic payloads between 650 and 900 kg can be delivered to 0.1 a.u. in flight times of 900-1000 days. Direct ballistic flights of only 100 days duration are possible if the mission objectives are limited to perihelion distances greater than 0.2 a.u. Here again, the SEP capability lies in the middle ground. The Titan IIIC matched to an optimum SEP spacecraft design can accomplish the 0.1 a.u. mission in a flight time of 400 to 500 days with a net mass capability of 300 to 400 kg. The

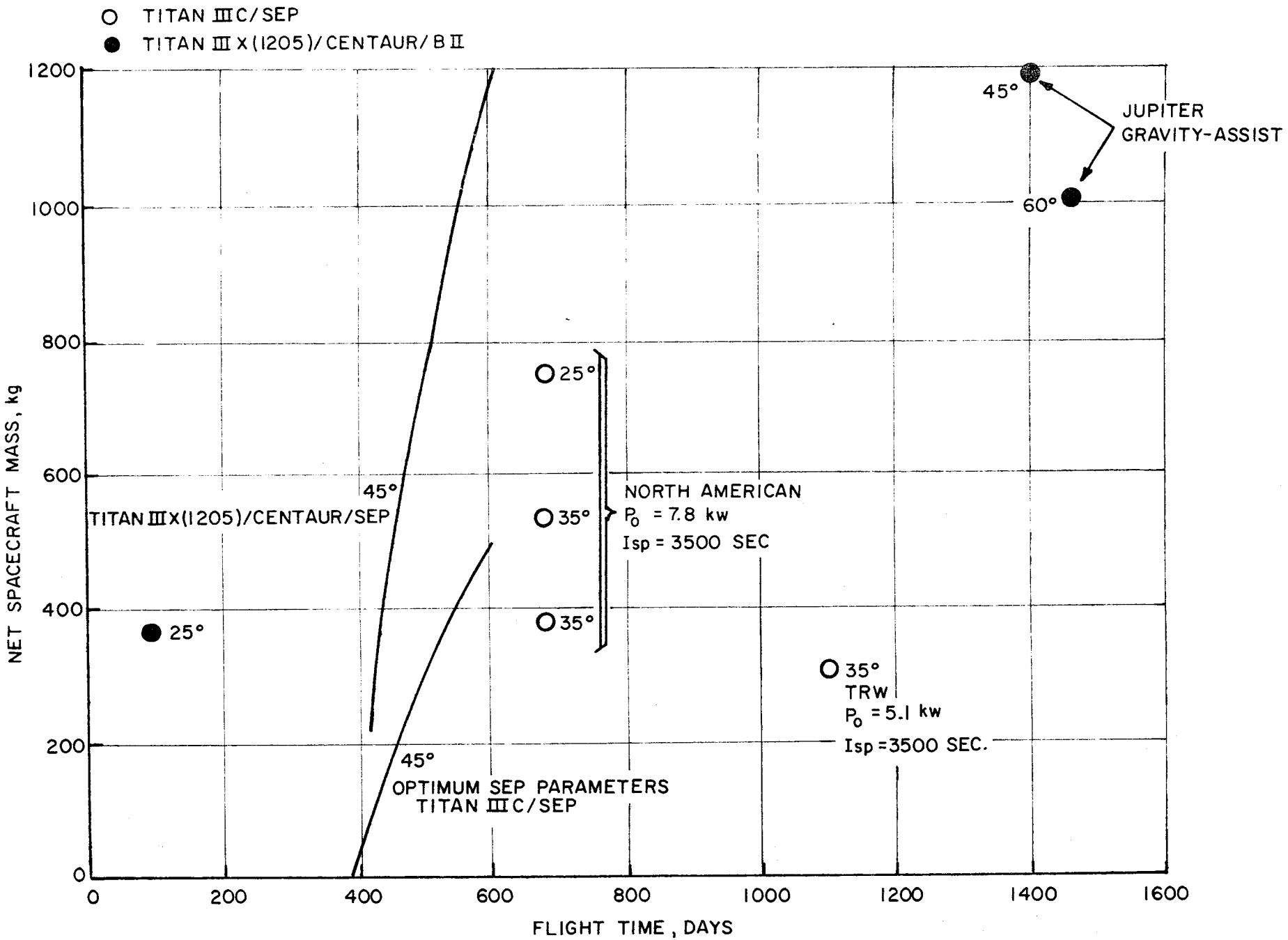

FIGURE 5-22. PERFORMANCE COMPARISON OF BALLISTIC AND SEP FLIGHT MODES FOR OUT-OF-ECLIPTIC MISSIONS AT I.A.U.

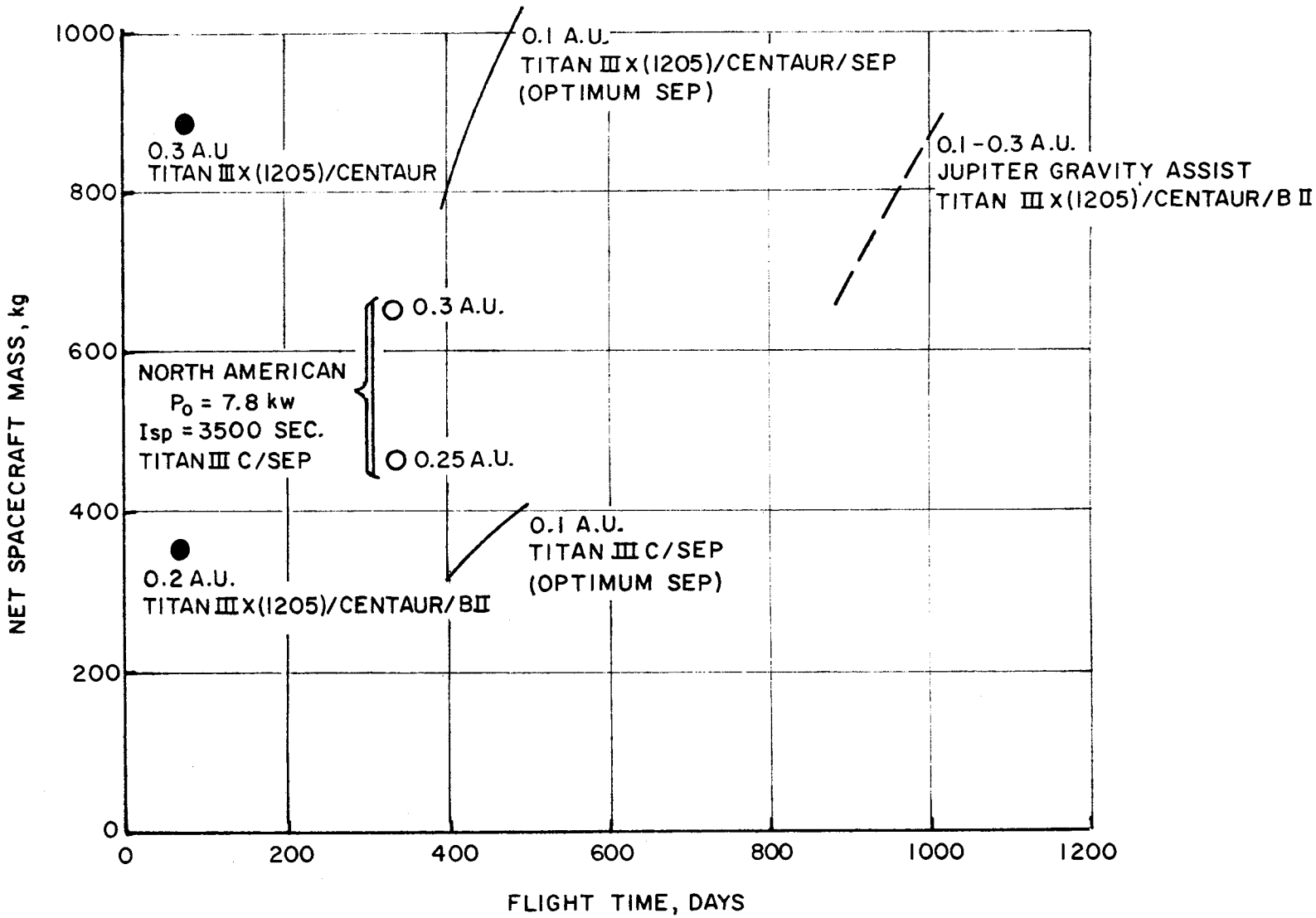

FIGURE 5-23. PERFORMANCE COMPARISON OF BALLISTIC AND SEP FLIGHT MODES FOR SOLAR PROBE MISSION.

Titan IIIX(1205)/Centaur/SEP offers a capability of 800-1000 kg. North American's baseline design SEP spacecraft (for the Asteroid Belt mission) matched to the Titan IIIC offers another example. In this case the 0.25-0.3 a.u. solar mission could be performed in about 320 days with a net mass capability of 460 to 640 kg.

The observational advantages of the SEP trajectory also apply to the 0.1 a.u. solar probe mission. Observation periods of the ballistic Jupiter swingby spacecraft near 0.1 a.u. would be restricted to only several days with a repeatability of about 2.5 years. In contrast, the SEP trajectory provides an observation period of about 15 days between 0.1 and 0.2 a.u. with a repeatability of 110 days.

5.3.6 Summary of Mission Capability

Highly energetic missions which are uniquely suited to SEP spacecraft are Mercury orbiter, comet rendezvous, large out-of-the-ecliptic excursions, and close solar probes. Performance advantages over ballistic spacecraft include significantly shorter flight times, high power availability at the target and, in some cases, a smaller launch vehicle. These missions can all be accomplished with the programmed Titan class vehicles; either the Titan IIIC or Titan IIIX(1205)/Centaur. The ballistic Mercury orbiter is completely infeasible even with the Saturn V/Centaur, and some comet rendezvous missions would require the (1207) version of the Titan IIIX. Other missions which show significant flight time reductions using SEP spacecraft are flybys and orbiters of all the outer planets but particularly flybys of Uranus and Neptune and orbiters of Saturn and Uranus. The Neptune orbiter mission, even with SEP, requires a flight time greater than 13 years. There does not appear to be any significant SEP advantage for orbiters of Venus and Mars except, perhaps, for high data-rate mapping missions requiring close circular orbits, very large orbiting payloads, and high power availability. If this were the case,

the Titan IIIX(1205)/Centaur/SEP could be employed to deliver a net mass of 2000 kg or more with power capability of at least 10 kw. For asteroid rendezvous missions, the ballistic flight mode may be adequate if a net spacecraft mass of 420 kg or less were acceptable. The advantage of SEP for this mission would depend upon the need to deliver a larger payload than the maximum ballistic capability of the Titan IIIX(1205)/Centaur/BII.

It should be noted that the above comparisons are based on a circular, coplanar model of planet motion, and a launch window of zero length. When a real planet ephemeris and finite-length launch window (15-30 days) are used, the comparative advantage of SEP spacecraft over ballistic spacecraft becomes significantly greater.

The optimum power rating depends on the mission, flight time and launch vehicle. This power falls within the range 10-25 kw for the Titan IIIC and 25-55 kw for the Titan IIIX(1205)/Centaur. It has been shown that off-optimum power operation, even down to 50 percent of optimum power, incurs only a modest payload penalty. The importance of this result is that a smaller solar array design allows a simpler SEP spacecraft configuration and lower cost. Another important result of the off-optimum power characteristic is that it becomes reasonable to consider a fixed SEP powerplant and spacecraft for multi-mission application. For example, a 10-15 kw SEP powerplant with thruster operation at about 3500 sec specific impulse could be launched by the Titan IIIC and perform many of the missions discussed previously with a net spacecraft mass of about 400 kg. Outer planet orbiters would likely require a common powerplant of 15-25 kw and the Titan IIIX(1205)/Centaur launch vehicle.

There has been an understandable reluctance among space program planners to accept the new technology of solar electric propulsion. Many missions of interest, particularly the high priority missions, can be flown with existing or soon to be

available chemical launch vehicles and ballistic spacecraft. It has not been possible to justify the SEP concept for most single mission applications. In the first instance, the single mission SEP cost would be about 10-15 percent higher than the ballistic mission. Secondly, the excess payload capability of SEP has not been readily appreciated in that the science payload matched to the ballistic capability is often said to be sufficient for the mission objectives. This may or may not be so but the question cannot be argued here.

It would seem that the acceptance and incorporation of SEP into flight programs depends first, on the demonstration of realistic hardware and reliable spacecraft operation, and, second, on showing the cost effectiveness of a given SEP design for multimission use. The technology demonstration has been essentially accomplished as of 1970 with the SERT II flight test, continuing laboratory development and test programs, and recently completed spacecraft design studies. Multimission cost advantages would result from the savings in existing launch vehicle cost and development of future high energy chemical upper stages and retro systems. However, SEP cost effectiveness can be established best if there exists a long range space exploration program encompassing many missions to which this propulsion concept could be applied.

6. REFERENCES

1. Molitor, J. H., Berman, D., Seliger, R. L. and Olson, R. N., "Design of a Solar-Electric Propulsion System for Interplanetary Spacecraft," Paper 66-214, March 1966, AIAA, New York, N. Y.

2. "Solar Powered Electric Propulsion Spacecraft Study," December 1965 and "Solar Powered Electric Propulsion Program Summary Report," December 1966, prepared for JPL under JPL Contract 951144, Hughes Aircraft Company, Culver City, California.

3. Strack, W. C., "Solar-Electric Propulsion System Performance for a Close Solar Probe Mission," Paper 66-496, June 1966, AIAA, New York, New York; ALSO, J. Spacecraft, July 1967.

4. Ramler, J. R., "Low-Thrust Orbit Raising in Continuous Sunlight While Thrusting in a Plane Perpendicular to the Earth-Sun Line," NASA TND-4104, August 1967.

5. Meissinger, H. F., Park, R. A. and Hunter, H. M., "A 3 KW Solar-Electric Spacecraft for Multiple Interplanetary Missions," Paper 67-711, September 1967, AIAA, New York, New York.

6. Flandro, G. A. and Barber, T. A., "Mission Analysis for Interplanetary Vehicles with Solar Electric Propulsion," AIAA Paper 67-708, September 1967.

7. "Flight Time and Mass Fraction Data for Out-of-Ecliptic Missions Utilizing Low-Thrust Propulsion," TRW Report 09661-6001-R000, October 29, 1967.

8. Strack, W. C. and Zola, C. L., "Solar-Electric Propulsion Probes for Exploring the Solar System," TMX-52318, 1967, NASA, Cleveland, Ohio.

9. Meissinger, H. F. and Greenstadt, E. W., "Use of Electric Propulsion for Exploring the Distant Regions of the Geomagnetic Tail," Paper 68-120, January 1968, AIAA, New York, New York.

10. Zola, C. L., "Jovian Planet Missions for Solar Cell Powered Electric Propulsion Spacecraft," Paper 68-118, January 1968, AIAA, New York, New York.

11. Flandro, G. A., "Solar Electric Grand Tour Missions to the Outer Planets," University of Utah Report ME 70-033, April 1970.

12. "1975 Jupiter Flyby Mission Using a Solar Electric Propulsion Spacecraft," Report No. ASD-760-18, March 1968, Jet Propulsion Laboratory, Pasadena, California.

13. Kerrisk, D. J. and Bartz, D. R., "Primary Electric Propulsion Technology-Toward Flight Programs for the Mid-1970's," Aeronautics and Astronautics, June 1968.

14. "Solar Electric Space Mission Analysis," Progress Reports on Contract NASR 31-001-078, January-March 1967, July 1968, prepared by Princeton University, Princeton, New Jersey.

15. Sauer, C. G., Jr., "Optimization of a Solar-Electric Propulsion Planetary Orbiter Spacecraft," September 1968, AIAA, New York, New York.

16. Mullin, J. P., Barber, T. and Zola, C., "A Survey of Solar Powered Electric Propulsion for Automatic Missions," NASA TMX-52488, October 1968.

17. Long, J. E., "To the Outer Planets," Astronautics and Aeronautics, June 1969.

18. Wrobel, J. R. and Driver, J. M., "Current Status of Solar-Propelled Asteroid Probe Studies," AIAA Paper No. 69-1105, October 1969.

19. Horsewood, J. L., "Solar Electric Performance Capabilities for Interplanetary and Outer Planetary Flybys and Orbiters," June 1969, Analytical Mechanical Associates, private communication (NASA CR-1524).

20. Zola, C. L., "Interplanetary Probe Missions with Solar-Electric Propulsion Systems," NASA TND-5293, July 1969.

21. Reader, P. D. and Regetz, J. D., Jr., "A Delta-Boosted Electrically Raised High Power Synchronous Satellite," AIAA Paper No. 69-1104, October 1969.

22. Park, R. A. et al., "Solar-Electric Propulsion Missions to the Comets," paper presented at the AAS Meeting, Boston, Mass., May 26, 1967.

23. Friedlander, A. L., Niehoff, J. C. and Waters, J. I., "Comet Rendezvous Opportunities," IIT Research Institute, ASC Report TM M-21, April 1970.

24. Bartz, D. R. and Horsewood, J. L., "Characteristics, Capabilities, and Costs of Solar Electric Spacecraft for Planetary Missions," AIAA Paper No. 69-1103, October 1969.

25. Lazar, J., "Current Status of Electric Propulsion Technology," AIAA Paper No. 69-1107, October 1969.

26. Kraemer, R. S., "A Forecast of Electrically-Propelled Spacecraft Applications," AIAA Paper No. 69-1108, October 1969.

27. "Solar Electric Propulsion Asteroid Belt Mission Study," Final Report SD 70-21-2, January 1970, North American Rockwell, Downey, California, JPL Contract 952566.

28. "Study of a Solar Electric Multi-Mission Spacecraft," Final Report 09451-6001-RO-3, March 1970, TRW Systems Group, Redondo Beach, California, JPL Contract 952394.

29. JPL Presentation to NASA-OSSA on Results of Contractor Studies for Asteroid Belt Mission, February 9, 1970.

30. Bartz, D., "Scaling of Electric Propulsion Mission Analysis Results," JPL Inter-office Memo, January 20, 1969.

31. "Electric Propulsion Mission Analysis, Terminology and Nomenclature," NASA SP-210, 1969.

32. "Large Area Solar Array," Final Report D2-113355-4 for JPL Contract 951653, the Boeing Company, Seattle, Wash., October 1967.

33. Carlson, A., "Development of Light Weight Solar Panels," Contract NAS7-428, Electro-Optical Systems, Inc., April 1968.

34. "A Proposal for Phase II 30 Watt Per Pound Rollup Solar Array, Volume 1," MSD Proposal No. F-20430, General Electric MSD, Valley Forge, Pa., May 31, 1968, JPL Contract 951970.

35. Sellen, J. M., Jr., "Interaction of Spacecraft and Engineering Subsystems with Electric Propulsion Systems," AIAA Paper No. 69-1106, October 1969.

Appendix A

SCALING LAW DEVELOPMENT AND VALIDITY

Appendix A

SCALING LAW DEVELOPMENT AND VALIDITY

Performance analysis of solar electric spacecraft is complicated by the interdependence of numerous trajectory, vehicle and propulsion system parameters as outlined in Section 3. For the purpose of this discussion, a single but useful measure of performance is adopted; namely, the net spacecraft mass m_n delivered to the target. The computation of the optimum trajectory and the associated selectable parameters (P_o, I_{sp}, V_{hL}, V_{hp}) which maximizes m_n generally requires a sophisticated computer optimization procedure. Suppose that such a computer result has been obtained for a given flight time and a specified set of input parameters such as launch vehicle, propulsion system specific mass, orbit size, etc. If the mission analyst is interested in the effect of changes in the input parameters on the spacecraft mass, it is clear that the reoptimization calculation may be both costly and time consuming. There is an incentive, therefore, to develop a greatly simplified method of calculation which yields the optimum performance, or nearly so, under the new input conditions. Results accurate to within a few percent would sufficiently justify the method.

It has been recognized that the optimum low thrust trajectory computed for one typical set of input parameters remains nearly optimum for another set. Hence one objective is to find the conditions for which the assumption of trajectory invariance would allow the performance calculation to be made "external" to the trajectory optimization loop. This external calculation is made easier if an appropriate set of scaling relationships

can be utilized. By scaling we mean a direct, noniterative algebraic expression of the form

$$m_{nB} = f\ (\underline{p}_A,\ \underline{p}_B,\ m_{nA}) \qquad (A.1)$$

where $\underline{p}_A$ and $\underline{p}_B$ are the input parameters under conditions A and B, respectively. Such a set has been proposed by Don Bartz of JPL.(30) These account for scaling of structure and tankage factors, propulsion system specific mass and efficiency, and launch vehicle. For example, in the case of launch vehicle scaling alone, the scaling law is simply

$$m_{nB} = \left(\frac{m_{oB}}{m_{oA}}\right) m_{nA} \qquad (A.2)$$

where m_{oA} and m_{oB} are the injected masses of launch vehicles A and B for the same value of hyperbolic launch velocity V_{hL}. In addition, trajectory invariance assumes the same values of flight time t_f, specific impulse I_{sp}, solar power dependence G(R), and hyperbolic approach velocity V_{hp}. Exact linear scaling as in the above expression requires that the launch vehicle performance curves (m_o vs V_{hL}) are linearly scalable over their entire range. This assumption is not always realistic and may lead to somewhat inexact results as will be discussed further.

Our task will be to check the validity of scaling as proposed by Bartz, and to attempt to extend the general usefulness of this concept to cover other input parameters as well. Adopting the basic scaling concept as proposed, the problem has been reformulated so as to describe the result in the general form of Equation (A.1) and in terms of readily accessible parameters. The scaling relationships may be applied to any combination of the following parameters:

(1) Launch vehicle, m_o.

(2) Electric propulsion system specific mass, $\alpha \equiv \alpha_{ps}$.

(3) Electric spacecraft structure factor, k_o.

(4) Electric propellant tankage factor, k_p.

(5) Electric thrust subsystem efficiency, η.

(6) Chemical retro propellant fraction, ρ (orbit size and retro I_{sp}).

(7) Chemical retro inert fraction, k_r.

The three mission operational modes for which scaling is treated are:

(1) No retro maneuver ($\rho = 0$); planet flyby, area missions, asteroid rendezvous, comet rendezvous.

(2) Retro maneuver without propulsion system jettison; planet orbiter.

(3) Retro maneuver with propulsion system jettison; planet orbiter.

A.1 Formulation of Scaling Laws

Invariance of the low thrust trajectory means that the acceleration time history a(t) is the same under input conditions A and B. Using the relationships given in Section 3 of this report, a(t) may be expressed as

$$a(t) = \frac{(2\eta/c)(P_o/m_o)\, G[R(t)]}{1 - \int_o^t \frac{\dot{m}_p}{m_o}\, dt} \qquad (A.3)$$

where the propellant flow rate is given by

$$\frac{\dot{m}_p}{m_o} = \left(\frac{2\eta}{c^2}\right)\left(\frac{P_o}{m_o}\right) G[R(t)] \quad . \qquad (A.4)$$

Assuming that the solar power function G(R), jet velocity c and efficiency η remain fixed, it is seen that acceleration invariance is satisfied by a constant ratio of initial power to mass

$$\frac{P_{oB}}{m_{oB}} = \frac{P_{oA}}{m_{oA}} \tag{A.5}$$

Consequently, the propellant mass fractions will also be in the constant ratio

$$\frac{m_{pB}}{m_{oB}} = \frac{m_{pA}}{m_{oA}} \tag{A.6}$$

Equations (A.5) and (A.6) are fundamental to the scaling law development. Some degree of relaxation in the assumption of fixed efficiency may be accommodated as shown later.

A.1.1 No Retro Maneuver

When the mission does not call for a chemical retro maneuver, the net spacecraft mass is given by the expressions

Condition A: $$m_{nA} = (1 \pm k_{oA})\, m_{oA} - (1 + k_{pA})\, m_{pA} - \alpha_A\, P_{oA} \tag{A.7a}$$

Condition B: $$m_{nB} = (1 \pm k_{oB})\, m_{oB} - (1 + k_{pB})\, m_{pB} - \alpha_B\, P_{oB} \tag{A.7b}$$

Solving (A.7a) for m_{pA}, using (A.5) and (A.6), and substituting into (A.7b) gives the desired scaling law after some rearrangement of terms

$$m_{nB} = \left(\frac{1 + k_{pB}}{1 + k_{pA}}\right)\left(\frac{m_{oB}}{m_{oA}}\right) m_{nA}$$

$$+\left[\left(\frac{1 + k_{pB}}{1 + k_{pA}}\right)\alpha_A - \alpha_B\right]\left(\frac{m_{oB}}{m_{oA}}\right) P_{oA} \qquad (A.8)$$

$$+\left[\left(\frac{1 + k_{pB}}{1 + k_{pA}}\right)(k_{oA} + k_{pA}) - (k_{oB} + k_{pB})\right]\left(\frac{m_{oB}}{m_{oA}}\right) m_{oA}$$

A.1.2 Retro Maneuver Without Propulsion System Jettison

In this case, the net spacecraft mass delivered into orbit about the target planet is

$$m_n = (1 - k_o)\, m_o - (1 + k_p)\, m_p - \alpha P_o - (1 + k_r)\, m_{pr}. \qquad (A.9)$$

The quantity m_{pr} is the chemical propellant mass expended

$$m_{pr} = (m_o - m_p)\rho \qquad (A.10)$$

where ρ has been defined in Section 3 as the retro propellant fraction which depends upon the planet gravitational constant, the orbit periapse and apoapse distances, the approach hyperbolic velocity, and the retro system specific impulse (see Eqs. 3.30 and 3.31). The approach velocity is the same under the scaling condition A and B as a result of the required trajectory invariance. Proceeding as outlined in Section A.1.1, the following scaling law is readily derived

$$m_{nB} = \left[\frac{(1 + k_{pB}) - \rho_B (1 + k_{rB})}{(1 + k_{pA}) - \rho_A (1 + k_{rA})}\right]\left(\frac{m_{oB}}{m_{oA}}\right) m_{nA}$$

$$+ \left\{\left[\frac{(1 + k_{pB}) - \rho_B (1 + k_{rB})}{(1 + k_{pA}) - \rho_A (1 + k_{rA})}\right] \alpha_A - \alpha_B\right\}\left(\frac{m_{oB}}{m_{oA}}\right) P_{oA} \qquad (A.11)$$

$$+ \left\{\left[\frac{(1 + k_{pB}) - \rho_B (1 + k_{rB})}{(1 + k_{pA}) - \rho_A (1 + k_{rA})}\right] (k_{oA} + k_{pA}) - (k_{oB} + k_{pB})\right\}\left(\frac{m_{oB}}{m_{oA}}\right) m_{oA}$$

It is noted that (A.11) reduces to (A.8) when $\rho_A = \rho_B = 0$.

A.1.3 Retro Maneuver With Propulsion System Jettison

Here it is assumed that the electric propulsion system including the propellant tankage is jettisoned prior to executing the orbit retro maneuver. The chemical propellant mass expended in the case of staging is thus reduced to

$$m_{pr} = (m_o - m_p - k_p m_p - \alpha P_o)\ \rho \ . \qquad (A.12)$$

Using (A.9) which still applies and proceeding as before, the scaling law may be expressed in the form

$$m_{nB} = \left[\frac{1 - \rho_B (1 + k_{rB})}{1 - \rho_A (1 + k_{rA})}\right]\left(\frac{1 + k_{pB}}{1 + k_{pA}}\right)\left(\frac{m_{oB}}{m_{oA}}\right) m_{nA} \qquad (A.13)$$

$$+ \left[1 - \rho_B (1 + k_{rB})\right]\left[\left(\frac{1 + k_{pB}}{1 + k_{pA}}\right)\alpha_A - \alpha_B\right]\left(\frac{m_{oB}}{m_{oA}}\right) P_{oA}$$

$$+ \left\{\left[\frac{1-\rho_B (1+k_{rB})}{1-\rho_A (1+k_{rA})}\right]\left(\frac{1+k_{pB}}{1+k_{pA}}\right)\left[(k_{oA}+k_{pA}) + \rho_A (1+k_{rA}) - (1+k_{pA})\right]\right.$$

$$\left. - \left[(k_{oB} + k_{pB}) + \rho_B (1 + k_{rB}) - (1 + k_{pB})\right]\right\}\left(\frac{m_{oB}}{m_{oA}}\right) m_{oA}$$

A.1.4 Scaling for Changes in Propulsion Efficiency

A change in propulsion system mass is directly related to a change in net spacecraft mass.

$$\begin{aligned} \Delta m_n &= \Delta m_{ps} \\ &= -\Delta(\alpha P_o) \end{aligned} \tag{A.14}$$

Now, relating m_{ps} to α, η and jet power at 1 a.u.

$$m_{ps} = \frac{\alpha}{\eta} P_{jo} \tag{A.15}$$

and assuming that I_{sp} and P_{jo} remain fixed (trajectory invariance requirement), the change in m_{ps} can be calculated for changes in both α and η.

$$(\Delta m_{ps})_\alpha = \frac{P_{jo}}{\eta} \Delta\alpha \tag{A.16}$$

$$(\Delta m_{ps})_\eta = -\frac{\alpha}{\eta 2} P_{jo} \Delta\eta \tag{A.17}$$

Hence, for an equivalent change in m_{ps} due to either α or η, the following first-order relationship holds

$$\frac{\Delta\alpha}{\alpha} = -\frac{\Delta\eta}{\eta} \tag{A.18}$$

This implies that a fractional (small) increase in efficiency has the same effect on net spacecraft mass as the same fractional decrease in propulsion system specific mass.
Equation (A.18) may be used together with either Equations (A.8), (A.11) or (A.13) to scale for changes in propulsion efficiency.

A.2 Validity of Scaling and Numerical Examples

While it is clear that mass scaling can always be performed, the question of interest is whether or not the results obtained are close to the optimum that would have been obtained via the computer program. It is assumed here that the original

data (Condition A) represents an optimized result for that set of input parameters. Thus, for example, the selectable parameters $(P_o, I_{sp}, V_{hL}$ and $V_{hp})_A$ have been optimized to maximize m_{nA}. This tends to benefit the accuracy of scaling since the effect of parameter variations are presumably least around the optimum point. The following discussion will attempt to delineate under which circumstances accurate scaling can be expected. In some cases an analytical argument can be invoked; in other cases resort has to be made to empirical results, i.e., numerical validity checks.

A.2.1 Launch Vehicle Scaling

Figure A-1 shows the injected mass capability of three Titan class launch vehicles. The slope of the performance curve is an important characteristic in arriving at the optimum value of V_{hL} for a given mission. If any two vehicles have performance curves which were linearly scalable over the entire range of V_{hL} of interest, i.e.,

$$m_{oB}(V_{hL}) = k_1 \, m_{oA}(V_{hL})$$

then it is intuitively evident that the same value of optimum V_{hL} would be obtained in both cases.

As an example, suppose that the Titan IIIX(1205)/Centaur mission optimizes at a value of V_{hL} = 4 km/sec. The broken line curves of Figure A-1 illustrate the scaling of this vehicle to the Titan IIIX(1207)/Centaur and the Titan IIIC, taking the constant scaling factors at V_{hL} = 4 km/sec. In the first case, the (1207) vehicle is fairly well scaled over a wide range of V_{hL}. However, since the scaled curve has a steeper slope, the Titan IIIX(1207)/Centaur would actually optimize at a V_{hL} somewhat higher than 4 km/sec. The second case (Titan IIIC) is an example of poor scalability. Here the scaled curve for the Titan IIIC has a shallower slope, and the actual value of optimum V_{hL} would be less than 4 km/sec.

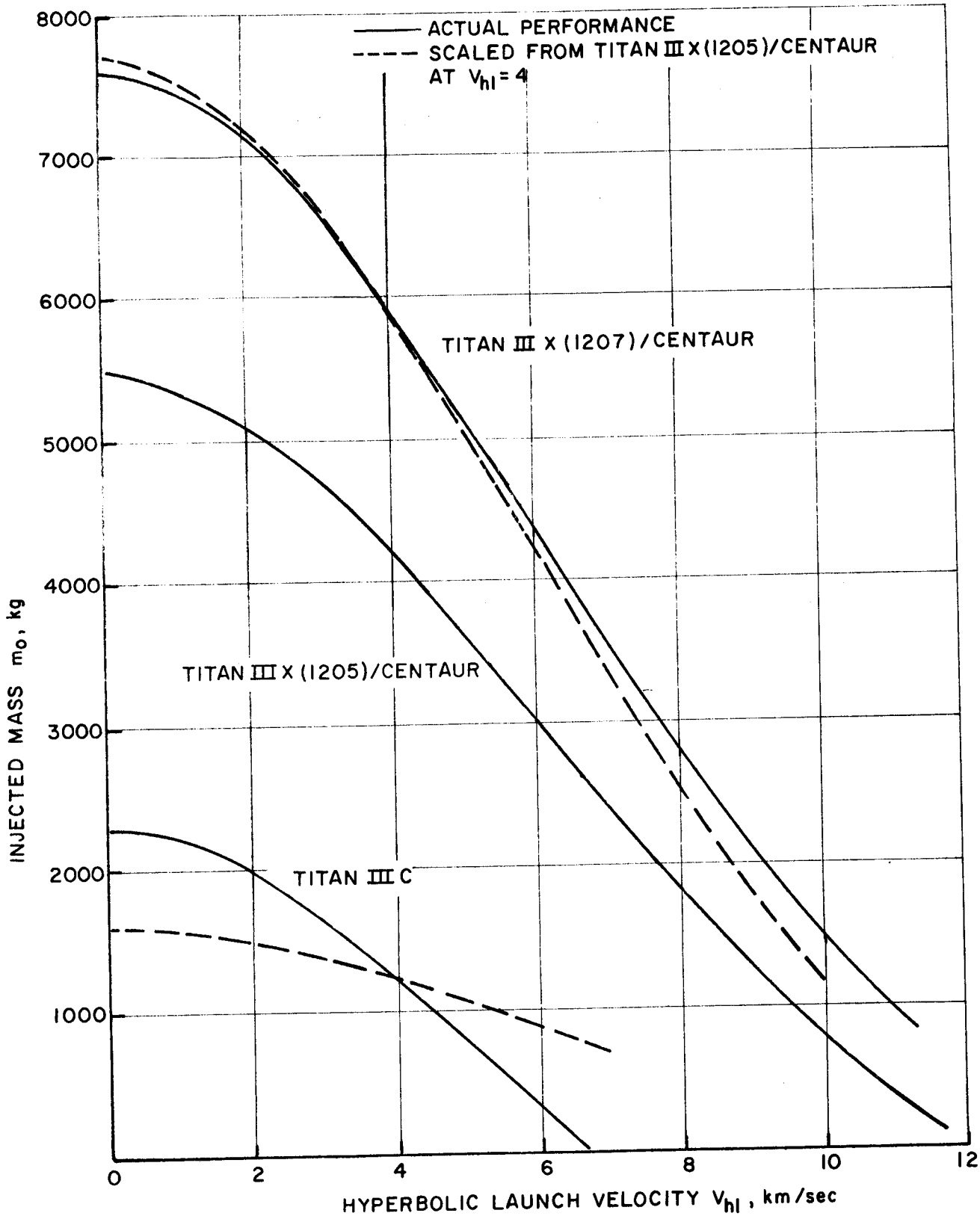

FIGURE A.I. LAUNCH VEHICLE PERFORMANCE CURVES, 1969 OSSA ESTIMATING FACTORS HANDBOOK.

Figure A-2 gives the scaling factor as a function of V_{hL} in each of these cases, and presents another way of describing the validity of scaling. Scaling between the (1205) and (1207) launch vehicles can be expected to be very accurate for an optimum V_{hL} less than about 4 km/sec, and increasingly less accurate for larger velocities. On the other hand, scaling between the Titan IIIX(1205)/Centaur and the Titan IIIC would lead to significantly off-optimum results except, perhaps, in the case of small values of optimum V_{hL}.

The above remarks are strengthened by a numerical check on scaling validity presented in Table A-1. Optimum data points are taken from recent results obtained by Horsewood.[19] The example is a 700 day Jupiter orbiter mission (2 x 38 radii orbit) utilizing the direct flight mode and with powerplant jettisoning prior to the retro maneuver. Reference data for the Titan IIIX(1205)/Centaur vehicle is listed in Table A-2. Table A-1 shows that the optimum trajectory is nearly invariant in the case of scaling to the Titan IIIX(1207)/Centaur. The scaled value of net spacecraft mass is accurate to 9 kg, or about 0.7 percent. Scaling to the Titan IIIC is not valid; m_n is 127 kg less than the optimum value which represents a scaling error of about 80 percent. Additional checks on scaling validity are presented in Figure A-3 which shows the net spacecraft mass over a range of flight times for the Jupiter orbiter mission. The validity of launch vehicle scaling has been tested for other mission examples. Again, the scaled results were found to be very accurate as long as the two launch vehicle performance curves are linearly scalable, or nearly so. Table A-3 gives a matrix of relative scaling validity between 6 different launch vehicles. Scaling is generally valid in the case of indirect trajectories because of the low values of launch velocity V_{hL}.

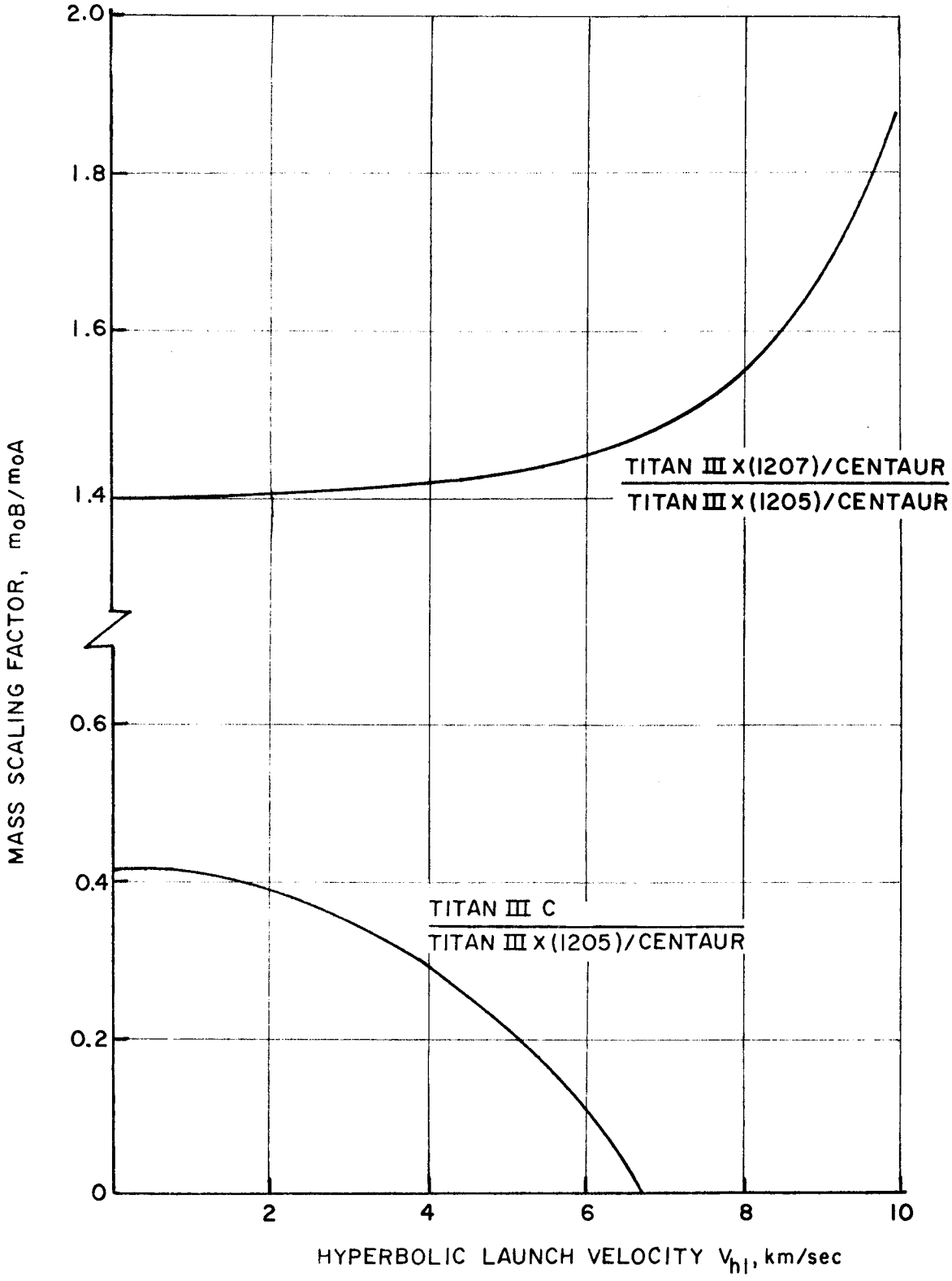

FIGURE A.2. MASS SCALING FACTORS FOR TITAN CLASS LAUNCH VEHICLES.

Table A-1

APPLICATION OF LAUNCH VEHICLE SCALING

Jupiter orbiter mission (see Table A-2)

Parameter	Vehicle B_1 (scaled)	Vehicle B_1 (optimized)	Vehicle B_2 (scaled)	Vehicle B_2 (optimized)
m_n, kg	1311	1320	156	283
I_{sp}, sec	2730	2770	2730	2720
P_o, kw	40.7	35.4	4.9	21.6
V_{hL}, km/sec	5.519	5.877	5.519	2.640
V_{hp}, km/sec	7.979	7.906	7.979	8.850
t_p, days	356	367	356	295

Vehicle A: Titan IIIX(1205)/Centaur (used for scaling).
Vehicle B_1: Titan IIIX(1207)/Centaur.
Vehicle B_2: Titan IIIC.

Table A-2

REFERENCE DATA FOR A JUPITER ORBITER MISSION EMPLOYING SOLAR-ELECTRIC PROPULSION

MISSION INPUTS

Launch vehicle	Titan IIIX(1205)/Centaur
Flight time	700 days, direct mode
Orbit size	$r_p = 2$, $r_a = 38$ Jupiter radii
Propulsion specific mass	$\alpha_{ps} = 30$ kg/kw
Propulsion efficiency	$\eta = 0.62$ at $I_{sp} = 3000$ sec
Tankage factor	$k_p = 0.03$
Structure factor	$k_o = 0$
Retro specific impulse	$I_{sc} = 300$ sec
Retro inert factor	$k_r = 0.111$

Propulsion system is jettisoned

OPTIMUM PARAMETERS

Initial power	$P_o = 28.5$ kw
Specific impulse	$I_{sp} = 2730$ sec
Hyperbolic launch velocity	$V_{hL} = 5.519$ km/sec
Hyperbolic arrival velocity	$V_{hp} = 7.979$ km/sec
Propulsion time	$t_p = 356$ days
Retro propellant fraction	$\rho = 0.46126$
Electric propellant mass	$m_p = 575$ kg
Retro system mass	$m_r = 967$ kg
Net spacecraft mass	$m_n = 920$ kg

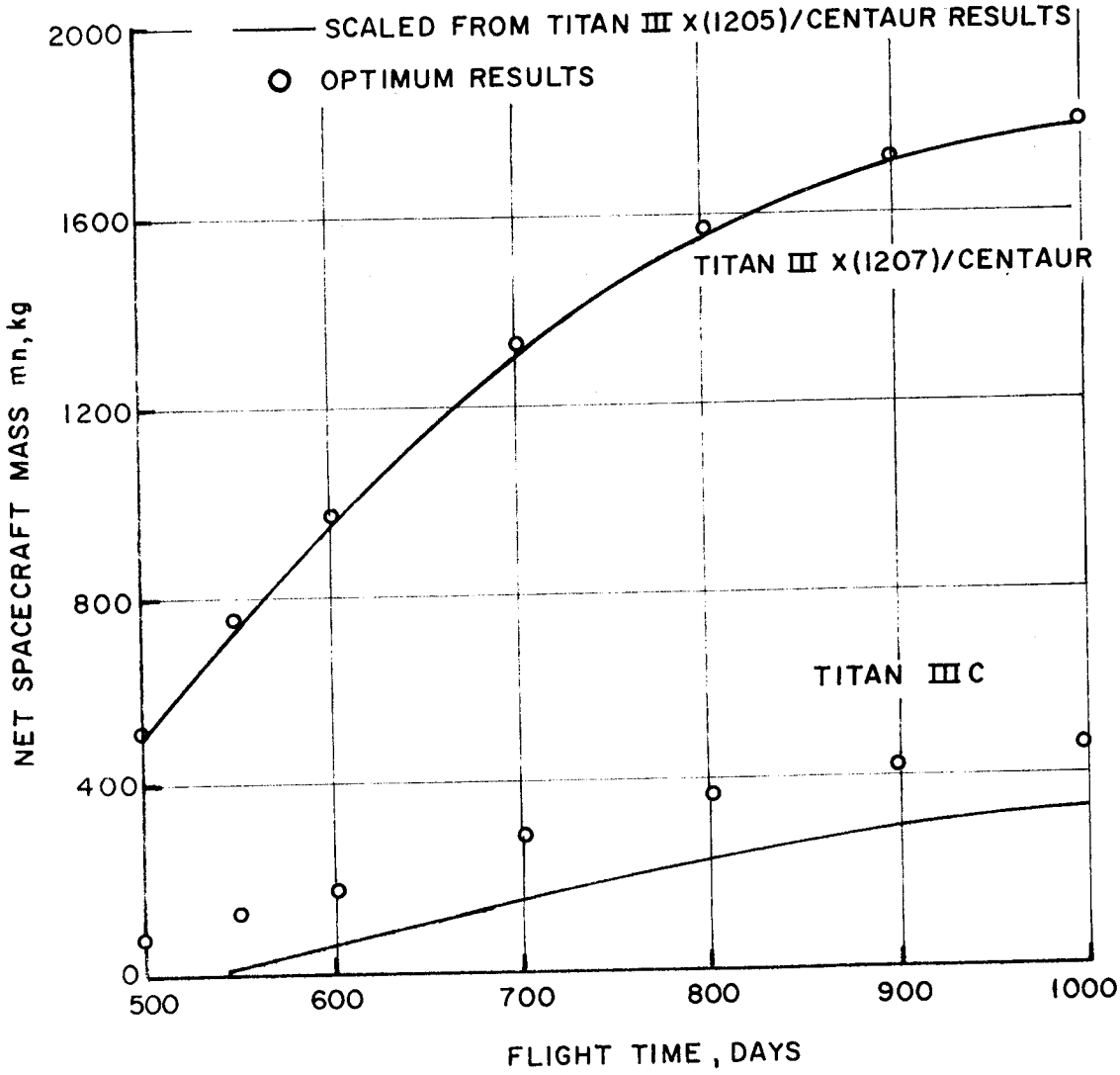

FIGURE A.3. APPLICATION OF LAUNCH VEHICLE SCALING FOR SOLAR-ELECTRIC PROPULSION JUPITER ORBITER MISSION.

Table A-3

LAUNCH VEHICLE SCALING FACTORS*, m_{oB}/m_{oA}

A \ B	Atlas(SLV3C)/ Cent	Titan IIIX/ Cent	Titan IIIC	Titan IIIX (1205)/Cent	Titan IIIX (1207)/Cent	SIC/SIVB/ Cent
Atlas(SLV3C)/Cent		(D) Yes (I) 1.24	(D) Yes (I) 1.82	(D) No (I) 4.40	(D) No (I) 6.19	(D) No (I) 18.2
Titan IIIX/Cent	(D) Yes (I) 0.805		(D) Yes (I) 1.47	(D) No (I) 3.56	(D) No (I) 5.00	(D) No (I) 14.7
Titan IIIC	(D) Yes (I) 0.550	(D) Yes (I) 0.680		(D) No (I) 2.42	(D) No (I) 3.40	(D) No (I) 10.0
Titan IIIX(1205)/ Cent	(D) No (I) 0.227	(D) No (I) 0.281	(D) No (I) 0.414		(D) Yes (I) 1.40	(D) Yes (I) 4.13
Titan IIIX(1207)/ Cent	(D) No (I) 0.162	(D) No (I) 0.200	(D) No (I) 0.294	(D) Yes (I) 0.715		(D) Yes (I) 2.94
SIC/SIVB/Cent	(D) No (I) 0.055	(D) No (I) 0.068	(D) No (I) 0.100	(D) Yes (I) 0.242	(D) Yes (I) 0.340	

*$m_{nB}/m_{nA} = P_{oB}/P_{oA} = m_{oB}/m_{oA}$

(D) Direct flight mode; Yes (scaling valid), No (scaling not valid).

(I) Indirect flight mode; scaling factor m_{oB}/m_{oA} at $V_{hL} = 0$ (escape energy).

A2.2 Scaling for Tankage and Structure Factors

There are two arguments for the validity of near-optimum scaling of tankage and structure masses. First, these masses can be traded off directly with m_n, at least in the case of no jettisoning of the propulsion system. Second, the parameters k_p and k_o have relatively small values. Structure and tankage mass together should account for less than 10 percent of the gross spacecraft mass at termination of low-thrust propulsion. One might expect, then, that any reasonable variation in these quantities would have negligible effect on the optimum parameters (P_o, I_{sp}, V_{hL}, V_{hp}). This conclusion has been verified by numerical results. Figure A-4 illustrates the effect of changes in the propellant tankage mass for the Jupiter orbiter mission discussed previously. As k_p varies between zero and one-tenth, the optimum net spacecraft mass decreases from 928.5 kg to 901.3 kg. The corresponding scaled values are 928.4 kg and 900.4 kg.

A2.3 Scaling for Propulsion System Specific Mass and Efficiency

A change in the assumed value of specific mass α will result in some variation of the optimum performance parameters. For example, as α is decreased with improved technology the optimum values of P_o and I_{sp} tend to increase while V_{hL} tends to decrease. Because of the lighter weight propulsion system, performance is increased by shifting the mass transportation burden more to the SEP stage and less to the chemical launch stage. However, if the variation of α under consideration is not too large, say less than 20 percent, previous studies have shown that the optimized values of P_o, I_{sp} and V_{hL} remain nearly the same. For those missions not calling for propulsion system jettisoning, the mass scaling law

$$m_{nB} = m_{nA} + (\alpha_A - \alpha_B) P_{oA}$$

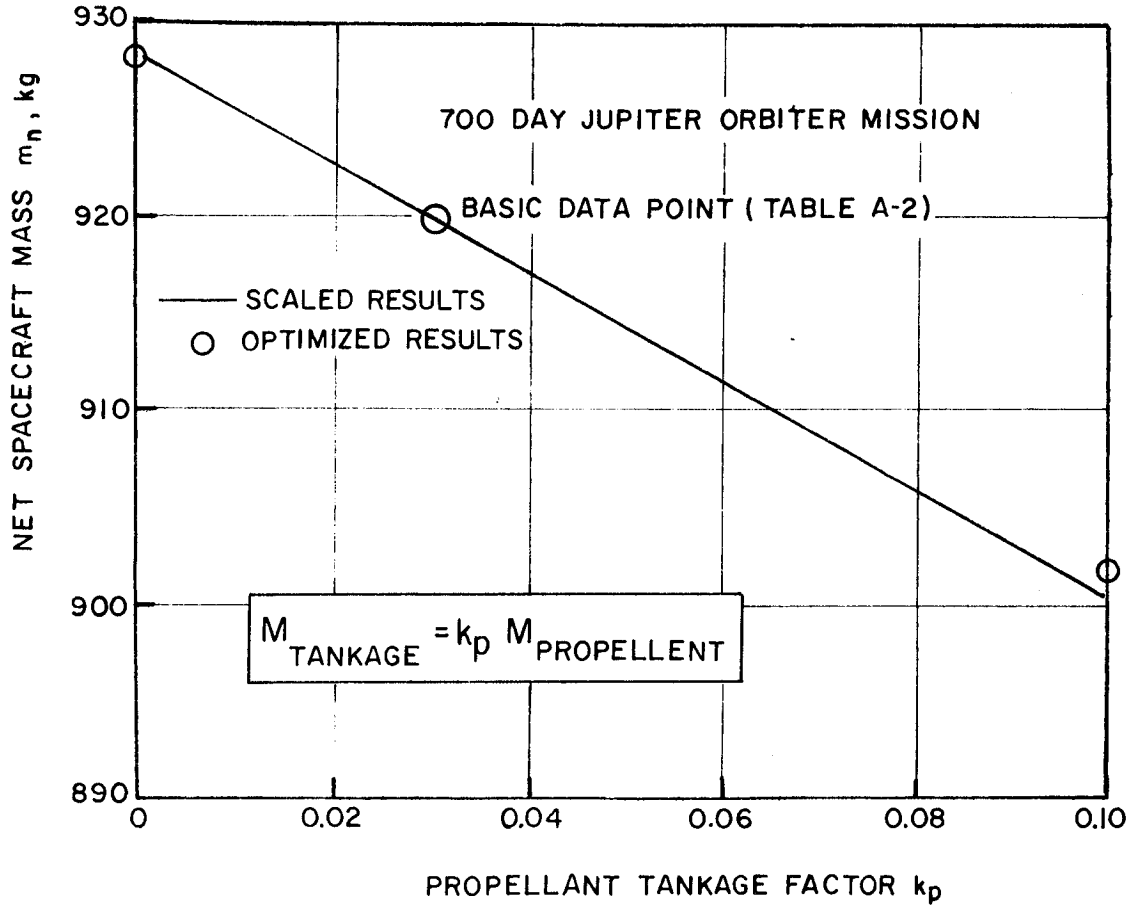

FIGURE A.4. ILLUSTRATION OF SCALING FOR PROPELLANT TANKAGE FACTOR.

would be expected to yield near-optimum values of m_{nB} providing that $(\alpha_A - \alpha_B)$ is relatively small. For orbiter missions calling for propulsion system jettisoning, the modified scaling law is

$$m_{nB} = m_{nA} + [1 - \rho_A(1 + k_{rA})] (\alpha_A - \alpha_B) P_{oA}$$

Figure A-5 illustrates the use of this expression for the reference Jupiter orbiter mission. Scaling accuracy is about 4 percent for a 33 percent change in α_{ps}.

The validity of scaling for changes in propulsion system efficiency η obviously depends on the validity of specific mass scaling (see Eq. A.18). In addition, it depends upon the invariance of specific impulse. As in the case of launch vehicle scaling, the optimum I_{sp} would depend on the shape of the η vs I_{sp} curve. If the two curves $\eta_A(I_{sp})$ and $\eta_B(I_{sp})$ are linearly scalable, I_{sp} should optimize at the same point. If this were not true, then the use of the scaling law would result in a value of m_n which is somewhat less than optimum. Figure A-6 shows an example of efficiency scaling for the Jupiter orbiter mission. Although scaling was found to be quite accurate, the reoptimized I_{sp} values did change even though η is linearly scalable in the factor b.

A.2.4 Scaling for Orbit Size and Retro System Parameters

The validity of orbit size scaling has been tested by numerical example with surprisingly accurate results. Figure A-7 compares the scaled and optimized values of m_n for a 600 day, direct mode, Jupiter orbiter mission utilizing the Titan IIIX(1207)/Centaur launch vehicle. The propulsion system is assumed to be jettisoned prior to the retro maneuver. Numerical results obtained over a wide range of orbit selections show excellent agreement between scaled and optimized performance -- less than 2 percent error. Since the question arose as to whether these results were peculiar to the example mission

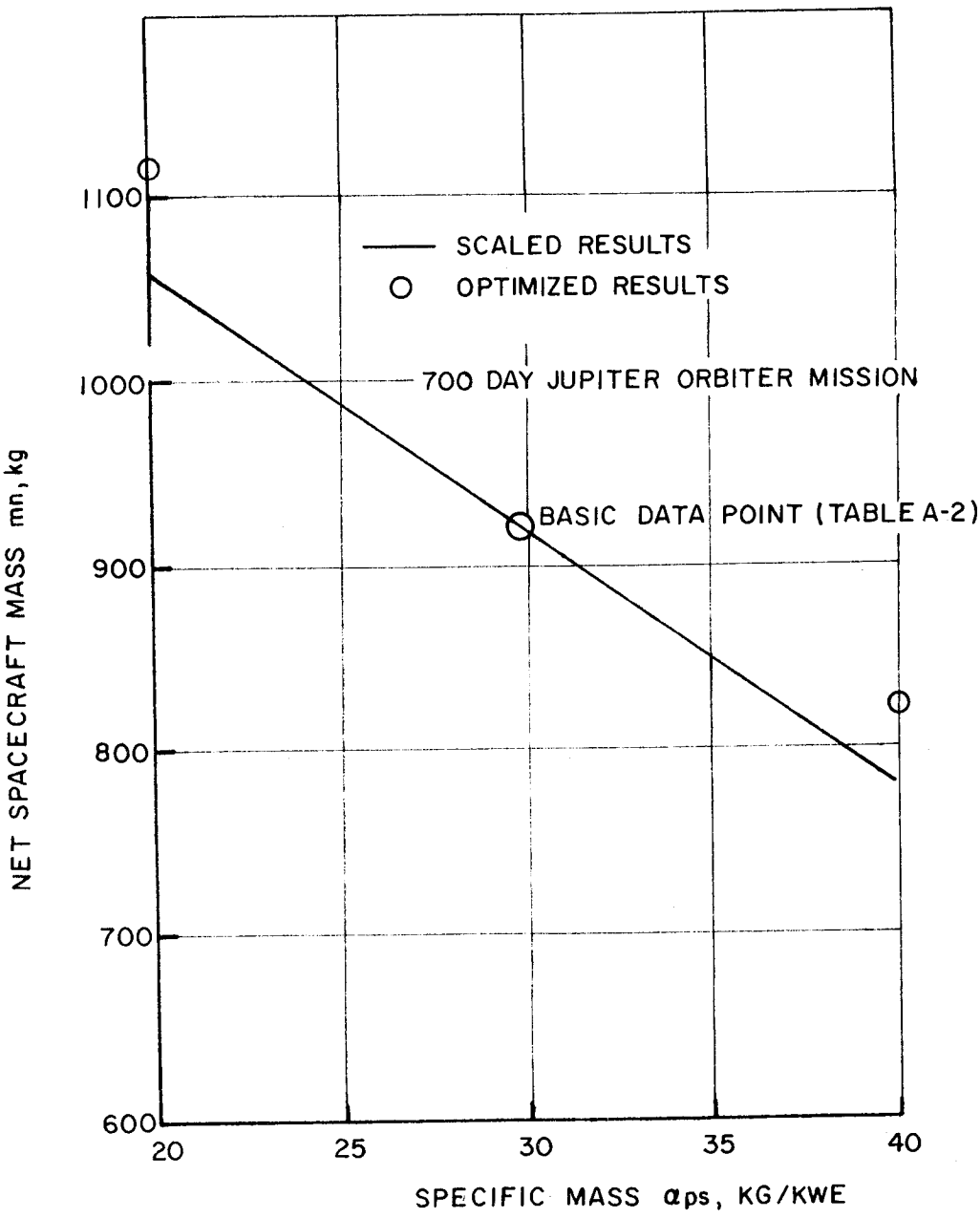

FIGURE A-5. ILLUSTRATION OF SCALING FOR PROPULSION SYSTEM SPECIFIC MASS.

$$\eta = \frac{b}{1 + \left(\frac{14300}{9.8066 I_{sp}}\right)^2}$$

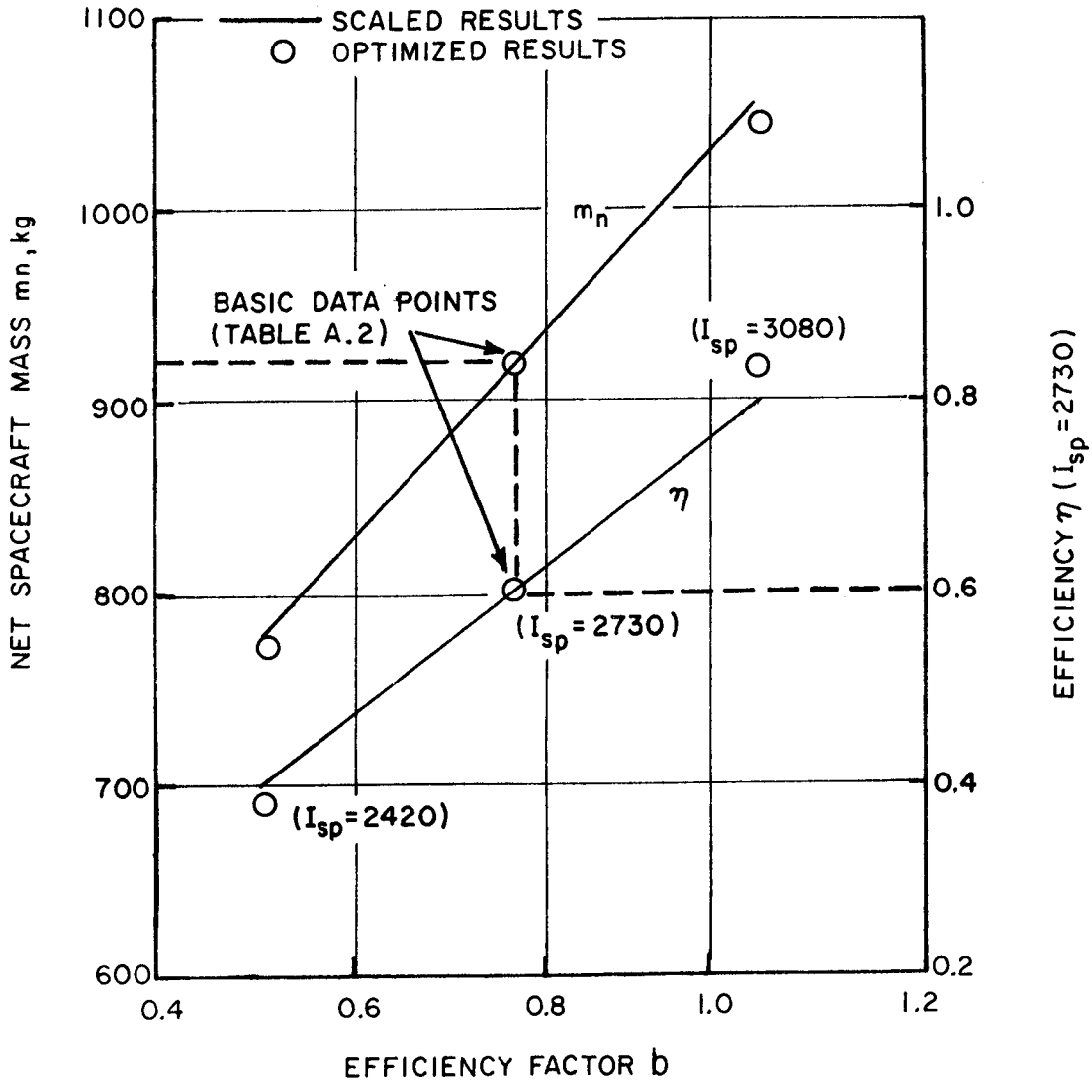

FIGURE A-6. ILLUSTRATION OF SCALING FOR PROPULSION SYSTEM EFFICIENCY (700-DAY JUPITER ORBITER MISSION).

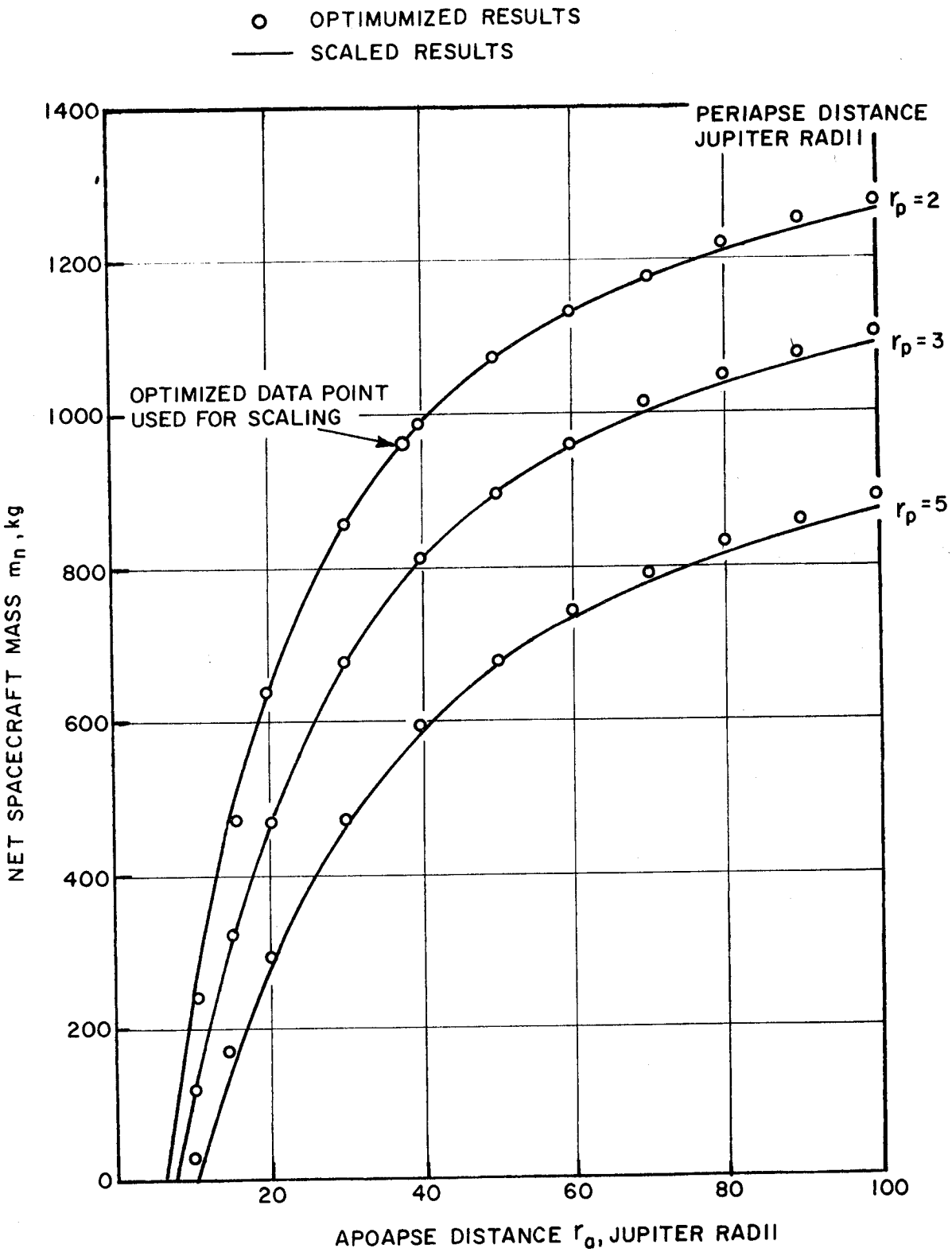

FIGURE A-7. ORBIT SIZE SCALING FOR SOLAR-ELECTRIC JUPITER ORBITER, 600 DAY FLIGHT, DIRECT MODE, POWER PLANT JETTISONED.

selected, a similar validity test was made for a 6000 day, indirect mode, Neptune orbiter mission. The low-thrust trajectory in this case bears no resemblance to the Jupiter trajectory. Scaling accuracy was again verified as shown in Figure A-8.

On the basis of these numerical validity tests, one could conclude that the optimum low-thrust transfer is essentially invariant with orbit size selection, at least for outer planet missions. This is akin to ballistic trajectory experience. The use of simple scaling relationships in place of trajectory reoptimization offers considerable savings in mission tradeoff analyses.

Orbit size scaling is shown in Figure A-9 for the 700 day Jupiter orbiter mission considered previously. Figures A-10 and A-11 illustrate the method of scaling for retro system specific impulse and inert fraction. Here again, the validity of scaling is shown empirically.

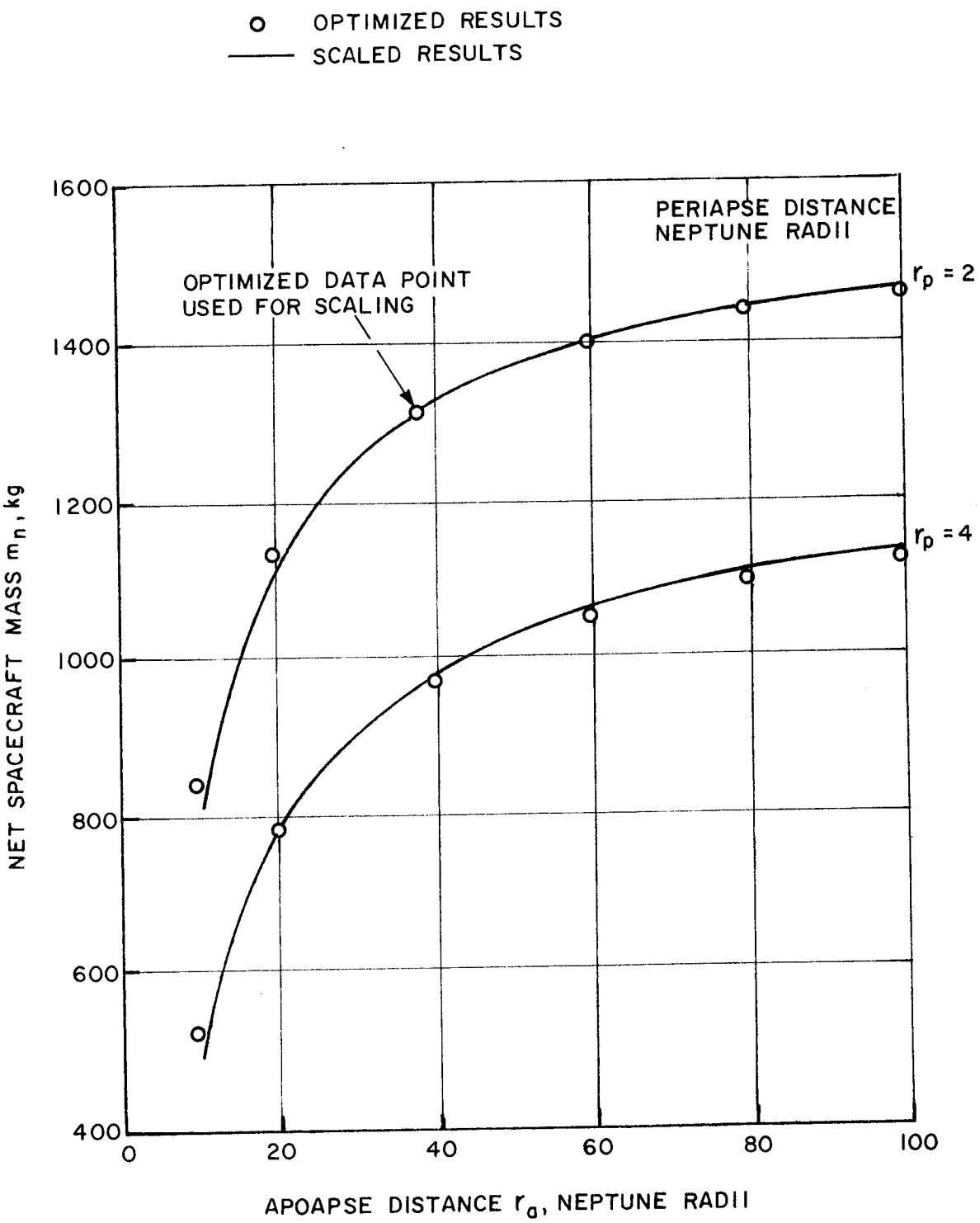

FIGURE A-8. ORBIT SIZE SCALING FOR SOLAR-ELECTRIC NEPTUNE ORBITER, 6000 DAY FLIGHT, INDIRECT MODE, POWER PLANT JETTISONED.

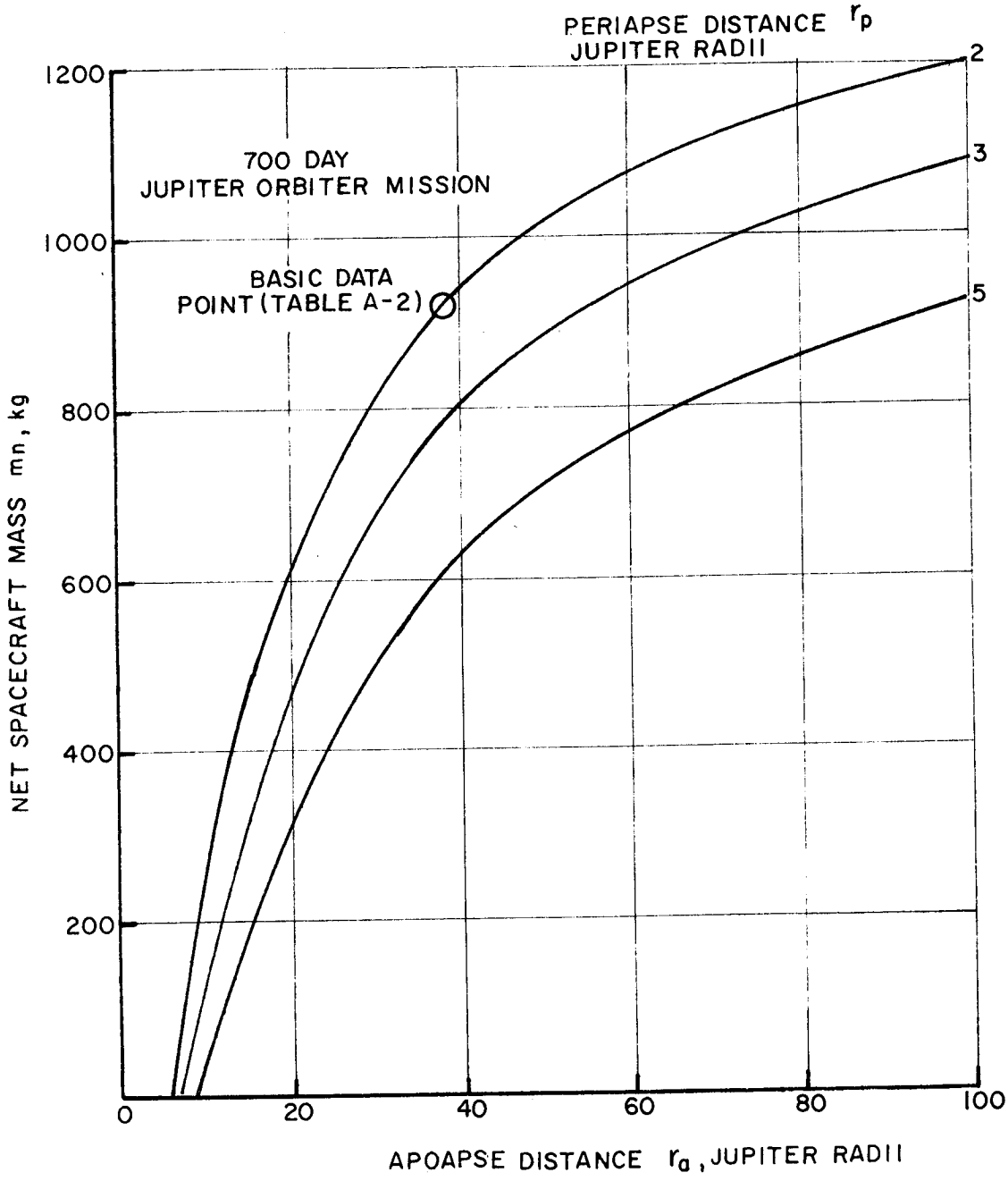

FIGURE A-9. ILLUSTRATION OF SCALING FOR ORBIT SIZE

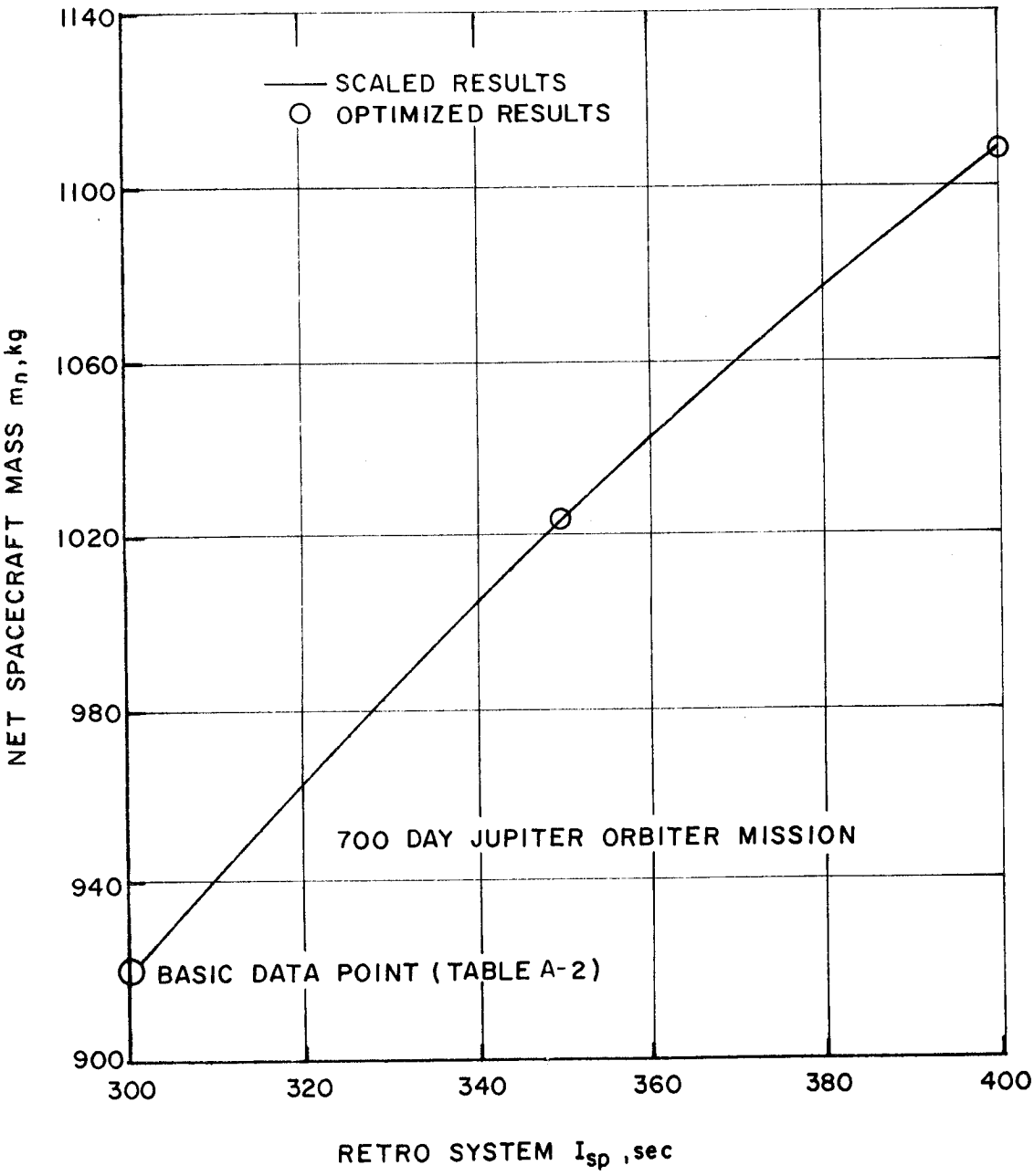

FIGURE A-10. ILLUSTRATION OF SCALING FOR RETRO SYSTEM SPECIFIC IMPULSE.

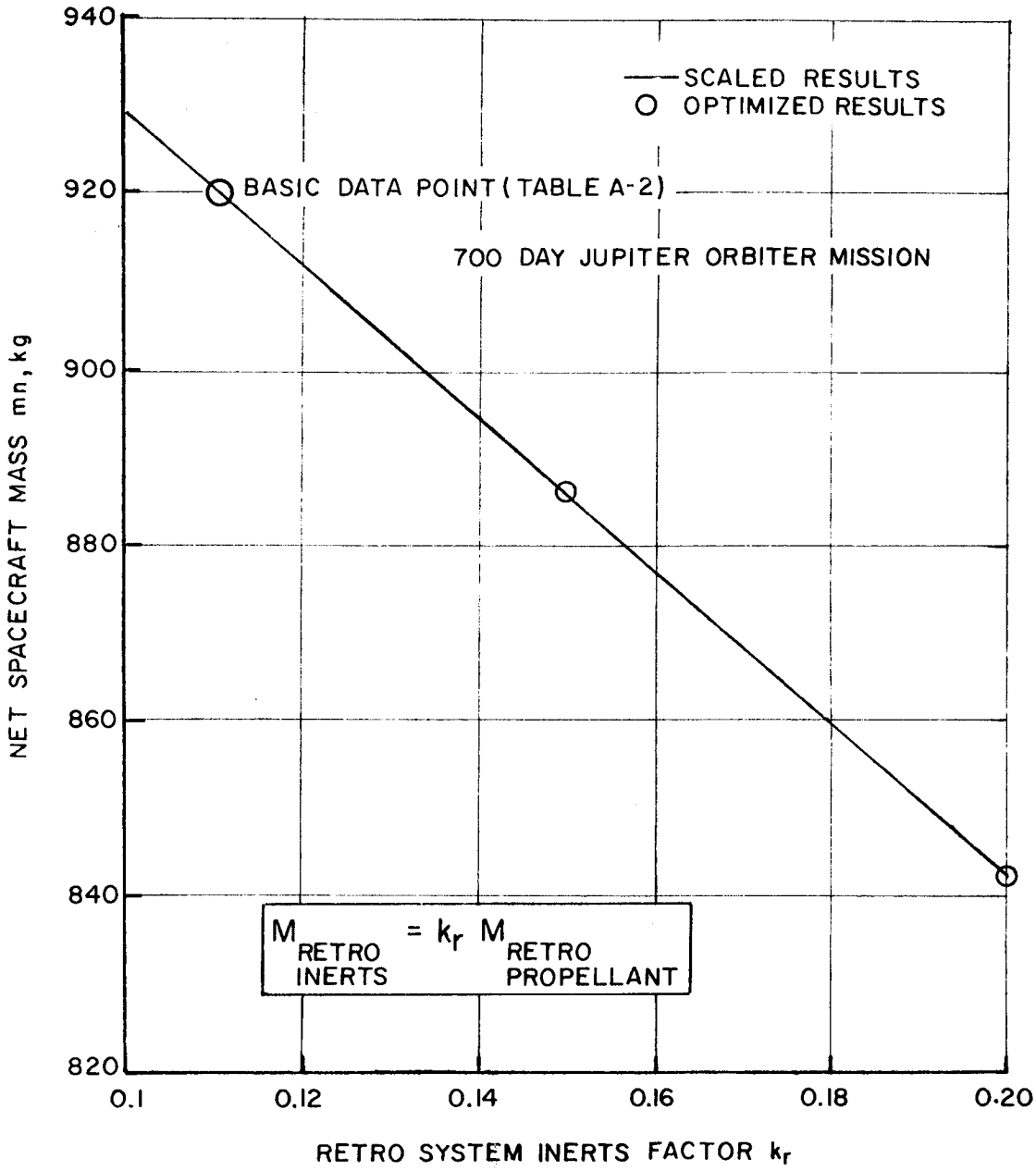

FIGURE A-11. ILLUSTRATION OF SCALING FOR RETRO SYSTEM INERTS.

Appendix B

ABSTRACTS OF SURVEY PAPERS

Appendix B

ABSTRACTS OF SURVEY PAPERS

This appendix includes one page abstracts of 17 papers and reports on the subject of solar-electric propulsion and mission applications. Additional documents that were reviewed are not abstracted here because they are discussed at some length within the main body of this report.

"LOW-THRUST ORBIT RAISING IN CONTINUOUS SUNLIGHT WHILE THRUSTING IN A PLANE PERPENDICULAR TO THE EARTH-SUN LINE," RAMLER[4]

This paper treats the problem of a SERT II type of ion engine system test in Earth orbit with power provided by solar panels. Maximizing the mission duration (i.e., time in continuous sunlight) can be accomplished by choosing appropriately the launch date and the initial orbit inclination for fixed values of initial altitude and thrust-weight ratio. The two main factors which influence the problem dynamics are (1) the apparent motion of the Sun along the ecliptic during the year, and (2) the precession of the orbit's line of nodes due to oblateness effects. Near-polar, retrograde orbits are necessary to allow the second factor above to counteract the first. The problem solution is obtained by analytical approximation methods deemed sufficiently accurate for the purpose; basically, an orbit averaging scheme is employed. Numerical optimization yields the best values of launch date and inclination. The scheme of thrust direction reversal is also analyzed as a means of increasing mission duration. In the case of no thrust reversal, a typical result for $F/W_o = 5 \times 10^{-6}g$ and $h_o = 300$ n. miles is a launch date of September 16, an inclination of 104°, a mission duration of 416 days and a final altitude of 2600 n. miles. The same thrust reversal case would extend the mission duration to 580 days but decrease the maximum altitude to 1800 n. miles.

"USE OF ELECTRIC PROPULSION FOR EXPLORING THE DISTANT REGIONS OF THE GEOMAGNETIC TAIL," MEISSINGER AND GREENSTADT(9)

The mission application discussed in this paper is an investigation of the solar proton wind interaction with the Earth's magnetotail as far as 200 Earth radii. An orbit-raising phase is accomplished in about 250 days employing a fixed thrust vector program (circumferential or normal to Sun-line in orbital plane). Holding the perigee to 2 radii the apogee is raised on successive elliptical orbits to the final radius desired. The second phase, uniquely appropriate for electric propulsion, consists of stationkeeping for about 8 months to permit continuous monitoring of the magnetotail environment. Launched by the low-cost Atlas/Burner II vehicle, the 600 lb conceptual spacecraft is powered by a 2.5 kw fold-out solar array (45 lbs/kw) and electron bombardment thrusters operating at a specific impulse of 3500 seconds. Flight readiness is projected to the early 1970's. Detailed descriptions of the scientific objectives, instruments, orbital characteristics and subsystem weight breakdowns are given in the paper.

"A DELTA-POWERED ELECTRICALLY RAISED HIGH POWER SYNCHRONOUS SATELLITE," READER AND REGETZ[21]

This paper presents an analysis and conceptual design of a solar-electric spacecraft employed to raise a 350 lb communications payload to a synchronous orbit. Once in final orbit, the solar array would be electrically reconfigured to provide up to 10 kw of power at 16 k volt potential to the communications experiment. The relatively low cost TAT/Delta vehicle with 9 Castor II's for thrust augmentation would be utilized to boost the SEP spacecraft to the initial orbit; either circular at about 2700 km altitude or elliptical at 370 x 5000 km altitude. Launch would take place from the Eastern Test Range; the subsequent 28.5° inclination of the initial orbit would have to be removed by the SEP spacecraft. The 10 kw solar array is articulated about a single vehicle - fixed axis to allow thrust orientation either circumferential in the orbit plane or normal to the orbit. Nominal thruster operation is at 2.25 kw and 3000 sec specific impulse (75% efficiency) -- 4 thrusters are used. The paper gives a subsystem weight breakdown and discusses the problem area of orbit shadowing effects, stationkeeping, attitude control and guidance.

"SOLAR-ELECTRIC PROPULSION SYSTEM PERFORMANCE FOR A CLOSE SOLAR PROBE MISSION," STRACK(3)

The mission application is a close (0.1-0.3 a.u.) solar flyby employing a hybrid chemical/SEP system. Propulsion system specific mass is assumed to be in the range 50-100 lbs/kw with a typical value of 75 lbs/kw (34 kg/kw). Thruster efficiency of 66 percent at a specific impulse of 4000 seconds assumes use of 50 cm mercury bombardment thrusters. The solar power curve used is based on a theoretical analysis of silicon cell properties and a design assumption of panel tilting for in-bound missions; panel tilting allows constant power operation for solar distances in the range 0.13-0.65 a.u. Comparisons are made with all-chemical systems and nuclear-electric systems. The basic launch vehicle considered is the Saturn 1B/Centaur. An all-chemical system with a high performance stage (I_{sp} = 460 sec) can deliver a 480 lb payload to 0.1 a.u. in 75 days. Assuming a specific weight of 75 lbs/kw, the nuclear-electric system provides a 1050 lb payload in 400 days, and the solar-electric system provides 1430 lb for the same flight time. The 2-1/2 revolution indirect trajectory is identified as being optimum for the solar-electric system. Optimum SEP specific impulse and power are 4100 seconds and 32 kw, respectively.

"A 3 KW SOLAR-ELECTRIC SPACECRAFT FOR MULTIPLE INTERPLANETARY MISSIONS," MEISSINGER, PARK AND HUNTER[5]

A small (under 300 kg) first-generation SEP spacecraft having multimission capability is proposed as an economical follow-on to the SERT II systems flight test. Mission applications include a 1 a.u. solar monitor, a 0.3 a.u. solar probe, a 40° out-of-the-ecliptic flight, and an asteroid belt fly-through. The science payload for each of these missions is about 50 lbs (23 kg). A weight and power breakdown of the basic SEP spacecraft subsystems and the science experiments is given along with trajectory and flight time data for the various missions. Propulsion system specific mass is assumed to be about 27 kg/kw. An Atlas/Burner II launch vehicle is suggested.

The major advantages of the light-weight spacecraft concept are attributed to the low power requirement, small launch vehicle cost, mission versatility, and growth potential for later planetary and comet intercepts. Spacecraft development is said to be based largely on existing technology and flight-proven systems. Operational readiness would be expected in the early 1970's.

"SOLAR-ELECTRIC PROPULSION PROBES FOR EXPLORING THE SOLAR SYSTEM," STRACK AND ZOLA(8)

This early study by the authors presents results of minimum flight time versus distance from the Sun for flyby and orbiter payloads of 500, 1000 and 2000 lbs. The three launch vehicles considered are (1) Atlas/Centaur, (2) Titan IIIC/Agena, and (3) Saturn 1B/Centaur. Study assumptions include planar trajectories, circular planet orbits, Strack's power curve allowing for panel tilting on inbound flights, specific weight of 75 lbs/kw, efficiency of 67 percent at 4000 sec specific impulse, and structure and tankage factors of 10 percent. Orbiter missions assume a highly elliptical orbit at 2 planet radii periapse, and a chemical retro system specific impulse of 300 seconds and a 20 percent inert fraction. Thrust direction and coast periods are optimized as needed. For optimum values of launch velocity and initial acceleration (or power), the thruster specific impulse is chosen to minimize the flight time; this generally results in continuous propulsion operation. Results are presented in graphical form. The reader of this report should be cautioned against one faulty conclusion by the authors: this refers to the statement that the chemical launch vehicle without the SEP stage can yield better performance than with the SEP stage for short flight times on certain missions. This being clearly not true, the explanation lies in the fact that the direct flight mode and not the indirect mode should have been the basis for comparison in the case of shorter flight times.

"JOVIAN PLANET MISSIONS FOR SOLAR CELL POWERED ELECTRIC PROPULSION SPACECRAFT," ZOLA(10)

This paper presents multimission application results for a fixed design SEP spacecraft launched by an Atlas(SLV3C)/ Centaur vehicle. Flyby and orbiter (2 x 200 planet radii) missions to Jupiter, Saturn, Uranus and Neptune are treated. The SEP design has an installed array power level of 11.1 kw (10 kw delivered to thrusters), a total propulsion system mass of 345 kg, a structure and tankage fraction of 10 percent each, and thrusters operating at a specific impulse of 4500 seconds with an efficiency of 70 percent. Launched to hyperbolic excess velocity, the SEP spacecraft has a total propulsion time constraint of 800 days or less. Apart from the fixed design and time constraint, the results presented assume optimization of travel angle (launch date), thrust direction and hyperbolic excess velocity.

It is shown that at least 200 kg of net spacecraft mass can be delivered to the outer planets (slightly less for Neptune orbiters). However, with the exception of Jupiter, the indirect flight mode is required,necessitating long flight times and the full 800 days of propulsion. Trip times range from 2-4 years for Jupiter missions and up to 12-18 years for the Uranus and Neptune missions.

"INTERPLANETARY PROBE MISSIONS WITH SOLAR-ELECTRIC PROPULSION SYSTEMS," ZOLA[20]

This report identifies optimum trajectory and propulsion system design parameters of SEP spacecraft for flyby and orbiter missions to the outer planets, Jupiter - Neptune, and also orbiters of Mercury and Mars. The orbit selection is highly elliptical with periapse distance at 2 planet radii. All example missions utilize the Atlas(SLV3C)/Centaur launch vehicle. Payload comparisons are made with the ballistic flight mode which assumes a high-performance (I_{sp} = 460 sec) chemical "kick" stage in place of the SEP spacecraft. The orbit retro stage common to both flight modes assumes an I_{sp} of 300 sec and a retro inert fraction of 20 percent. Assumed SEP input parameters are a propulsion system specific mass of 34 kg/kw and tankage and structure factors of 10 percent each.

Both direct and indirect SEP trajectories are analyzed for two classes of initial conditions: Earth-escape spiral and launch to hyperbolic excess velocity. The escape spiral-indirect transfer combination offers the best performance in the case of large payload ($>$ 600 kg) requirements but necessitates the use of longer flight times and higher power levels. Payload capability of the SEP system is at least 300 kg for the outer planet flybys and 200 kg for the loose orbiters. The all-chemical system has a definite performance edge only for Mars and Jupiter missions. It is noted, however, that the Atlas/Centaur launch vehicle is probably not adequate for delivering the payload sizes needed for planet orbiter missions.

"MISSION ANALYSIS FOR INTERPLANETARY VEHICLES WITH SOLAR ELECTRIC PROPULSION," FLANDRO AND BARBER(6)

This paper presents a thorough qualitative discussion of the problem areas facing the mission analyst and the techniques which may be employed in mission design. The increased complexity of low-thrust mission analysis stems from the inability to separate the performance chracteristics of the interplanetary trajectory from the high-thrust launch phase. Also, the presence of the continuous propulsion device gives rise to a complex set of interactions involving trajectory design, guidance and navigation, attitude control and spacecraft configuration. A case is made for the development and use of a graded set of low-thrust trajectory programs. A Level 1 program, employing approximate solution methods for purposes of fast compututation, would be used for generating maps of mission opportunity and parametric data. It is primarily a good "performance simulator" rather than a good "path simulator." The Level 2 program, also a performance simulator, would employ numerical integration, have full optimization capability, and be used for more detailed mission definition and constraint analysis. Level 3 and 4 programs are primarily good path simulators employing very accurate computation procedures; the first would be used for advanced mission definition, error analysis and targeting; the second would be used for actual mission support operation.

Application of the analysis techniques described is illustrated for a 1975 Jupiter flyby mission. Curves of the key mission performance parameters are given as a function of launch date. The tradeoff analysis leading to the specification of fixed SEP design parameters is described.

"SOLAR ELECTRIC GRAND TOUR MISSIONS TO THE OUTER PLANETS," FLANDRO[11]

This report presents an analysis of the hybrid low thrust/gravity assist trajectory mode. The SEP spacecraft is utilized only for the Earth-Jupiter leg of the multi-planet mission. This ground rule, adopted for analysis simplicity, results in performance data which is not fully optimum, but, probably, nearly so. The "optimum" trajectories described are those which deliver the maximum payload to the intermediate planet Jupiter for a given hyperbolic excess velocity at encounter; the total mission flight time is, hence, a dependent parameter of the first leg characteristic.

Among the various missions analyzed are: (1) Earth-Jupiter-Saturn, (2) Earth-Jupiter-Uranus, (3) Earth-Jupiter-Saturn-Pluto, and (4) Earth-Jupiter-Uranus-Neptune. Optimum launch years, time of flight, and payload for each mission are presented in graphical form. It is shown that application of SEP on the first leg offers a significant performance advantage over the completely ballistic flight mode. Utilizing the Titan IIIX(1205)/Centaur as the basic launch vehicle, this performance advantage is primarily in terms of reduced flight time. SEP Grand Tour missions, E-J-S-P (1977 launch) and E-J-U-N (1979 launch) require total flight times of about 6 years and 7.5 years, respectively. Net spacecraft mass in each case is at least 650 kg (1435 lbs). The all-ballistic Grand Tours utilizing the Titan IIIX(1205)/Centaur/BII deliver a 650 kg payload in flight times of 8.5 years and 9.1 years, respectively.

"SOLAR ELECTRIC SPACE MISSION ANALYSIS-FINAL REPORT," PRINCETON UNIVERSITY (ASMAR)[14]

Characteristics of the optimum trajectory and payload capability of solar electric propulsion are discussed for the Jupiter flyby mission and asteroid belt missions. The propulsion system specific mass is taken to be 30 kg/kwe nominally, but is varied over the range 20-30 kg/kwe in a sensitivity analysis. Thruster efficiency, representative of a cesium electron bombardment engine, is nominally 60 percent at a specific impulse of 4000 seconds; this parameter is also varied to determine sensitivity effects. The Jupiter flyby mission is investigated for flight times from 600 to 1000 days. Net spacecraft mass (payload) delivered varies from 100 to 420 kg assuming the Atlas(SLV3C)/Centaur launch vehicle. The indirect flight mode, having a transfer angle greater than 360°, is identified and shown to result in greater payload than the direct flights for the longer trip times. Useful information on the optimum values of power, specific impulse and hyperbolic launch velocity is given in the report as well as the sensitivity of off-optimum design. Asteroid rendezvous missions are shown to be uniquely suited for electric propulsion application. Trajectory and payload data are given for several launch vehicle candidates. Also discussed is the less ambitious asteroid belt fly-through mission and the possible application of on-board radar experiments.

"OPTIMIZATION OF A SOLAR-ELECTRIC PROPULSION PLANETARY ORBITER SPACECRAFT," SAUER[15]

An optimization is made of a 1971 Mars orbiter mission using a Titan IIIC launch vehicle and a SEP spacecraft employing mercury bombardment thrusters operating with an efficiency of 65.5 percent at a specific impulse of 3500 seconds. The overall propulsion system specific mass is assumed to be 34 kg/kw. The net spacecraft mass in Mars orbit (1.3 x 4 radii) is maximized with respect to the solar panel output power, the launch energy and the arrival energy. A constant power drain of 400 watts for operating spacecraft subsystems is considered. Performance comparisons between SEP and ballistic flight systems are described. For example, the ballistic spacecraft launched by the Titan IIIC on a 216 day flight (30 day launch window) can deliver a net spacecraft mass of 370 kg which does not include 224 kg of solar panels for power. The SEP system delivers 831 kg on a 248 day trajectory, again not including the 224 kg of solar panels (power output at Mars is 4.8 kw). The installed power level at 1 a.u. is 8.4 kw.

The first several sections of this paper describe the mathematical formulation of the trajectory/payload optimization problem. Sufficient detail and interpretive discussion is given to make these sections quite useful in understanding the SEP mission analysis problem.

"TO THE OUTER PLANETS," LONG(17)

This article is concerned with a general explanation of possible flight modes to the outer planets. Three specific multiple-planet missions are identified and analyzed subject to the broad constraints of the planet's orbital alignment in the years 1976-80. The four-planet "grand tour" to Jupiter, Saturn, Uranus and Neptune is available from 1976 to 1979 with the middle two years offering the best launch opportunity in terms of launch energy, flight time and swingby distances. A modified grand tour of Jupiter, Saturn and Pluto is available during the same time period, with 1977 and 1978 again being the best launch years. A second modification would tour Jupiter, Uranus and Neptune with 1979 being the best year. These missions can be accomplished with the programmed Titan/Centaur launch vehicle.

Basic scientific objectives of such missions are discussed, and a moderate science payload of 80 lbs is selected for discussion purposes. Consideration is given to the ballistic and SEP flight modes, and spacecraft design configurations for each mode are presented and compared. The SEP spacecraft would utilize the low-thrust propulsion system only during the transit to Jupiter, and its main advantage lies with increased payload capability or a smaller version of the Titan/Centaur launch vehicle.

"A SURVEY OF SOLAR POWERED ELECTRIC PROPULSION FOR AUTOMATIC MISSIONS," MULLIN, BARBER AND ZOLA(16)

The status (as of 1968) of solar-electric propulsion technology and mission application studies is described in this comprehensive survey paper. Major subsystems, such as the solar array, power conditioning and thrusters, are summarized in terms of their design and operational characteristics and the parameter set relevant to mission analysis. Solar array specific mass lies in the range 15-22 kg/kw depending upon the use of roll-up or fold-out array designs. The thruster subsystem, including power conditioning, thrusters and thrust vector control, is estimated to have a specific mass of 10 kg/kw consistent with hardware modularization in the 2-2.5 kw range and total power level in the 5-20 kw range. A description of the SERT II flight test (launched 2/70) is given. Mission analysis procedures are discussed and study results are summarized for geocentric and solar system area missions as well as flyby and orbiter missions to the planets. System analysis and spacecraft design procedures are reviewed with reference to the two conceptual spacecraft design studies by Hughes (Mars orbiter) and JPL (Jupiter flyby) -- problem areas discussed include thrust vector control, attitude control, navigation, launch vehicle interface, sensor field-of-view, auxiliary power, and thermal control.

"CURRENT STATUS OF SOLAR ELECTRIC-PROPELLED ASTEROID PROBE STUDIES," WROBEL AND DRIVER(18)

NASA sponsored, JPL contracted, studies were initiated in June 1969 with the Space Division of North American Rockwell (NAR) and with TRW Systems for the preliminary design and program planning of a SEP probe of the asteroid region for launch in the 1974-75 time period. Although operating with the same basic guidelines and constraints, the NAR study effort was directed at a reference spacecraft design solely for the asteroid flight, while the TRW study emphasized a multimission spacecraft for the asteroid belt, Jupiter flyby and out-of-the-ecliptic missions. This paper, by the contract technical monitors, presents the interim results of these two study efforts. Launch vehicle options considered are the Atlas/Centaur and the Titan IIIC. The trajectory profile evolved for the asteroid belt fly-through has an aphelion distance of 3.5 a.u. (maximum asteroid flux). Thrust cut-off occurs at about 2 a.u. (240 days) after which the probe coasts to aphelion (750 days) and then inward to 2 a.u. (1260 days). The paper describes the mission science rationale, trajectory/payload analysis, solar array and thruster subsystems, and the spacecraft configuration of each contractor. The reader is referred to the final reports of NAR and TRW to obtain the completed study results.

"CHARACTERISTICS, CAPABILITIES, AND COSTS OF SOLAR ELECTRIC SPACECRAFT FOR PLANETARY MISSIONS," BARTZ AND HORSEWOOD[24]

This survey article reviews previous studies of solar electric propulsion with the intent of summarizing and updating the overall picture of this new technology applied to planetary missions. Basic characteristics are described in terms of current subsystem performance and specific weight, functional requirements, and example spacecraft designs. The capabilities of SEP spacecraft are presented in terms of the net spacecraft mass delivered as a function of flight time. These results are for a uniform set of assumptions and system input parameters, and for one launch vehicle -- Titan IIIX(1205)/Centaur. Approximate conversion factors are given for other launch vehicles. Mission applications are discussed for the four categories: outer planet flybys, outer planet orbiters, inner planet orbiters, and area missions. Performance results are compared against those of ballistic missions assuming the Titan IIIX(1205)/Centaur/BII launch vehicle. It is shown that SEP performance advantages are especially significant for flybys of Uranus and Neptune, orbiters of Mercury, Saturn and Uranus, solar probes and out-of-the-ecliptic missions. The cost of initial SEP missions will likely cost 10-15 percent more than the ballistic counterpart. Cost advantages will accrue only when the ballistic approach requires a Saturn class launch vehicle and when the total exploration program envisions multiple launches; i.e., multimission capability.

"INTERACTION OF SPACECRAFT SCIENCE AND ENGINEERING SUBSYSTEMS WITH ELECTRIC PROPULSION SYSTEMS," SELLEN[35]

A series of possible processes have been detailed through which the operation of electrical thrusting units may impact upon the data pool or upon the operation of the data chain. Possible contaminants affecting the data pool are (1) particles released in the thrust beam, (2) electromagnetic contamination due to the waves in the frequency range from VLF to optical, (3) the radial component of the magnetic field produced and (4) the effects of the electrical field.

System configurations and constraints to reduce or eliminate various possible contaminants are discussed. To eliminate some data pool contamination it is suggested to include appropriate placement in the back-wiring of the solar cell arrays, include field cancellation configurations for ion thruster operations and incorporate neutralizer coupling to yield a minimized electrostatic field. To eliminate some data chain contamination it is suggested to place certain constraints on antennae placements and "look angles" and to look closer at the problem of material deposition on spacecraft surfaces due to the effects of changed ions.

In all of the areas of contamination listed the author points out that even without significant payload or configuration penalties the contamination can be reduced below the level of interference. He even suggests that electrically-propelled spacecraft may provide a more hospitable environment for the collections and processing of data than has previously been possible with ballistic spacecraft.